

2017

Target Identification Strategies for MMV Malaria Box Inhibitors of *Toxoplasma gondii* Growth

Jenna Elizabeth Foderaro
University of Vermont

Follow this and additional works at: <https://scholarworks.uvm.edu/graddis>

 Part of the [Genetics and Genomics Commons](#), [Microbiology Commons](#), and the [Molecular Biology Commons](#)

Recommended Citation

Foderaro, Jenna Elizabeth, "Target Identification Strategies for MMV Malaria Box Inhibitors of *Toxoplasma gondii* Growth" (2017). *Graduate College Dissertations and Theses*. 698.
<https://scholarworks.uvm.edu/graddis/698>

This Dissertation is brought to you for free and open access by the Dissertations and Theses at ScholarWorks @ UVM. It has been accepted for inclusion in Graduate College Dissertations and Theses by an authorized administrator of ScholarWorks @ UVM. For more information, please contact donna.omalley@uvm.edu.

TARGET IDENTIFICATION STRATEGIES FOR MMV MALARIA BOX
INHIBITORS OF *TOXOPLASMA GONDII* GROWTH

A Dissertation Presented

by

Jenna E. Foderaro

to

The Faculty of the Graduate College

of

The University of Vermont

In Partial Fulfillment of the Requirements
for the Degree of Doctor of Philosophy
Specializing in Microbiology and Molecular Genetics

May, 2017

Defense Date: December 19, 2016
Dissertation Examination Committee:

Gary E. Ward, Ph.D., Advisor
Jeanne M. Harris Ph.D., Chairperson
Christopher D. Huston, M.D.
Douglas I. Johnson, Ph.D.
Cynthia J. Forehand, Ph.D., Dean of the Graduate College

ABSTRACT

Small molecule screening is commonly used to discover lead compounds for drug development, but it can also be a powerful way to identify chemical probes for studying biological mechanisms. Our lab uses small molecules to study the mechanisms by which the protozoan parasite *Toxoplasma gondii* infects and replicates within its hosts. In this work, we employed a fluorescence-based assay to screen the Medicines for Malaria Venture (MMV) Open Access Malaria box for compounds that affect *T. gondii* growth. The box contains 400 previously identified small-molecule inhibitors of the related parasite, *Plasmodium falciparum*. We identified 79 hits, including a 2,4-diaminoquinazoline (MMV006169; $IC_{50}=1.15\mu M$) that strongly inhibits *T. gondii* intracellular replication and invasion with no evidence of toxicity to mammalian cells. Extensive structure-activity relationship analyses with *T. gondii* identified a number of analogs with changed potency and altered effects on replication and invasion. These structure-activity analyses provided the information necessary to synthesize a bivalent chemical inducer of dimerization (CID) containing MMV006169 for use in yeast three-hybrid experiments. Yeast growth competition assays showed that this CID is capable of entering the yeast nucleus, as required for yeast three-hybrid screening. Yeast three-hybrid was used in a targeted format to test the hypothesis that MMV006169 works by inhibiting parasite CDC48, an ATPase involved in trafficking and the degradation of misfolded proteins. Large-scale cDNA library screening by yeast three-hybrid suggests that the compound may instead be working through inhibition of a host cell target. This work has provided insight into how MMV006169 affects the parasite's lytic cycle and generated a testable hypothesis for the biologically relevant target of the compound.

CITATIONS

Material from this dissertation has been published in the following form:

Bessoff, K., Spangenberg, T., **Foderaro, J. E.**, Jumani, R. S., Ward, G. E., and Huston, C. D.. (2014). Identification of *Cryptosporidium parvum* active chemical series by Repurposing the open access malaria box. *Antimicrob Agents Chemother*, 58(5), 2731-2739. doi:10.1128/AAC.02641-13

Odell, A. V., Tran, F., **Foderaro, J. E.**, Poupart, S., Pathak, R., Westwood, N. J., and Ward, G. E.. (2015). Yeast three-hybrid screen identifies TgBRADIN/GRA24 as a negative regulator of *Toxoplasma gondii* bradyzoite differentiation. *PLoS ONE*, 10(3), e0120331. doi:10.1371/journal.pone.0120331

ACKNOWLEDGEMENTS

First, I would like to thank my advisor, Gary Ward. Gary welcomed me into his lab without hesitation and I am incredibly grateful for the opportunities he has afforded me. Gary's patience, professionalism, and approach to science have influenced me greatly during my time here and will continue to shape me in the future. I would also like to acknowledge the members of my dissertation committee: Douglas Johnson, Christopher Huston, and Jeanne Harris for their patience, guidance, and encouragement. I must extend extra gratitude to Jeanne Harris, my committee chair, for the time we spent discussing science, life, and the importance of overall happiness. I would also like to thank Nicholas Westwood, Fanny Tran, Christopher Huston, Kovi Bessoff, and Rajiv Jumani for our continued collaboration throughout the years.

I must acknowledge Steven Schmidt and Martin Thaler. Steven and Martin are amongst the most compassionate and generous men I have encountered. Seven years ago, they welcomed me into their home and family without question. I am tremendously grateful for the love and support they have shown me during this process.

Stephen and Amanda Everse have made massive contributions to my success. They made themselves available when I needed it most and showed me love and compassion during my darkest days. They have helped me to understand the true meaning of friendship and trust, without which I would not be here.

I would also like to thank K.P. Smith, who began this journey with me in 2010. While he has since moved on to become a wildly successful scientist, he is still an endless source of support, compassion, and honesty. At this point in my life, K.P. is family. His patience, drive for success, and genuine nature have helped shape me into the scientist and person I am today. I am incredibly thankful for his on-going friendship.

It is truly difficult to put into words the extent to which I need to thank my family. My parents, Melissa and Vito Foderaro, have been unwavering in their support throughout my life. From the attendance of early morning swim meets to late night trips to the lab, they have always been there. Their patience, love, and endless encouragement will never leave me. I also have to thank my brother, Anthony. We have been through so much together and I am thankful each and everyday that he is a part of my life. His persistence and continued desire for personal growth have helped me to develop into the person I am today. This dissertation would not have been a possibility without the love and support of one last family member, Roland Jean. He was the light of my life and the greatest person I have ever known. He taught me more than I can express about being an honest, compassionate, and diligent person. This is for you, Grandpa. I did it!

TABLE OF CONTENTS

CITATIONS	ii
ACKNOWLEDGEMENTS	iii
LIST OF TABLES	viii
LIST OF FIGURES	ix
CHAPTER 1: LITERATURE REVIEW	1
1.1 Introduction to <i>Toxoplasma gondii</i>	1
1.1.1 The phylum Apicomplexa	1
1.1.2 <i>Toxoplasma gondii</i> and toxoplasmosis in humans	2
1.1.3 Current treatments and limitations.....	5
1.1.4 The model Apicomplexan parasite	6
1.2 <i>T. gondii</i> drug development.....	8
1.2.1 Target- and phenotype-based compound screening	8
1.2.2 SAR studies	12
1.2.3 Mechanisms for Target Identification	14
1.3 Yeast three-hybrid	17
1.3.1 Applications.....	17
1.3.2 CID Development.....	21
1.3.3 False negatives and positives.....	23
CHAPTER 2: SMALL-MOLECULE SCREEN AND STRUCTURE ACTIVITY RELATIONSHIPS IDENTIFIES 2,4 DIAMINOQUINAZOLINE AS INHIBITOR OF T. GONDII AND C. PARVUM	31
2.1 Introduction	31
2.2 Materials and Methods	33
2.2.1 Host cell and parasite culture.....	33
2.2.2 YFP-based growth assay.....	34
2.2.3 MMV Malaria box screening.....	35
2.2.4 ATPase assay	35

2.2.5 Replication assay	36
2.2.6 Invasion assay	37
2.2.7 Two-Dimensional trail assay	37
2.2.8 Construction of pGADCDC48Ap and pGADCDC48Cy	38
2.2.9 CID competition assay.....	39
2.2.10 Targeted yeast three-hybrid liquid assay	40
2.3 Results	41
2.3.1 MMV box screen identifies 79 inhibitors of <i>T. gondii</i> growth.....	41
2.3.2 MMV006169 inhibits <i>T. gondii</i> invasion, but not motility	42
2.3.3 MMV006169 inhibits <i>T. gondii</i> replication.....	43
2.3.4 Structure activity relationship analyses	43
2.3.5 CDC48 does not interact with Mtx-MMV006169.....	46
2.4 Discussion.....	48
CHAPTER 3: APPROACHES TO IDENTIFYING THE TARGET(S) OF MMV006169	81
3.1 Introduction	81
3.2 Materials and Methods	83
3.2.1 Parasite culture.....	83
3.2.2 N-ethyl-N-nitrosourea titration and plaque assay	83
3.2.3 ENU mutagenesis	84
3.2.4 Compound-induced cyst staining	84
3.2.5 YFP-based growth assay.....	85
3.2.6 cDNA library preparation and negative selection	86
3.2.7 Titering 3-Amino-1, 2, 4-triazole (3-AT) for library screens.....	87
3.2.8 Yeast three-hybrid library screens	88
3.2.9 Yeast three-hybrid reporter confirmation	88
3.2.10 Construction of pGADNDH2-1 and pGADNDH2-2	89
3.2.11 Targeted yeast three-hybrid liquid assay	90

3.3 Results	91
3.3.1 Isolation of MMV006169 resistant mutants	91
3.3.2 Yeast three-hybrid system optimization	92
3.3.3 A host cell target for MMV006169	94
3.4 Discussion.....	95
CHAPTER 4: DISCUSSION AND FUTURE DIRECTIONS.....	108
COMPREHENSIVE BIBIOLOGRAPHY	117
APPENDIX A: ANALYSIS OF THE REPLICATION INHIBITOR MMV403679	128
APPENDIX B: ATTEMPTS TO IDENTIFY THE TARGET(S) OF QQ-437.....	137
APPENDIX C: SCREENING A SUBSET OF THE NIH CLINICAL COLLECTION	142
APPENDIX D: TARGETED YEAST THREE-HYBRID FOR INTERACTION BETWEEN 118793 AND EG5	144
APPENDIX E: GENERATING THE TgUNC ANTIBODY AND DEFINING CELLULAR LOCALIZATION	146
APPENDIX F: DRUG AFFINITY RESPONSIVE TARGET STABILITY AS AN APPROACH TO TARGET IDENTIFICATION	158
APPENDIX G: DETERMING IF TgBRADIN CAN INTERACT WITH p38 α MAP KINASE.....	162
APPENDIX H: USING 3-DIMENSIONAL MOTILITY ASSAYS TO EXAMINE THE ROLE OF CALCIUM IN <i>T. GONDII</i> MOVEMENT	166

LIST OF TABLES

Chapter 2 – Table 1: Summary of MMV box hits against <i>T. gondii</i>	54
Chapter 2 – Table 2: Subset of MMV Malaria box molecules of interest.....	56
Chapter 2 – Table 3: MMV006169 structural analogs	57
Chapter 2 – Table 4: SAR for phenotypic separation.....	68
Chapter 2 – Table 5: Primers for cloning <i>T. gondii</i> CDC48Ap and CDC48Cy	69
Chapter 3 – Table 1: IC ₅₀ values for MMV006169 resistant parasite clones	100
Chapter 3 – Table 2: Titering 3-AT	101
Chapter 3 – Table 3: Primers for cloning <i>T. gondii</i> NDH2-1 and NDH2-2	102
Appendix A – Table 1: MMV403679 structural analogs	129
Appendix B – Table 1: QQ-437 structural analogs	138
Appendix C – Table 1: Efficacy of NIH Clinical Collection compounds on <i>T. gondii</i> growth.	143

LIST OF FIGURES

Chapter 1 – Figure 1: Life cycle of <i>T. gondii</i>	26
Chapter 1 – Figure 2: Lytic cycle of <i>T. gondii</i>	27
Chapter 1 – Figure 3: Schematic of yeast three-hybrid system	28
Chapter 1 – Figure 4: A modular approach to CID Synthesis	29
Chapter 1 – Figure 5: 5-FOA-based negative selection strategy	30
Chapter 2 – Figure 1: Effect of MMV006169 on <i>T. gondii</i> growth kinetics	70
Chapter 2 – Figure 2: MMV006169 is not toxic to HFFs	71
Chapter 2 – Figure 3: MMV006169 inhibits <i>T. gondii</i> invasion and replication, not motility.....	72
Chapter 2 – Figure 4: MMV006169 analogs are not toxic to host cells after 24 hours.....	73
Chapter 2 – Figure 5: Effect of MMV006169 structural analogs on replication.....	74
Chapter 2 – Figure 6: Effect of MMV006169 structural analogs on <i>T. gondii</i> invasion.....	75
Chapter 2 – Figure 7: MMV006169 structural analogs cannot initiate replication	76
Chapter 2 – Figure 8: Targeted yeast three-hybrid and structure of Mtx-MMV006169	77
Chapter 2 – Figure 9: CID Competition Assay with Mtx-MMV006169.....	78
Chapter 2 – Figure 10: Targeted yeast three-hybrid liquid growth assay suggests MMV006169 does not interact with CDC48Ap.....	79
Chapter 2 – Figure 11: Targeted yeast three-hybrid liquid growth assay suggests MMV006169 does not interact with CDC48Cy.....	80
Chapter 3 – Figure 1: Titration of ENU.....	103
Chapter 3 – Figure 2: MMV006169 resistant clone forms cysts after compound treatment	104
Chapter 3 – Figure 3: Clone 14 interacts with Mtx-MMV006169.....	105
Chapter 3 – Figure 4: MMV006169 analog toxicity after 8 days.....	106
Chapter 3 – Figure 5: MMV006169 does not interact with TgNDHs by yeast three-hybrid	107
Appendix A – Figure 1: MMV403679 is not toxic to human foreskin fibroblasts.....	135
Appendix A – Figure 2: MMV403679 inhibits <i>T. gondii</i> replication.....	136
Appendix B – Figure 1: Structures of QQ-437-based CIDs	140

Appendix B – Figure 2: Targeted yeast three-hybrid suggests QQ-437 does not interact with AP3B.....	141
Appendix D – Figure 1: Targeted yeast three-hybrid suggests Eg5 does not interact with 118793.	145
Appendix E – Figure 1: Subcellular localization of TgUNC.....	150
Appendix E – Figure 2: IPTG Induction of TgUNC UCS domain expression.	151
Appendix E – Figure 3: Screening pre-bleed samples against RH lysate.....	152
Appendix E – Figure 4: Immunofluorescence with pre-bleeds against <i>T. gondii</i>	153
Appendix E – Figure 5: Western blot against <i>T. gondii</i> lysates using UVT149 and UVT150	154
Appendix E – Figure 6: Immunofluorescence of UCS3xMYCCln1 parasites using UVT149 and UVT150	155
Appendix E – Figure 7: Western blot against recombinantly expressed TgUNC (full-length and truncations) using UVT150.....	156
Appendix E – Figure 8: Inducible knock-out of TgUNC results in loss of TgMyoA	157
Appendix F – Figure 1: Schematic of DARTS mechanism.....	160
Appendix F – Figure 2: DARTS using TgMLC1 and TachypleginA	161
Appendix G – Figure 1: Hypothesized role of p38 α MAPK in yeast three-hybrid complex.....	164
Appendix G – Figure 2: p38 α MAPK is not present in yeast three-hybrid complex	165
Appendix H – Figure 1: Increases in calcium precede increases in velocity along parasite trajectories	168
Appendix H – Figure 2: Oscillations in intracellular parasite calcium levels during motility.....	169

CHAPTER 1: LITERATURE REVIEW

1.1 Introduction to *Toxoplasma gondii*

1.1.1 The phylum Apicomplexa

The phylum Apicomplexa is diverse, containing 6,000 known and likely more than one million unstudied obligate intracellular protozoans (Adl et al. 2007). These organisms are so successful that every vertebrate and invertebrate is parasitized by at least one species belonging to this phylum (Portman and Slapeta 2014). Apicomplexans are known for their unique invasive stages, which involve an apical complex of secretory organelles and cytoskeletal elements (Morrison 2009). This complex is used to aid in the entry of host cells, which is essential for at least one stage of each organism's life cycle.

The phylum contains a variety of important veterinary pathogens, all of which have adopted a parasitic life-style. *Neospora caninum* has a broad host range; however, it causes significant economical loss in the cattle industry as infection results in spontaneous abortion of calves. Treatment of neosporosis is limited by the ability to detect infection in animals (Dubey et al. 2007). *Babesia* spp. cause babesiosis, which also affects the cattle industry, but can impact humans and other domestic animals as well. Recently, efforts to develop treatments for babesiosis have suggested areas for drug targeting, but no successful treatments have resulted (Mosqueda et al. 2012).

Apicomplexans are also an important medical concern for humans. Arguably, the most notorious of the Apicomplexan parasites are *Plasmodium* spp., which cause malaria. Between 2000 and 2015, the World Health Organization estimates that of the 218 million

people infected by *Plasmodium* spp., 438,000 lives were lost each year (W.H.O. 2015). This is due to the continual ability of the parasite to develop resistance to anti-malarial drugs. *Cryptosporidium* spp. cause the diarrheal disease cryptosporidiosis. Diarrheal disease is one of the leading causes of death amongst children under the age of 5, killing 800,000 children annually (Bhutta and Black 2013). Despite its clinical importance, the drugs available for the treatment of cryptosporidiosis are minimal due to wide efficacy ranges in patients (Manjunatha et al. 2016). As a theme, despite the broad host range and worldwide prevalence of Apicomplexans, minimal therapeutics are available to treat the infections they cause.

1.1.2 *Toxoplasma gondii* and toxoplasmosis in humans

Toxoplasma gondii infects nearly 30% of the United States population, and up to 80% of the population in some parts of the world, causing a condition termed toxoplasmosis (Dubey 1994, Remington et al. 1995, Pappas et al. 2009). The life cycle of *T. gondii* has both sexual and asexual phases and involves three infectious forms of the organism: sporozoites, tachyzoites, and bradyzoites (Chapter 1 – Figure 1). The sexual phase takes place in the definitive host, which can be any domestic or wild feline (Tenter et al. 2000). Oocysts containing sporozoites form within the intestines and are shed in feline feces. Humans and other intermediate hosts ingest these oocysts, which then transform into tachyzoites (Speer et al. 1995). Tachyzoites, the fast replicating asexual form of the parasite, are responsible for the lytic cycle (Chapter 1 – Figure 2). The lytic cycle begins when a tachyzoite invades a host cell. *T. gondii* has a broad host-range and

is capable of invading any nucleated mammalian cell (Black and Boothroyd 2000). The parasite replicates via endodyogeny within a newly formed parasitophorous vacuole. Once the host cell is filled with tachyzoites, the parasites secrete perforin-like protein 1 (TgPLP1), and egress from the host cell (Kafsack et al. 2009). These newly egressed tachyzoites then disseminate and invade new host cells. It is the repeated cycling of host cell lysis via invasion, replication, and egress that cause noticeable symptoms in humans.

When the tachyzoite senses stress, such as assault by immune cells or lack of nutrients, the parasite will undergo a stage conversion to form the bradyzoite. The bradyzoite is the slow-replicating asexual form of the parasite. During stage conversion, the parasitophorous vacuole is modified to form a cyst wall and matrix within which the bradyzoite resides (Weiss and Kim 2000). The resulting tissue cysts are commonly found in the brain, heart, skeletal muscle, and retina of the host. Within these cysts, the parasite can lay dormant until the host immune system becomes impaired. At this point the bradyzoites convert back to tachyzoites and the lytic cycle begins again.

Toxoplasmosis can manifest in a variety of ways depending on the immune state of the host. The immunocompetent host typically experiences either no symptoms at all, or mild flu-like symptoms that are self-limiting and resolve within a few weeks. In the immunocompromised individual, toxoplasmosis typically manifests as toxoplasmic encephalitis (TE) or ocular toxoplasmosis. Toxoplasmic encephalitis (TE) is commonly caused by the reactivation of a chronic *T. gondii* infection that manifests as hemisensory loss, visual field defects, headache, weakness, disorientation, seizures, coma, and death (Luft and Remington 1992). TE is of particular importance in AIDS patients as it is often

diagnosed before the patient knows of their HIV-status (Porter and Sande 1992). As such, it is the most common infection of the central nervous system for those not receiving appropriate anti-retrovirals (Walker and Zunt 2005). Ocular toxoplasmosis results from the mass infection of the eye tissue and immune cells, resulting in necrosis and retinal pigment epithelial cells migrating to, entering the eye, and aiding in phagocytosis (Jones et al. 2006). In the United States, ocular toxoplasmosis is considered the most common infection of the retina (Jones and Holland 2010). Congenital toxoplasmosis has severe effects on neonates, including spontaneous abortion, retinochoroiditis, and cerebral calcifications (Dubey and Jones 2008).

In humans, transmission of infection can take place through carnivorousism, a fecal-oral route, or congenitally. In 1965, it was shown that the consumption of undercooked meat containing tissue cysts resulted in increased levels of *T. gondii* seropositivity in a population of children. The connection between infection and carnivorousism was later confirmed epidemiologically by looking at seropositivity in areas known for consumption of raw meat. It was shown that 80% of the adult population tested in Paris was positive for *T. gondii* specific antibodies (Dubey 2014). The fecal-oral route of infection occurs when humans ingest *T. gondii* oocysts from cat feces. This route has been confirmed through experimentation on mice (Dubey et al. 1997). Congenital transmission occurs when a pregnant woman becomes infected with *T. gondii*. During pregnancy, the parasite can pass the placental barrier and infect the fetus. The first record of a *T. gondii*-like infection in humans was reported in 1923 in a child born with

hydrocephalus (Dubey 2014). The child became blind within three months and died at 11 months.

1.1.3 Current treatments and limitations

Despite its prevalence, there are minimal therapeutics available for use in the treatment of toxoplasmosis due to specificity of drugs for specific forms and life-cycle stages of the parasite as well as high levels of relapse and serious side effects that result in the therapeutics' discontinuation (Tomavo and Boothroyd 1995). The most common treatment for infection is a cocktail of pyrimethamine, sulfadiazine, and folinic acid (Derouin and Santillana-Hayat 2000). Pyrimethamine is an inhibitor of dihydrofolate reductase. While it demonstrates strong anti-*Toxoplasma* activity, it is associated with bone marrow suppression and is potentially teratogenic (van der Ven et al. 1996, Montoya and Remington 2008). To avoid the issue of bone marrow suppression, small quantities of folinic acid are added to the cocktail. Folinic acid can be used to generate purines and pyrimidines when dihydrofolate reductase is inhibited. However, the addition of folinic acid has only been marginally successful, as many patients still suffer from marrow suppression (Hakes and Armstrong 1983).

Sulfadiazine works in synergy with pyrimethamine by inhibiting dihydropteroate synthase in the same pathway, and is also associated with side effects; sixty percent of HIV-patients develop a rash and fever upon sulfadiazine treatment (Porter and Sande 1992, van der Ven et al. 1996). It should also be noted that some anti-retrovirals, such as Zidovudine, reverse the effects of both pyrimethamine and sulfadiazine (Israelski et al.

1989). For patients who are unable to tolerate sulfa drugs, sulfadiazine can be replaced with clindamycin or azithromycin (Montoya and Liesenfeld 2004, Andrews et al. 2014). Women that become infected with *T. gondii* while pregnant are prescribed a course of spiramycin, which has been shown to reduce transmission to the fetus by 60% (Montoya and Remington 2008). If congenital transmission has already occurred, the standard course of pyrimethamine and sulfadiazine must be administered, as spiramycin cannot pass the placental barrier (Montoya and Remington 2008). These present therapeutics are insufficient for control of toxoplasmosis not only based on the detrimental side effects, but also because they are ineffective against the dormant form of the parasite, the bradyzoite.

1.1.4 The model Apicomplexan parasite

Like other Apicomplexan parasites, *T. gondii* is a single-celled pathogen that requires a host cell for survival. *T. gondii* is the model organism for its phylum. The asexual, pathogenic form of the parasite can be easily maintained by continuous culture through a variety of cell lines, such as human foreskin fibroblasts, hTERT, and HeLa cells. Parasites can also be preserved indefinitely in liquid nitrogen using DMSO as a cryoprotectant (Roos et al. 1994). Methods for continuous culture of other Apicomplexans, such as *Cryptosporidium* spp. are not available, which in turn limits the ability to genetically manipulate these organisms. Efficient means of preserving *Cryptosporidium* are also lacking, meaning that fresh oocysts must be isolated regularly from animal feces and then prepared for experimental procedures (Gut and Nelson 1999).

Animal models for the study of *T. gondii* infection are plentiful, relevant, and used for the study of cerebral, ocular, and congenital toxoplasmosis. The mouse model alone has been used to study acute infection, toxoplasmic encephalitis, and retinochoroiditis (Dubey 1997, Dubey et al. 1997, Subauste 2012). Other successfully utilized animal models include: rat, rabbit, hamster, guinea pig, and primate (Luder et al. 2014). *Plasmodium* spp. can be studied in mouse and non-human primate models; however, speculation exists as to how relevant these models are (Langhorne et al. 2011). For example, in cerebral malaria, it is infected leukocytes that accumulate in the brain of mice, and not red blood cells as seen in human infection (Carvalho 2010). Additionally, mechanisms for controlling infection in animal models of malaria do not always translate to control of human infections (Carvalho 2010).

The genome of *T. gondii* has been sequenced and is readily accessible (<http://toxodb.org/toxo>) along with community annotation, gene expression data, ESTs, and proteomics data (Gajria et al. 2008). Diverse approaches to genetic manipulation have been developed in the last decade that aid in understanding the complex life cycle of *T. gondii*. The development of $\Delta ku80$ parasite lines, which prevent non-homologous end joining, have made the generation of tagged proteins, gene deletions, promoter swapping, and allelic replacements more straight-forward (Fox et al. 2009, Huynh and Carruthers 2009, Sheiner et al. 2011). The recent use of CRISPR technology for genetic manipulation of *T. gondii* has dramatically decreased the time needed to clone complex parasite lines and has been used genome-wide to define essential vs. nonessential genes (Shen et al. 2014, Sidik et al. 2014, Sidik et al. 2016). Historically, genes have been

considered essential only after efforts toward generating a clean deletion have failed. Now armed with data from a genome-wide CRISPR screen, researchers can move directly towards the generation of parasites with inducible down-regulation or deletion of essential genes (Mital et al. 2005, Andenmatten et al. 2012). Taken together, the ability to continuously culture and preserve parasites, relevant animal models, and abundant genetic tools make *T. gondii* the model Apicomplexan parasite.

1.2 *T. gondii* drug development

1.2.1 Target- and phenotype-based compound screening

Small molecule screening is commonly used to discover lead compounds for drug development, but it can also be a powerful way to identify chemical probes for studying biological mechanisms. A more comprehensive understanding of the mechanisms of infection utilized by *T. gondii* will lead to the generation of drugs with minimal off-target effects. Historically, small-molecule screens have taken either a target- or phenotype-based approach. Target-based approaches involve the identification of molecules that alter the activity of a specific protein target *in vitro*. This approach comes with the advantage of having defined assays for use in screening molecules of interest and for confirming putative targets. Knowledge of the target of a compound can also guide in the development of meaningful structure activity relationship analyses and toxicology studies (Zheng et al. 2013). Disadvantages of this approach involve lack of efficacy of compounds *in vivo*. Screening assays are not always biologically relevant as the molecule of interest may not be able to access the particular protein of interest. This approach is

also limited by our inability to predict mechanisms of biological compensation. When the goal is drug development, target-based approaches can be limiting as potential chemical diversity is lost upfront and the ability to discover new targets along the way is reduced.

Phenotype-based approaches are used to identify molecules that induce a desired effect (phenotype) on an entire cell or organism (Kotz 2012). Advantages associated with these approaches include knowing that the molecule can enter the cell of interest, the screening methodology is biologically relevant, and multiple targets can be modulated at once to create a synergistic effect resulting in a desired phenotype. As mentioned above, when drug development is a goal, phenotype-based approaches can be associated with broad chemical diversity that is not limited to interaction with a specific target. As such, this allows for the identification of new/multiple targets throughout the process. However, this means that target deconvolution can be more arduous as multiple genes must be examined at once. SAR is also more difficult to develop as metabolism and cell-permeability must be constant considerations (Khurana et al. 2015). The differences between target- and phenotype-based approaches can be likened to reverse and forward genetics respectively. In a reverse genetics approach the goal is to identify a phenotype associated with a gene disruption, whereas in forward genetics screens one identifies a gene responsible for a specific phenotype.

Both target- and phenotype-based screens have been used to study *T. gondii*. In 2010, it was shown that bumped kinase inhibitors (BKIs) can inhibit TgCDPK1 (Murphy et al. 2010, Ojo et al. 2010). Using structural and sequence-based analysis of the ATP-binding site of mammalian kinases versus TgCPDK1, it was found that TgCDPK1 has a

unique glycine gate-keeper residue in its active site. Three novel BKIs were synthesized to improve the specificity of compound binding. Two of these BKIs (NA-PP2, and NM-PP1) were specific, potent inhibitors of TgCDPK1 as determined by a radiometric scintillation assay, an ATP consumption assay, and co-crystallization.

In 2011, a Hybrid Structure Based method was used to identify small molecules capable of disrupting the interaction between Myosin A (TgMyoA) and Myosin Light Chain-1 (TgMLC1) (Kortagere et al. 2011). The approach involved structural modeling of the TgMyoA-TgMLC1 interaction, custom design of a pharmacophore that could disrupt this interaction, computational compound library screening, and identification of the compounds that best match the designed pharmacophore. The identified compounds were then screened against *T. gondii* for defects in invasion, and one compound was chosen as a potential lead for drug development. At this point, no new drugs have resulted from either study.

While the aforementioned target-based approaches for isolation of lead compounds was useful to better aid in the understanding of general parasite biology, the majority of small-molecule screens against *T. gondii* are phenotype-based. These small-molecule screens have been completed using diverse compound libraries containing varied classes of compounds or targeted libraries containing only specific types of compounds. Complete compound libraries screened against *T. gondii* have been examined to identify inhibitors of invasion. Carey et al. screened 12,160 molecules and identified 24 inhibitors and 6 enhancers of invasion (Carey et al. 2004). In addition to invasion, these compounds were found to have varying effects on microneme secretion, conoid extension, and

motility. One compound from this screen, tachypleginA, was shown to target TgMLC1 by formation of an adduct on C58, which decreases the parasites myosin motor activity (Heaslip et al. 2010, Leung et al. 2014). This compound, however, does have additional targets and was shown to have cytotoxic effects after 24 hours. The second study looking for compounds impacting parasite invasion identified WRR-086 (Hall et al. 2011). WRR-086 modifies C127 in the gene encoding DJ-1. This mutation results in the inability of the parasite to attach to host cells and successfully invade. While both of these screens helped to better understand parasite invasion and other associated processes, no successful drugs have been developed as a result of these studies.

Kamau et al. screened a targeted library of 527 kinase inhibitors for an effect on *T. gondii* growth (Kamau et al. 2012). Fourteen different compounds were identified as altering (increasing or decreasing) parasite growth kinetics and having varying effects on motility and parasite morphology. To date, the targets of these compounds in the parasite are unknown. Recently, a drug-repurposing screen was performed using the Tocriscreen Total Library of compounds (1,120), which identified tamoxifen and pimozide as potential anti-*T. gondii* drugs (Dittmar et al. 2016). While drug repurposing has the potential to quickly identify new therapeutics, the authors acknowledge that target confirmation is necessary, since off-target effects may be playing a role in parasite inhibition. It should now be apparent that simply identifying a compound of interest is not enough to lead to the development of a successful drug. The process requires compound optimization and a straightforward approach to target identification.

1.2.2 SAR studies

Both target- and phenotype-based approaches to drug development require extensive compound optimization based on the ligand of choice through a process termed structure-activity relationship (SAR) analyses. SAR analyses can be used to reveal how biological processes are related to chemical structures. In one sense, they can be used to improve small molecules of interest by strategically adding and removing portions of a compound to increase its affinity for a single protein target. In cell culture, one is working with a homogenous system of a single cell type where a drug may only bind to one specific target. Once administered to an intact organism, the potential for secondary and tertiary targets becomes possible. For example, in *T. gondii*, Compound 2 is an anti-parasitic compound effective against multiple targets, including TgCDPK1, TgPKG, and TgCK1 α (Donald et al. 2006). Recently, it was shown that this compound has a fourth target; TgBRADIN (Odell et al. 2015). To prevent compound promiscuity, SAR can identify structural analogs with increased compound specificity. For example, the 5-aminopyrazole-4-carboxamide chemical scaffold has been shown to be an effective inhibitor of TgCDPK1. The C-3 substitution of a 2-cyclopropoxy group on this chemical scaffold resulted in a compound with increased solubility and potency against TgCDPK1 (0.22 μ M to 0.089 μ M), and was able to better eliminate *T. gondii* from the brain, spleen, and peritoneal fluid (Huang et al. 2015). SAR was also used to determine novel substrates of uracil phosphoribosyltransferase. The study screened 100 different analogs of uracil and identified 5 novel substrates with increased affinity for the enzyme (Iltzsch and Tankersley 1994).

In addition to identifying and increasing potency for protein-binding partners, SAR is pivotal in ensuring that small molecules can traverse necessary biological membranes and as such work the same way *in vivo* as they do *in vitro* (Lien 1981). A common limitation of drug development is getting the intact small molecule of interest within proximity of its intended target. A potent compound may appear to function perfectly *in vitro*, but fail when applied to an *in vivo* model. This lack of an effect may be due to the drug being degraded to a non-functional form by the pH or enzymes present in the gastrointestinal tract (Sousa et al. 2008). In addition to host enzymes that may degrade the drug to a useless product, a score of enzymes provided by the gut microflora may contribute to degradation. The microbiota mainly digest drugs via hydrolytic and reductive reactions that result in non-polar byproducts (Sousa et al. 2008). These byproducts themselves may be useless or, due to their non-polar nature, associate with fatty tissue and be sequestered from the bloodstream preventing delivery of the drug to its site of action (Qureshi 2010). In addition to storage in adipose tissue, degraded drug products can also be secreted through urine without ever being absorbed (Qureshi 2010). Altering a compound's lipophilicity can help to ensure it will reach an environment of interest. For example, if one wishes to design a drug that can pass biological membranes and find a receptor, the lipophilicity should be increased (Lien 1981). Conversely, if a one wishes to prevent a compound from passing the blood-brain barrier, the lipophilicity should be reduced (Lee 1991).

SAR is also useful in making small molecules of interest more “drug-like”. Lipinski's rule of five has been considered the standard when designing a membrane

permeable, easily absorbed drug. The rules include having a molecular weight less than 500 Daltons, a partition coefficient of less than 5 (see above discussion for optimizing lipophilicity), fewer than 5 hydrogen bond donors, and fewer than 10 hydrogen bond acceptors (Leeson 2012). By optimizing these qualities, SAR can make a compound easier to synthesize and alter its pharmacokinetic properties, such that the compound has an increased likelihood of working *in vivo*.

1.2.3 Mechanisms for Target Identification

Once a compound of interest has been selected and optimized, one must next identify the biologically relevant target(s) of the molecule to truly understand any phenotypes resulting from compound treatment. A variety of approaches for small-molecule target identification exist, both direct and indirect, each with its own set of limitations and advantages. Direct approaches to target identification look specifically at small molecule-target interactions, while indirect approaches look at protein or gene expression profiling, morphological changes, and sensitivity of the target to the drug to determine the target. The most common direct approach to target identification is through affinity chromatography. This technique involves the compound of interest being derivatized to a solid matrix. One successful use of this technique involved the derivatization of an analog of trapoxin, K-trap, to a resin matrix. Mammalian cell extract was run over the column, followed by washing, and two distinct compound interacting partners were identified (Taunton et al. 1996). In 1999, epoxomicin was derivatized to biotin at the amino terminus and incubated with cell lysate. The resulting

mixture was probed by western blot with streptavidin-horseradish peroxidase, and three catalytic components of the 20s proteasome were identified (Meng et al. 1999).

A phage display approach to target identification involves the biotinylation of the compound, its immobilization on a streptavidin coated plate, and screening of phage libraries. The libraries are panned across the plate and any interacting proteins remain on the plate after washing. The phage is then eluted, phagemid is isolated, and the gene encoding the target can be sequenced. This technique was successfully used to show that UQCRB is the target of terpestacin (Jung et al. 2010). Along similar lines, protein microarrays can be used to identify compound targets. Tagged versions of the compound are flowed over protein microarrays, washed to remove non-specific interactions, and the array imaged to determine where the tagged molecule resides. This approach was validated by showing direct biotin-streptavidin, anti-digoxigen antibody-digoxigen, and FKBP12-AP1497 binding (MacBeath and Schreiber 2000).

These direct techniques are limited by the inherent nature of the compound-target interaction. The interaction needs to be high affinity to survive the vigorous washing steps involved and/or the target needs to be abundant enough to be visualized on and isolated from a gel for follow-up identification (Burdine and Kodadek 2004). These approaches also require extensive SAR analyses to ensure the molecule is linked to the matrix/affinity-label in a manner that still allows it to interact with its unknown target.

Drug Affinity Responsive Target Stability (DARTS) is an indirect approach to target identification that does not rely on derivatization of the small molecule (Lomenick

et al. 2009, Pai et al. 2015). The technique relies on a small molecule stabilizing or protecting its target from proteolysis. In the proof of principle experiment, human Jurkat cells were exposed to didemnin B, a known inhibitor of EF-1 α , and thermolysin (Crews et al. 1994). Samples were run on SDS-PAGE gels, coomassie stained, and a single enriched band (didemnin B and thermolysin treated) was confirmed to be that of EF-1 α (Lomenick et al. 2009). This approach is useful in that it can be used in any cell or tissue type, is not enzyme specific, and has a simple readout. However, as with the aforementioned affinity-based approaches, DARTS is limited by the strength of the small molecule-target interaction.

Genomics-based approaches to target identification involve screening the expression level of genes in the presence and absence of a compound. Scherf et al. analyzed the expression levels of 8,000 genes in untreated human cancer cell lines and then treated those cancer cell lines with over 1,400 compounds of interest (Scherf et al. 2000). Correlations between compound treatments and changes in gene expression were then mapped, enabling target identification to be performed. An alternate approach is whole-genome mutagenesis, where one treats mutagenized cells with a compound of interest and selects for resistant organisms. This has proven useful in the study of *T. gondii* where the n-ethyl-n-nitrosourea (ENU) mutagenized genome of resistant parasites can then be sequenced and the relevant target confirmed (Pfefferkorn and Pfefferkorn 1979, Gubbels et al. 2008, Coleman and Gubbels 2012, Farrell et al. 2014). Metabolomics- and proteomics-based approaches are similar in that the data set is analyzed in the absence and presence of the drug, and changes in metabolite or protein

expression are noted for further hypothesis-driven work (Watkins et al. 2002, Plavec et al. 2004). Similar to the DARTS approach discussed above, Thermal Proteome Profiling (TPP) looks at the ability of a small molecule to stabilize, or prevent the denaturation of, a protein during heating (Savitski et al. 2014). TPP was validated by using human K562 chronic myeloid leukemia cells heated to different temperatures in the presence and absence of kinase inhibitors (staurosporine or GSK3182571). The resulting cellular supernatants are analyzed by SDS-PAGE and mass spectrometry to determine which proteins demonstrate a thermal shift and as such interact with the small molecule (Franken et al. 2015).

The aforementioned indirect approaches to target identification are advantageous in that they require no additional chemical derivations be performed on the molecule of interest. However, they are limited by the fact that they rarely identify a single target; rather they reveal only a focused area of cellular physiology in which the molecule is involved. This becomes further complicated when a compound is promiscuous and interacts with multiple targets. In most cases, these indirect approaches must then be followed by direct hypothesis-driven approaches.

1.3 Yeast three-hybrid

1.3.1 Applications

Genetically modified yeast can be used in an alternate approach to small-molecule target identification. The system was originally described as yeast two-hybrid, in which the *Saccharomyces cerevisiae* GAL4 transcription factor was split into two functional

domains, the DNA-binding domain (DBD) and activation domain (AD). The Gal4-DBD is incapable of activating transcription unless physically associated with an activation domain. The DBD was fused to SNF1, a serine-threonine-specific kinase, while the AD was fused to SNF4, a protein known to associate with SNF1, and is required for it to function maximally. The yeast genome was also engineered to encode *lacZ* under the control of the *GALI* (galactose inducible) promoter. Using yeast expressing both halves of the transcription factor, it was shown that when SNF1 and SNF4 associate, the transcription factor is reconstituted and can thus up-regulate the expression of the *lacZ* reporter gene by interacting with the upstream activating sequence (Fields and Song 1989). Based on this proof of principle experiment, it was suggested that any two proteins (a bait and prey) could be fused to either half of a split transcription factor and be used to demonstrate direct protein-protein interactions.

The yeast-two hybrid system was modified over time to include components from additional proteins such as the DBD of the *E. coli* repressor LexA, the AD from the “acid blob” protein B42, and the AD of the herpes virus protein VP16 (Triezenberg et al. 1988, Ruden et al. 1991, Golemis and Brent 1992, Gyuris et al. 1993, Vojtek et al. 1993). Together, the yeast two-hybrid system has been successful in the identification of direct protein-protein interactions for proteins as small as 8-10 amino acids and as large as 755 amino acids (Heery et al. 1997, Young 1998). The reporter genes used in yeast two-hybrid systems have been broadened beyond the use of *lacZ*. Common “primary reporters” include genes required for the synthesis of amino acids. The use of these synthetic genes makes it easy to measure reporter activation by plating yeast on selective

media. The most commonly used reporters include *LEU2* and *HIS3*, which are required for successful yeast growth on media lacking leucine and histidine respectively (Chien et al. 1991, Gyuris et al. 1993). Colorimetric reporters, such as *lacZ* and *MEL1* can be used as “secondary reporters” (Aho et al. 1997). Other variations to the yeast two-hybrid system include the fusion of entire cDNA libraries to the AD in place of a single protein, which allows for high-throughput screening for protein interacting partners.

The concept of including a linker molecule in the system led to the development of the yeast three-hybrid methodology (Chapter 1 – Figure 3). First implemented in 1996, the yeast three-hybrid was used to detect protein-RNA and protein-small molecule interactions (Licitra and Liu 1996, SenGupta et al. 1996). The system is fundamentally the same as the yeast two-hybrid, where the activation of a transcriptional reporter is dependent upon the functional assembly of a transcription factor. Instead of looking at the direct interaction of two fusion proteins, the system now depends upon the interaction of each end of a bivalent molecule with those fusion proteins. This bivalent molecule was named the chemical inducer of dimerization (CID) since it is necessary to dimerize proteins. Originally, a dexamethasone-FK506-based CID was used in conjunction with fusion proteins expressing the rat glucocorticoid receptor fused to the LexA-DBD and human FKBP12 fused to the B42-AD. Upon interaction of the CID with each fusion protein, the *lacZ* gene was activated and was detected using media containing 5-bromo-4-chloro-indolyl- β -D-galactopyranoside (Licitra and Liu 1996). The same CID was then used to determine if yeast three-hybrid could be used to identify receptors for a ligand. They screened a Jurkat cell cDNA library fused to the B42-AD for targets of FK506 and

isolated two variants of FKBP12, indicating that the system was capable of identifying known interacting partners of FK506. Yeast three-hybrid methodology has been used to identify a variety of compound-protein interactions, but it was not until 2002 that the use of a GAL4-based system was implemented (Henthorn et al. 2002). Since large number of GAL4-AD containing cDNA libraries are available, this allows for the screening of small molecules against a variety of organisms and tissue sources. Odell et al. reported the first use of the yeast three-hybrid methodology in the study of a pathogen in 2015. A CID was generated linking Compound 2, an imidazopyridine known to inhibit the *T. gondii* lytic cycle, to methotrexate. Using this CID and a *T. gondii* cDNA library, it was found that Compound 2 inhibits TgBRADIN (Odell et al. 2015).

An alternate approach to yeast three-hybrid was developed using a SNAP-tag system (Chidley et al. 2011). The CID is comprised of the small molecule of interest linked to an O6-benzylguanine (BG) derivative. This BG derivative can covalently bind to a SNAP-tagged DBD. This generates a stable anchor between the CID and DBD. Upon association of the target protein with the small molecule, reporter genes are expressed as previously described. Using this approach, eight different CIDs were generated containing methotrexate, dasatinib, purvanol b, erlotinib, atorvastatin, sulfasalazine, furosemide, and indomethacin. These CIDs were screened against different human cDNA libraries where both known and novel targets were identified. This approach is useful in that the same CID (BG linked to small molecule) can be coupled to glutathione S-transferase (GST). Affinity chromatography can be performed using glutathione sepharose beads in the presence and absence of GST-tagged CID exposed to cellular

lysate. The subsequent interacting/target protein can be eluted and identified by western blot or mass spectrometry.

1.3.2 CID Development

In order to perform a successful yeast three-hybrid screen, one must first obtain an optimally constructed CID. A typical CID contains a small molecule of interest, a linker unit, and a compound with a known binding partner (e.g., dexamethasone) (Chapter 1 - Figure 3). In an attempt to make the generation of CIDs more straightforward, systems were designed to work with commercially available components. The first successful CID generated from these components contained dexamethasone fused to methotrexate, which was successful in the dimerization of the glucocorticoid receptor with dihydrofolate reductase (DHFR) (Lin et al. 2000, Baker et al. 2003). A major consideration when synthesizing CIDs is how to derivatize each component into one molecule such that it still retains the ability to bind to its target. For example, one must be certain that methotrexate is properly attached to a small molecule of interest such that it can still interact with DHFR. Walton et al. performed extensive SAR studies on methotrexate and was able to identify a functional position for attachment to other molecules (Walton et al. 2009). Thorough SAR studies must also be performed to determine how to attach the small molecule of interest to the other end of the linker.

Another important property of CIDs is the length of the linker unit present between methotrexate and the small molecule of interest. Initially, it was believed that the chemical nature and length of CIDs had no impact on the ability to bridge proteins. This

was based on the use of three CIDs containing chemically distinct linker units of varying lengths. Each of these CIDs was capable of bridging FK506 with FKBP12 (Spencer et al. 1993). In the context of yeast three-hybrid, the impact of CID structure was first analyzed in 1997, when four FK1012-based CIDs with linkers of varying length and composition were compared with regards to reporter activation. It was determined that, while all the CIDs were functional, dramatic differences in potency exist, suggesting that linker length and composition is important for optimal transcriptional activation (Amara et al. 1997). In contrast, a similar study was performed with respect to *lacZ* transcriptional activation using four different dexamethasone-methotrexate CIDs. The linkers were all generated using similar chemistry and were comprised of varying length methylene subunits. While the shortest linker unit (3 methylene subunits) was incapable of activating transcription, the authors concluded that there was otherwise no correlation between CID size and transcriptional activation (Abida et al. 2002). Discrepancies between studies may be due to differences in affinity between CIDs and target proteins, steric hindrance created by the proteins, or the distance required between proteins for optimal binding (Tran et al. 2013).

CID development is also rate-limited by the number of synthetic steps necessary to achieve the desired chemical structure. It was reported that generation of a single CID containing a standard polyethylene glycol (PEG) linker took 21 synthetic steps, 7 of which were required only to generate the linker unit (Odell et al. 2015). In an attempt to streamline CID development, the concept of modular CID synthesis was proposed (Chapter 1 – Figure 4). This approach involves the coupling of methotrexate to an azide

and the small molecule of interest to an alkyne. Each of these components could be coupled to varying lengths of PEG linker and then attached via click chemistry to create a triazole containing CID (Chapter 1 – Figure 4) (Tran et al. 2013). This new approach has streamlined CID development, making it easier to develop families of CIDs simultaneously.

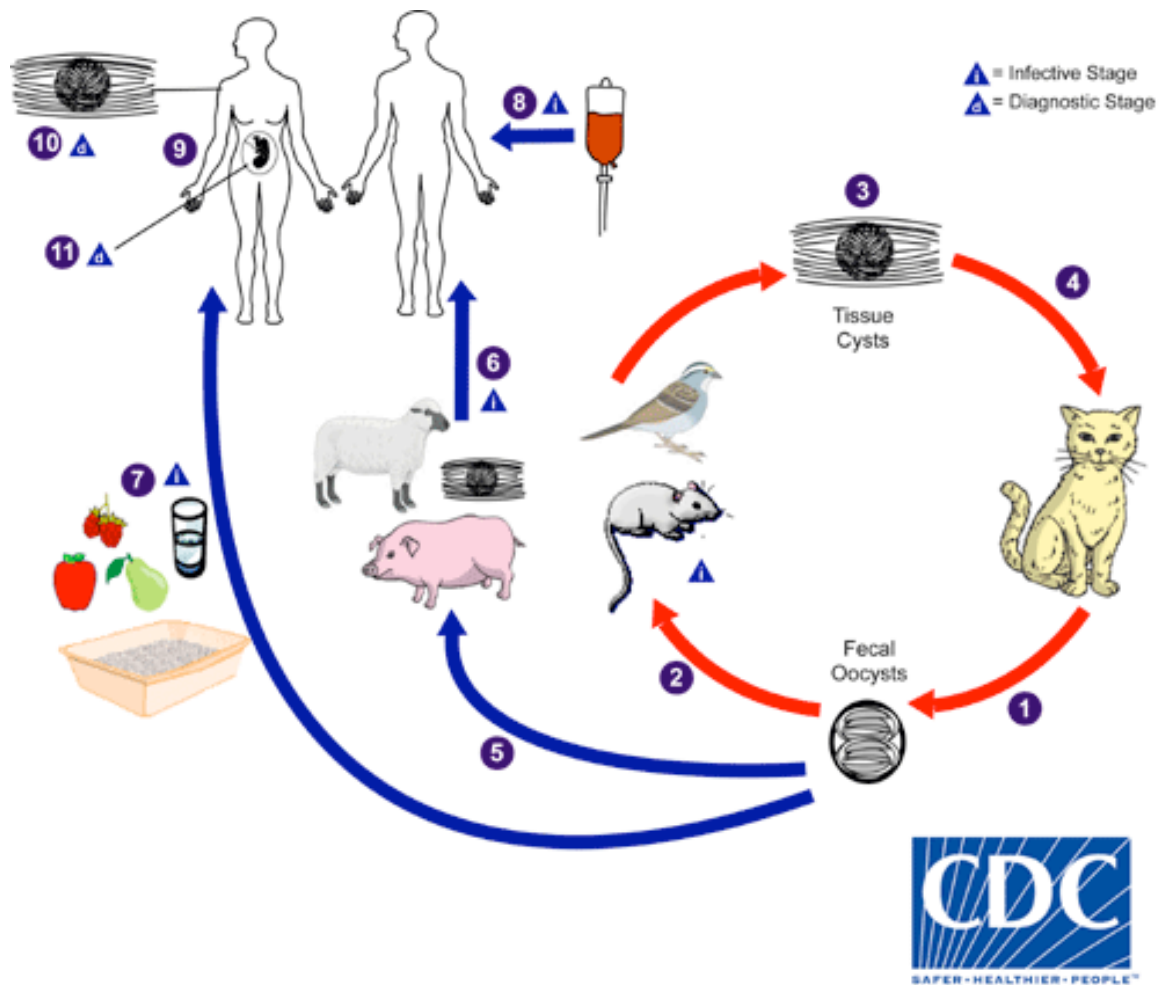
1.3.3 False negatives and positives

Yeast three-hybrid technology is limited by the presence of false negatives and positives in the system. A false negative is defined as a small molecule-protein interaction, which cannot be detected by the chosen screening method. These false negatives can be membrane bound proteins, which are not detectable in standard yeast three-hybrid experiments that require the target protein to be shuttled into the yeast nucleus. To avoid this issue, the yeast three-hybrid strategy must be chosen carefully to ensure that the desired proteome is being probed (Bruckner et al. 2009). Steric hindrance is a common cause of false negatives. Fusing a cDNA library or hypothesized protein target to a transcription factor may prevent the protein conformation needed to interact with the small molecule of interest. Troubleshooting can be done with hypothesized targets by swapping the half of the transcription factor fused to the bait with that of the prey or by fusing the transcription factor to the other terminus (e.g., fusing the transcription factor at the carboxy- instead of amino-terminus). Additionally, expressing these fusion proteins in yeast may result in changes in or the absence of necessary post-translational modifications to the target protein that prevent small molecule-protein

interactions from occurring as they would in the target organism. To avoid this issue, the transcription factor fusion proteins can be co-expressed in the presence of those enzymes needed for a given post-translational modification (Osborne et al. 1996). Lastly, an inherent issue in the reproducibility of library screens leads to a large number of false negatives. Yeast two-hybrid system experiments performed under identical conditions have been shown to be only 30% reproducible and identify only 12.5% of known targets (Ito et al. 2001). This means that a number of true positive interactions are often excluded based on the inability to repeat a given result.

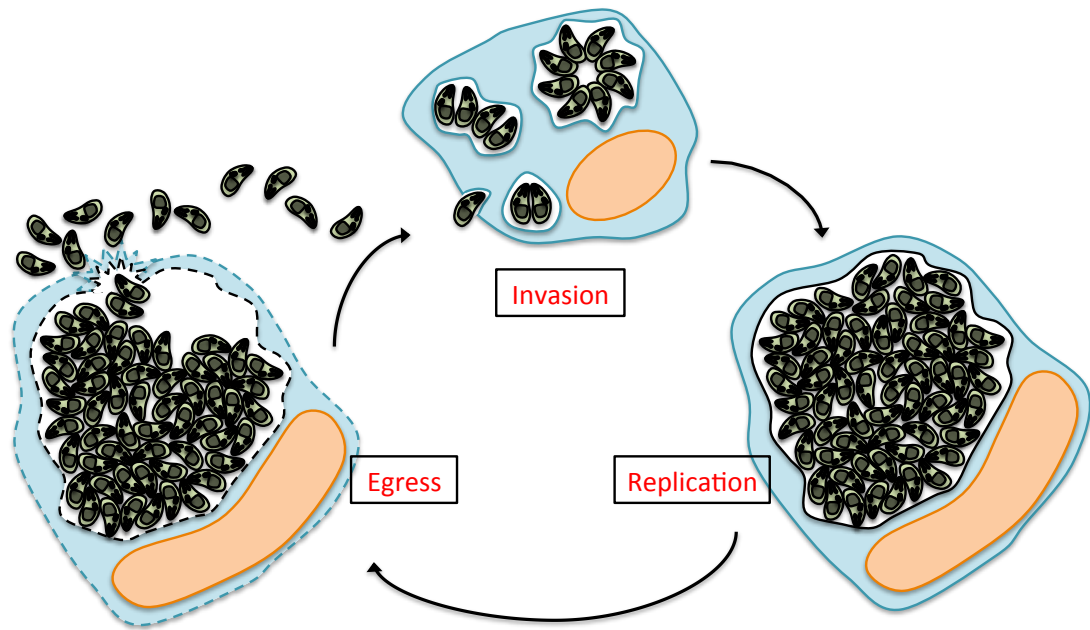
False positive results are obtained when the activation of reporter genes happens in the absence of a direct small molecule-target protein interaction. The fact that transcription factor fusion proteins are being overexpressed in a non-native environment (e.g., the yeast nucleus) can contribute to this problem. As a result, yeast proteins can interact with the small molecule and parts of the fusion protein resulting in reporter activation. Since these proteins are not found in the target organism, they are called false positives. Lastly, “sticky” or misfolded proteins can result in non-specific interactions with the bait and prey and result in reporter activation. One way to minimize the presence of false positives in yeast “n”-hybrid systems is to implement a negative selection step (Chapter 1 – Figure 5). This selection requires the presence of the *URA3* reporter gene under the control of an inducible promoter matching that of the other reporters used in the yeast “n”-hybrid screen. An aliquot of pre-transformed yeast (containing bait and prey) is plated on media containing 5-fluoroorotic acid (5-FOA). 5-FOA converts precursor molecules in the uracil biosynthetic pathway to a toxic product (5-FUMP). This means

that anything expressing *URA3* in the absence of a functional transcription factor will be killed. Yeast that survives this selection is pooled and used in conjunction with CID to perform full-scale library screens (Chidley et al. 2011). While this can significantly reduce the number of false positive interactions seen, it likely will not eliminate them all.



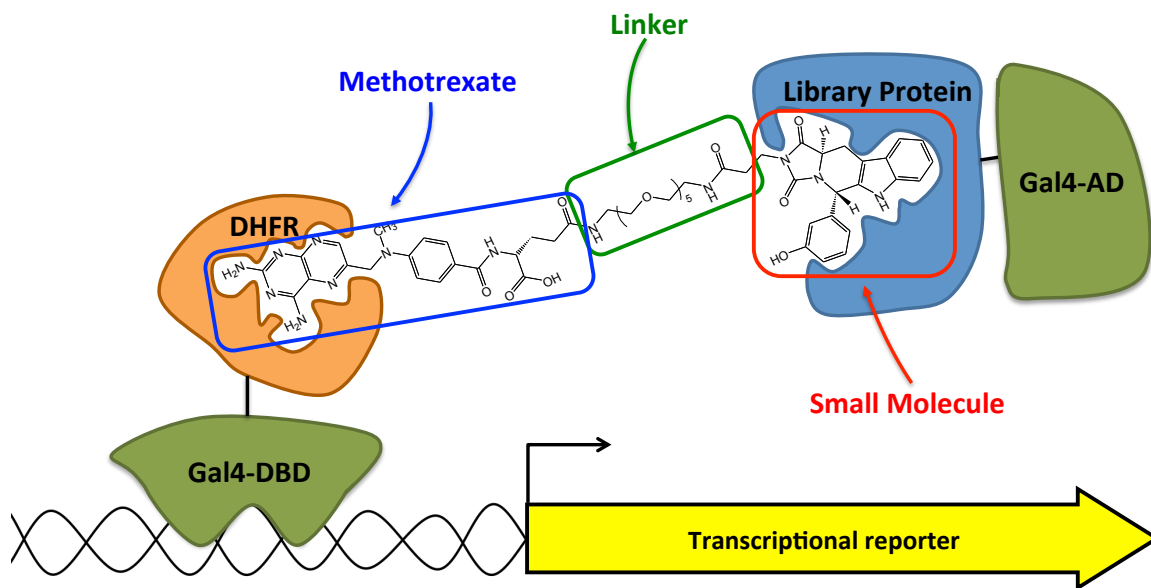
Chapter 1 – Figure 1: Life cycle of *T. gondii*

T. gondii oocysts shed in feline feces (1) are consumed by and encyst in intermediate hosts (2, 3, 5 and 6). Humans become infected through the consumption of tainted food or water (7), blood transfusions (8), changing kitty litter (7), or through consumption of undercooked meat containing tissue cysts (6). Once in the human, the parasite can infect neonates (9, 11) or become cysts in the brain and skeletal muscle (10). Image courtesy of the CDC; <http://www.cdc.gov/parasites/toxoplasmosis/biology.html>.



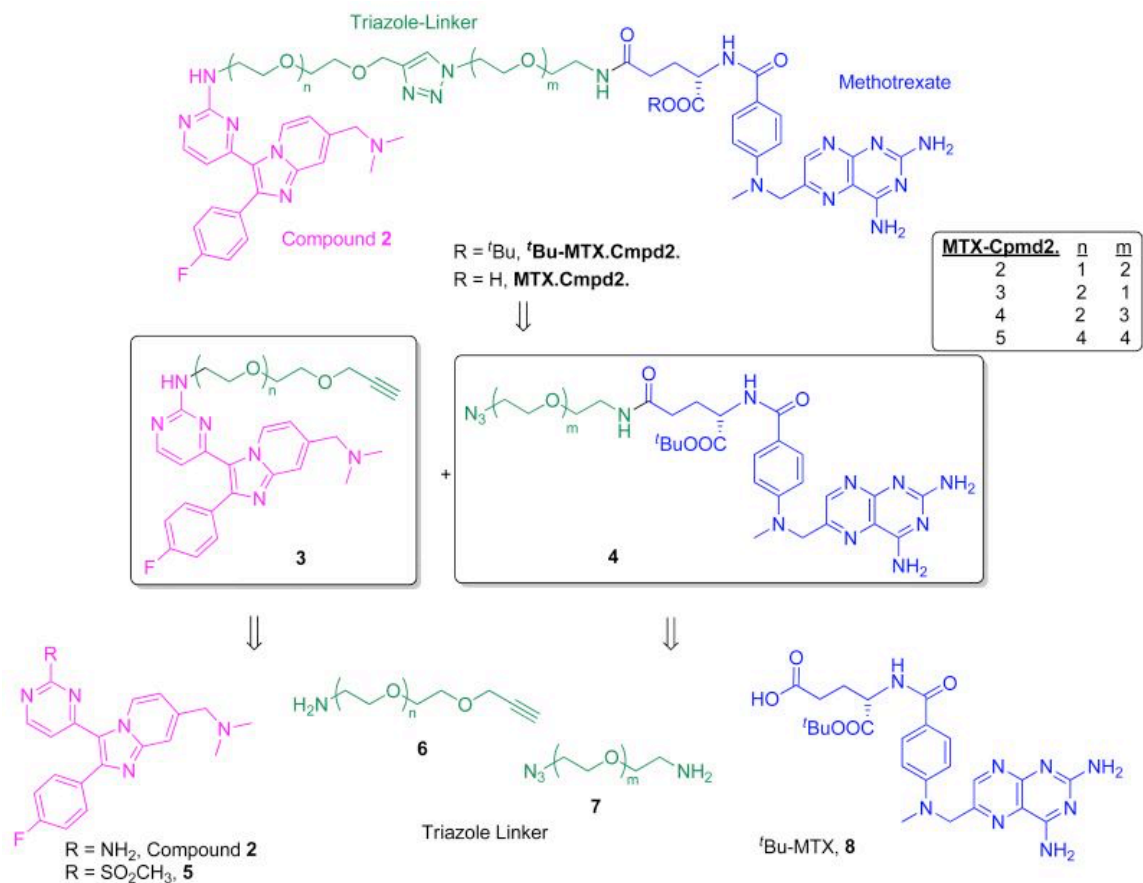
Chapter 1 – Figure 2: Lytic cycle of *T. gondii*

T. gondii tachyzoites form an intimate attachment with a host cell and invade through the formation of a moving junction. Within a parasitophorous vacuole, parasites replicate via endodyogeny. Parasites egress from the vacuole through a myosin-driven process coupled with perforin-like protein secretion.



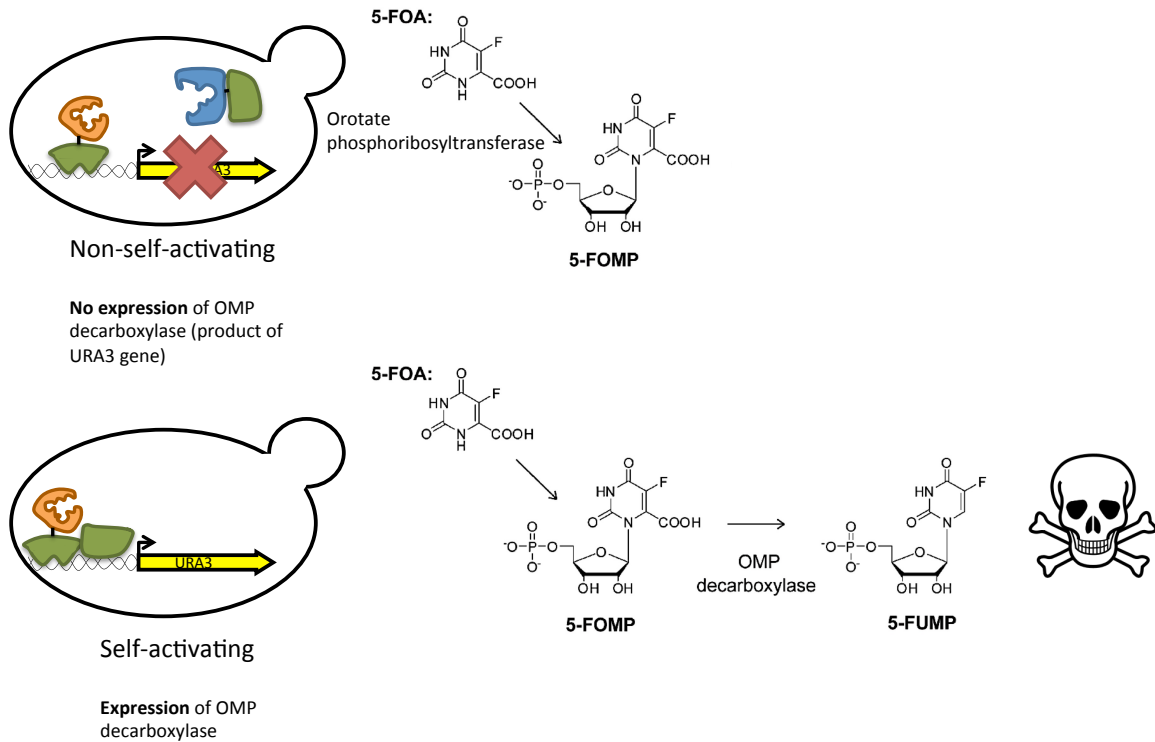
Chapter 1 – Figure 3: Schematic of yeast three-hybrid system

Yeast three-hybrid systems rely on the separation of a transcription factor into its DNA-binding (DBD) and activation (AD) domains. These domains are expressed as fusion proteins to DHFR and a cDNA library protein, respectively. Upon addition of a CID composed of methotrexate, a linker, and a small molecule of interest (above), the transcription factor will assemble and activate the expression of reporter genes.



Chapter 1 – Figure 4: A modular approach to CID Synthesis

Schematic of modular CID synthesis with compound of interest shown in pink, methotrexate in blue, and components of the linker shown in green. From (Tran et al. 2013). Copyright © 2013, Tran et al; licensee MDPI, Basel, Switzerland. Used under the terms of the Creative Commons Attribution license 3.0.



Chapter 1 – Figure 5: 5-FOA-based negative selection strategy

Non-self-activating clones do not activate the expression of URA3 (OMP decarboxylase). 5-FOA is metabolized to 5-FOMP, which is non-toxic, allowing yeast cell survival. Self-activating clones, which induce the expression of URA3, convert 5-FOA to toxic 5-FUMP, resulting in cell death. 5-FOA: 5-fluoroorotic acid; 5-FOMP: 5-fluoroorotidine monophosphate; 5-FUMP: 5-fluorouridine monophosphate. Adapted with permission from Macmillan Publishers Ltd: Nature Chemical Biology (Chidley et al. 2011), copyright © 2011.

**CHAPTER 2: SMALL-MOLECULE SCREEN AND STRUCTURE ACTIVITY
RELATIONSHIPS IDENTIFIES 2,4 DIAMINOQUINAZOLINE AS INHIBITOR
OF T. GONDII AND C. PARVUM**

[N.B. Some material from this chapter has been published in the following form:

Bessoff, K., T. Spangenberg, J. E. Foderaro, R. S. Jumani, G. E. Ward and C. D. Huston (2014). "Identification of Cryptosporidium parvum active chemical series by repurposing the open access malaria box." Antimicrob Agents Chemother 58(5): 2731-2739]

2.1 Introduction

Toxoplasma gondii, the causative agent of toxoplasmosis, is a highly infectious protozoan parasite infecting roughly 30% of the United States population and up to 80% of the population in some parts of the world (Dubey 1994, Remington et al. 1995, Pappas et al. 2009). *T. gondii* is a member of the phylum Apicomplexa, which contains many important human (e.g., *Plasmodium* and *Cryptosporidium* spp.) and veterinary (e.g., *Neospora* and *Babesia* spp.) protozoan pathogens. *T. gondii* has a multi-stage life cycle involving sexual reproduction in the definitive feline host, and asexual reproduction in a number of intermediate hosts. In the human host, an acute infection involves the fast replicating tachyzoite stage invading, replicating in, and egressing from host cells resulting in cell lysis. The host immune system controls these acute infections by forcing the parasite to differentiate into the slow replicating bradyzoite. As a result the infection

becomes chronic with bradyzoites forming tissue cysts, primarily in the brain, cardiac, and skeletal muscle.

As with other Apicomplexan parasites, there is a need for additional drugs to treat toxoplasmosis. Current therapeutics available for the treatment of *T. gondii* include a cocktail of pyrimethamine, sulfadiazine, and folinic acid (Derouin and Santillana-Hayat 2000). In some cases sulfadiazine can be replaced with clindamycin or azithromycin (Montoya and Liesenfeld 2004, Andrews et al. 2014). However, due to the high incidence of relapse and occurrence of side effects, these treatments often must be discontinued (Porter and Sande 1992, Tomavo and Boothroyd 1995, van der Ven et al. 1996). To date, no effective therapeutics are available for the treatment of chronic *T. gondii* infections. In order to develop better drugs against *T. gondii*, a deeper understanding of parasite biology is necessary.

The Medicines for Malaria Venture (MMV) is a partnership founded to reduce the global burden of malaria by aiding in the development of affordable anti-malarial therapeutics. Recently, the MMV presented the Open Access Malaria box, a battery of 200 drug-like and 200 probe-like commercially available small molecule inhibitors. These inhibitors were selected from >19,000 compounds originally identified as inhibitors of erythrocyte-stage *P. falciparum* by the screening efforts of GlaxoSmithKline, St. Jude Children's Research Hospital, and Novartis (Gamo et al. 2010, Guiguemde et al. 2010, Meister et al. 2011, Spangenberg et al. 2013). The MMV Open Access Malaria box has been useful in identifying inhibitors of a variety of apicomplexans including *P. falciparum*, *Cryptosporidium parvum*, *T. gondii*, and

Theileria annulata (Spangenberg et al. 2013, Bessoff et al. 2014, Boyom et al. 2014, Hostettler et al. 2016, Van Voorhis et al. 2016).

In the present study, we screen the MMV Open Access Malaria box to identify inhibitors of *T. gondii* growth. We focus on MMV006169, which inhibits the growth of both *T. gondii* and *C. parvum* (Bessoff et al. 2014), and find that it also reduces *T. gondii* invasion and replication, but has no effect on motility. Extensive structure activity relationship (SAR) analyses of MMV006169 against both *T. gondii* and *C. parvum* are reported. Lastly, we use yeast three-hybrid technology to test the hypothesis that MMV006169 interacts with TgCDC48 (TgCDC48Cy and TgCDC48Ap, respectively), and find no evidence of a direct interaction with either.

2.2 Materials and Methods

2.2.1 Host cell and parasite culture

Human foreskin fibroblasts (HFFs) (ATCC CRL-1643) were maintained in Dulbecco's Modified Eagle's Medium (DMEM), supplemented with 10 units/mL penicillin G sodium salt, 10 units/mL streptomycin sulfate, 10 mM HEPES, pH 7.2, and containing 1% heat-inactivated fetal bovine serum (FBS; 1% DMEM) at 37°C, 5% CO₂, and constant humidity. Cells were split by the addition of trypsin to release host cells from the surface of tissue culture flasks and resuspended in DMEM supplemented as above but containing 10% FBS (10%DMEM) as described in (Roos et al. 1994) .

T. gondii 2F1 YFP₂ tachyzoites (Gubbels et al. 2003), kindly provided by Dr. Marc-Jan Gubbels, were serially passaged in confluent monolayers of HFFs.

2.2.2 YFP-based growth assay

Growth of *T. gondii* strain 2F1 YFP₂ parasites expressing yellow fluorescent protein (YFP) was monitored as previously described (Gubbels et al. 2003) with a few modifications. Briefly, parasites and HFFs were cultured in HyClone DMEM/high modified medium lacking phenol red (Thermo Fisher Scientific), supplemented with 10 units/mL penicillin, 10 units/mL streptomycin sulfate, 10 mM HEPES, pH 7.2, and containing 1 or 10% v/v fetal bovine serum (FBS). Approximately 5×10^3 HFFs (in 50 μ L medium containing 10% v/v FBS) were seeded into each well of a Special Optics black/clear 384-well tissue culture-treated plate (BD Falcon) and grown at 37°C, 5% CO₂, and constant humidity. Upon confluence, culture medium was removed, wells were washed once with culture medium containing 1% v/v FBS, and then replaced with 30 μ L of the same medium. Parasites were harvested by syringe release, passed through a 3- μ m Nuclepore filter (Whatman, Piscataway, NJ) to eliminate host cell debris, and gently pelleted (1,100 x g, 4 minutes). The resulting parasite pellets were resuspended in medium supplemented with 1% v/v FBS, counted, and diluted to 1×10^5 parasites/mL. Each well of the assay plate was inoculated with 20 μ L (2000) parasites, followed by the addition of test compounds serially diluted from DMSO stocks in culture medium supplemented with 1% v/v FBS. Assay plates were incubated at 37°C in 5% CO₂, and fluorescence was read daily for 8 days from the bottom of the plate with the lid in place using a Synergy 2 microplate reader (BioTek, Winooski, VT). The program was optimized to a set sensitivity of 60, with excitation filter of 485/20 and emission filter of

528/20. Positive controls were included in all assays (typically pyrimethamine). The IC₅₀ of each compound was determined as described previously (Bessoff et al. 2014).

2.2.3 MMV Malaria box screening

The 400 small-molecules included in the MMV box (Spangenberg et al. 2013) were diluted to 1.67 mM in DMSO and consolidated into two V-bottom polypropylene 384-well plates (Whatman, Piscataway, NJ). Vehicle (DMSO) and positive control (pyrimethamine) wells were scattered throughout the plate. Prior to each use these plates were warmed to 37°C and centrifuged to ensure compounds were concentrated at the bottom of each well. Compounds were transferred to the wells of HFF seeded Special Optics black/clear 384-well tissue culture-treated plates (BD Falcon) using a 384 solid pin Multi-Blot replicator tool (V&P Scientific) as previously described (Bessoff et al. 2014). Compounds were screened using the YFP-based growth assay at a final concentration of 2.3 μM in duplicate. Upon completion of the eight-day assay, each well was visually screened for evidence of compound cytotoxicity, precipitation, and parasite plaque formation.

2.2.4 ATPase assay

To assess host cell viability in the presence of compounds of interest we performed ATPase assays using the CellTiter-Glo Luminescent Cell Viability Assay according to manufacturer's instructions (Promega, Madison, WI). Briefly, Special Optics white 384-well tissue culture-treated plates (Corning, Corning, NY) were seeded with

5×10^3 HFFs (in 50 μ L medium containing 10% v/v FBS) and grown at 37°C, 5% CO₂, and constant humidity. Upon confluence, culture medium was removed and replaced with 30 μ L of 1% DMEM. Compounds diluted in DMEM were added to each well to a final concentration of 10 μ M (5 μ L). Positive and negative controls (sodium azide 143 mM final and DMSO) were included in each plate. Plates were incubated at 37°C, 5% CO₂, and constant humidity. After 24 hours, an equal volume of CellTiter-Glo Reagent was added to each well. Plates were agitated by shaking for 2 minutes, followed by stabilization of the luminescence accomplished by incubating the plate for 10 minutes at room temperature. Luminescence was recorded using a Synergy 2 microplate reader (BioTek, Winooski, VT) and presented as relative luminescence units (RLU).

2.2.5 Replication assay

HFFs were grown to confluence on 12 mm circular coverslips in 12-well plates. 2F1 YFP₂ parasites were harvested by syringe release, passed through a 3- μ m Nuclepore filter (Whatman, Piscataway, NJ) to eliminate host cell debris, and gently pelleted (1,100 x g, 4 minutes). 4×10^5 parasites were added to each coverslip in the presence of each compound of interest. Coverslips were removed 36 hours post infection and incubated in fixative solution (1X PBS + 4% v/v paraformaldehyde) for 20 minutes, permeabilized (1X PBS + 0.25% v/v Triton X-100) for 15 minutes, and blocked for 30 minutes in 1X PBS + 1% w/v bovine serum albumin. Coverslips were incubated in mouse anti-IMC1 (mAb 45.36, 0.75 μ g/mL) at a 1:1000 dilution in block solution for 1 hour and then goat anti-mouse IgG conjugated to Alexa 546 (Invitrogen, 2mg/mL) at a 1:500 dilution for 30

minutes. Coverslips were then sealed to the surface of glass slides using nail polish. One hundred fields of each sample were counted blindly at 100X on a Nikon Eclipse TE300 epifluorescence microscope.

2.2.6 Invasion assay

Invasion assays were performed in a manner similar to that previously described (Carey et al. 2004). Harvested 2F1 YFP₂ tachyzoites were counted and 5×10^5 parasites were added to confluent HFFs grown on 12 mm circular coverslips in 12-well plates in the presence of each compound of interest (or DMSO). Plates were left at room temperature for 15 minutes to allow the parasites to settle and were then shifted to 37°C for 1 hour. Loosely attached parasites were washed away with 1x PBS and each coverslip was then prepared for immunofluorescence as described above with the following modifications. Cells were fixed in 1X PBS + 3.1% v/v paraformaldehyde, 0.06% glutaraldehyde. Fixed coverslips were stained with mouse anti-SAG1 (DG52) diluted 1:200 for 30 minutes and then goat anti-mouse IgG conjugated to Alexa 546 (Invitrogen, 2 mg/mL) at a 1:500 dilution for 30 minutes. Coverslips were then permeabilized and stained again with mouse anti-SAG1 (DG52) diluted 1:200 for 30 minutes and then goat anti-mouse IgG conjugated to Alexa 488 (Invitrogen, 2 mg/mL) at a 1:500 dilution for 30 minutes. All intracellular parasites (green) in 100 fields were counted blindly at 100X on a Nikon Eclipse TE300 epifluorescence microscope.

2.2.7 Two-Dimensional trail assay

Trail assays were performed similarly to that described previously (Dobrowolski and Sibley 1996, Carey et al. 2004). Briefly, wells of a Special Optics black/clear 384-well tissue culture-treated plate (BD Falcon) were coated with Cell-Tak per manufacturer's instructions (Corning, Corning, NY). NaHCO₃ (100 mM, pH 8.0) was used for adsorption. Wells were washed twice with PBS prior to parasite loading. 2F1 YFP₂ parasites were harvested, counted, and diluted (in 10mM Hepes buffered Hank's Buffered Saline Solution (HBSS) containing 1% v/v dialyzed FBS) to 1.5x10⁷ parasites/mL. Compounds were diluted in Hepes buffered HBSS. To each well containing Cell-Tak, 20 µL of parasites was mixed with 30 µL of each compound and incubated for 15 minutes at room temperature followed by 30 minutes at 37°C. The contents of each well were aspirated, washed, and replaced with 2.5% paraformaldehyde for 10 minutes. After fixation, wells were treated with 1x PBS + 0.5% w/v bovine serum albumin for 15 minutes. Parasites were stained with mouse anti-SAG1 (DG52) diluted 1:500 for 15 minutes and then goat anti-mouse IgG conjugated to Alexa 488 (Invitrogen, 2 mg/mL) at a 1:500 dilution for 15 minutes. A thin layer of overlay (1X PBS containing 75% glycerol and 0.05% NaN₃) was used to keep wells from drying out. The number of trails per field was scored blindly across each well in duplicate.

2.2.8 Construction of pGADCDC48Ap and pGADCDC48Cy

Plasmid construction was performed using restriction enzymes and Phusion high fidelity polymerase purchased from New England BioLabs (Ipswich, MA). Primers used were synthesized by Sigma Aldrich (The Woodlands, TX). To construct

pGADCDC48Ap, the plasmid pGADT7 (Clontech Laboratories, Mountain View, CA) was digested with SacI and NdeI. CDC48Ap was amplified from RH $\Delta hxgprt\Delta ku80$ cDNA using primers 1 and 2. Purified digested plasmid and CDC48Ap PCR product were co-transformed into competent AH109 yeast as previously described (Gietz and Schiestl 2007). Transformants were plated on yeast drop out plates (SC +Glu –leu) and incubated at 30°C for 48 hours. The resulting plasmid was screened by restriction digest and DNA sequencing using primers 3-7 (Chapter 2 – Table 5). pGADCDC48Cy was cloned as described above using primers 8-13 (Chapter 2 – Table 5).

2.2.9 CID competition assay

CID competition assays begin with yeast co-transformed with a plasmid encoding *E. coli* dihydrofolate reductase fused to the Gal4 DNA-binding domain (pGBKeDHFR, cloned by Anahi Odell, unpublished) and a plasmid encoding the Gal4 activation domain fused to TgCPDK1. A single colony was grown at 30°C overnight in 3 mL of synthetic complete liquid media (SC +Glu –trp –leu). The next morning, 4 mL SC +Glu –trp –leu was inoculated with 200 μ L of the turbid yeast culture and incubated for 4 hours with shaking. Log phase cells (determined by OD₆₀₀) were diluted to 2×10^5 cells/mL and 25 μ L was used to inoculate each test well in a 96-well plate (BD Falcon) containing 125 μ L SC +Glu –trp –leu –his. CID7 (1.5 μ L of 2.5 mM or DMSO) and 3-AT (1.5 μ L of 50 mM) was added to each well. To half of the experimental samples, 1 μ L of 40 mM Mtx-MMV006169 was added. Plates were parafilm and incubated with shaking (200 rpm) at 30°C. With the lid in place, the OD₆₀₀ for each well was recorded

from the bottom of the plate using a Synergy 2 microplate reader (BioTek, Winooski, VT). Plates were read daily and the assay was terminated when robust growth was observed in positive control wells that lack Mtx-MMV006169.

2.2.10 Targeted yeast three-hybrid liquid assay

To perform targeted yeast three-hybrid assays a plasmid containing the hypothesized compound target (pGADCDC48Ap or pGADCDC48Cy) and a plasmid encoding *E. coli* dihydrofolate reductase fused to the Gal4 DNA-binding domain (pGBKeDHFR) was co-transformed into competent AH109 yeast cells, plated on yeast drop out plates (SC +Glu –trp –leu) and incubated at 30°C for 48 hours. A single colony of the resulting transformants was grown overnight in 3 mL of synthetic complete liquid media (SC +Glu –trp –leu). The next morning, 200 µL of turbid yeast culture was used to inoculate 4 mL of SC +Glu –trp –leu and incubated for 4 hours. Log phase cells (determined by OD₆₀₀) were counted and diluted to 2x10⁵ cells/mL and 25 µL was used to inoculate each test well in a 96-well plate (BD Falcon) containing 125 µL SC +Glu –trp –leu –his. CID (1.5 µL of 2.5 mM or DMSO) and 3-AT (1.5 µL of 50 mM) were added to test wells. As a negative control, 1.5 µL DMSO and 1.5 µL 3-AT were added to wells containing 150 µL of media alone. Yeast expressing pGBKeDHFR and a plasmid encoding the Gal4 activation domain fused to TgCPDK1 were used as a positive control (125 µL media, 1.5 µL 2.5 mM CID7, 1.5 µL 50 mM 3-AT, and 25 µL yeast). Plates were parafilm and incubated with shaking (200 rpm) at 30°C. With the lid in place, the OD₆₀₀ for each well was recorded from the bottom of the plate using a Synergy 2

microplate reader (BioTek, Winooski, VT). Plates were read daily and the assay was terminated when robust growth was observed in positive control wells.

2.3 Results

2.3.1 MMV box screen identifies 79 inhibitors of *T. gondii* growth

Given that many proteins and biochemical processes are conserved between *P. falciparum* and *T. gondii*, we hypothesized that a high percentage of the molecules included in the MMV Malaria box as inhibitors of *P. falciparum* would also function as *T. gondii* inhibitors. We screened the MMV Malaria box in duplicate against *T. gondii* using a YFP-based growth assay (Gubbels et al. 2003). For simplicity and to aid in the identification of potent compounds of interest, all 400 compounds in the box were added to assay plates using a pin transfer device that deposits compound at a final concentration of 2.3 μM (Bessoff et al. 2014). Upon completion of the 8-day growth assay, monolayers were visually scored for evidence of compound toxicity, insolubility, and host cell integrity. Seventy-nine compounds, a 19.8% hit rate, were found to alter *T. gondii* growth kinetics at 2.3 μM in both replicates (Chapter 2 – Table 1). By comparing these screen results with data previously generated against *C. parvum* (Bessoff et al. 2014) and by closely examining each chemical scaffold for synthetic accessibility, we were able to narrow our focus down to 5 compounds of interest: MMV000720, MMV403679, MMV001246, MMV000642, and MMV006169 (Chapter 2 – Table 2). Each of these compounds was reordered and screened for an effect on *T. gondii* growth at 11 different concentrations to extrapolate IC_{50} values (Chapter 2 – Table 2). From these 5

compounds, we chose MMV006169 as our focus based on potency against *T. gondii* (1.15 μM), a similar IC_{50} against *C. parvum* (1.50 μM) (Bessoff et al. 2014), ease of chemical synthesis, and the availability of analogs commercially (Chapter 2 – Figure 1). MMV006169 showed no evidence of host cell toxicity based on visual examination of wells during each growth assay (maximum 18 μM) or by ATPase assay (10 μM) (Chapter 2 – Figure 2).

2.3.2 MMV006169 inhibits *T. gondii* invasion, but not motility

The lytic cycle of *T. gondii* in human cells is a complex, multi-step process (see Chapter 1). In order to better understand how MMV006169 inhibits *T. gondii* growth, we tested individual steps of this lytic cycle to determine if the compound could inhibit invasion, replication, and/or motility. Parasite invasion is dependent on its ability to glide along, attach to, and enter host cells, so in a sense, motility is essential for invasion (Black and Boothroyd 2000, Carey et al. 2004). We tested the parasite's ability to invade host cells using a two-color immunofluorescence invasion assay where the surface antigen, TgSAG1, of intracellular parasites is stained green, and extracellular parasites are stained red (Carey et al. 2004). Upon quantification of the number of intracellular parasites per field we found that MMV006169 did inhibit invasion at 10 μM (green, $p \leq 0.05$), but not the lower concentration tested (5 μM , red) compared to vehicle control (blue) (Chapter 2 – Figure 3A).

Parasite motility was analyzed by 2D trail assay, which exploits the fact that Apicomplexans deposit surface antigen “trails” as they glide along a substrate

(Dobrowolski and Sibley 1996). As with the invasion assay, the surface antigen, TgSAG1, can be stained on a given substrate and these trails can be quantified. No significant difference in the mean number of trails per field was seen at 5 (red) or 10 μM (green) compared to a vehicle control (blue) (Chapter 2 – Figure 3B).

2.3.3 MMV006169 inhibits *T. gondii* replication

T. gondii replication occurs via a process termed endodyogeny, where two daughter parasites form within the mother (Sheffield and Melton 1968). The mother's inner membrane complex, a series of flattened vesicles underlying the plasma membrane, serves as the scaffold for new daughters (Hu et al. 2002). During cell division, the mother's organelles are partitioned between the newly formed daughters and any remnants are left in a small residual body (Hu et al. 2002). Replication can be quantified by recording the number (e.g., 2, 4, 8, and 16 or more) of surface stained parasites present in individual parasitophorous vacuoles over time. Parasites exposed to MMV006169 (5 μM , red, Chapter 2 – Figure 3C) for 36 hours, show a severe replication defect where 98% of the vacuoles seen contain only two parasites.

2.3.4 Structure activity relationship analyses

In order to better understand how MMV006169 inhibits *T. gondii* replication and invasion, we expanded our compound library to include structural analogs containing a conserved 2,4-diaminoquinazoline scaffold (Chapter 2 – Figure 1C, red). We hypothesized that structural changes to MMV006169 might differentially affect

replication and invasion. To test this, we purchased 26 and synthesized 48 analogs containing the 2,4-diaminoquinazoline scaffold, screened each of them by growth assay, and calculated associated IC₅₀ values. The majority of screened analogs (n=68) ranged in potency from 0.26 – 11.54 μM, while 6 analogs were found to have IC₅₀ values outside the range tested (Chapter 2 – Table 3). These compounds were screened in parallel against *C. parvum* for inhibitory effects on growth ((Bessoiff et al. 2014) and Rajiv Jumani, personal communication). To differentiate between effects on invasion and replication, we chose 11 molecules with different potencies against *T. gondii* and *C. parvum*, as well as analogs with major changes to the chemical backbone (Chapter 2 – Table 4). None of the analogs chosen have toxic effects against the host cells after 24 hours (Chapter 2 – Figure 4). By changing the chemical structure of these compounds we are able to determine which parts of the compound are essential for an effect on replication and/or invasion.

The majority of structural analogs examined inhibit *T. gondii* replication in a manner similar to the parent molecule (Chapter 2 – Figure 5). However, treatment with either C-6 or C-10 resulted in only partial inhibition of replication. Here, we define partial inhibition of replication as having 40% (or more) of vacuoles containing 4-8 parasites per vacuole, with no vacuoles containing 16 or more parasites. C-11 has only a minor effect on replication, where fewer vacuoles (19% vs. 56%) containing 16 or more parasites were seen in comparison with the vehicle control. This analog has three modifications: a trifluoromethyl group on position 3 of R¹, a methoxy group on position 8 of R¹, and a methoxy group on position 4 of R³. C-4 contains the same modifications on

R¹ and R³, but still inhibits replication. FT14.025.2, not included in the replication analyses, contains both the modifications on R¹ and R², and can still inhibit *T. gondii* growth (Chapter 2 - Table 3). This suggests that the combination of methoxy groups on R² and R³ prevent the small molecule from interacting with its target(s). All other analogs tested appear to inhibit replication, suggesting that having more than 2 modifications (C-6 and C-11) to the structure prevent the analog from properly associating with its replication associated target(s) and that hindrance of the amine on R³ (C-10) leads to only partial inhibition (an isopropylamine is sufficient).

To analyze the effects of structural analogs on invasion we chose to use a subset of 5 analogs that included structural modifications to each of three portions of the molecule (R¹, R², and R³) and also included representatives of each of the three replication phenotypes described above: inhibition, partial inhibition, and no effect. These assays suggest that only single modifications made on R¹ and R³ retain the ability to inhibit invasion (Chapter 2 – Figure 6 and Chapter 2 – Table 4). Specifically, the single modification of R¹ on C-1 with a single trifluoromethyl group on position 3 and the single modification of R³ on C-7 with a methoxy group on position 2, both result in inhibition of invasion. More than one modification of R¹ results in invasion levels equal to that of the DMSO control (C-5, C-6). C-11, with modifications to R¹, R², and R³ (discussed above), yield invasion levels equivalent to that of DMSO. C-11 does not inhibit *T. gondii* growth at concentrations up to 18 μM, this correlates with the lack of an effect seen in both invasion and replication assays. Similarly, C-11 does not inhibit *C. parvum* growth at concentrations up to 10 μM.

In our replication assays, we only scored vacuoles containing two or more parasites (i.e., vacuoles in which at least one round of replication had taken place) and the data are expressed as the percentage of the total vacuoles containing at least two parasites. However, we noted that the total number of two-parasite containing vacuoles was low in all compound-treated samples. This led us to ask if the small number of two-parasite containing vacuoles in these samples was due to inhibition of invasion or the inability to initiate endodyogeny. To test this, we measured the total number of one- and two-parasite containing vacuoles 36 hours post-infection using the differential two-color staining strategy typically used in invasion assays (Carey et al. 2004). We found that for those analogs that caused the most severe invasion defect in a 60-minute invasion assay ($p \leq 0.0001$, C-1 and C-7, Chapter 2 – Figure 6), the number of two-parasite containing vacuoles was considerably lower after 36 hours than one-parasite vacuoles (Chapter 2 – Figure 7). This suggests that while the parasites are able to eventually invade, they are not successfully initiating endodyogeny.

2.3.5 CDC48 does not interact with Mtx-MMV006169

Structure-based searches aimed toward the identification of the target(s) of MMV006169 identified the inhibitor N_2N_4 -dibenzylquinazoline-2,4-diamine (DBeQ) as a previously characterized structural analog of MMV006169 (Bessoff et al. 2014). DBeQ is a potent, reversible inhibitor of an AAA ATPase (ATPase associated with diverse cellular activities) known as p97 (or CDC48) that is involved in protein trafficking and the degradation of misfolded proteins (Chou et al. 2011). Previous work suggested that

p97 functions in the *P. falciparum* endoplasmic reticulum-associated degradation (ERAD) pathway and showed that treatment of parasites with DBEq inhibits growth (Harbut et al. 2012). We reordered and tested DBEq for an effect on *T. gondii* growth and found it to inhibit growth with similar potency (1.42 μ M) to MMV006169, but having lost potency against *C. parvum* (4.73 μ M) (Bessoff et al. 2014) (Chapter 2 – Table 3, OSSL_324373). Interestingly, *T. gondii* has two isoforms of CDC48 (TgCDC48Cy and TgCDC48Ap) with three different cellular localizations (TgCDC48Cy to the plasma membrane and endoplasmic reticulum; TgCDC48Ap to the apicoplast) (Agrawal et al. 2009). While CDC48 proteins are highly conserved, these isoforms are of divergent phylogenetic evolution. Consistent with vertical evolution, TgCDC48Cy exists in a clade with homologs found in chromalveolates, while TgCDC48Ap groups with proteins found in organisms that contain secondary plastids (Agrawal et al. 2009). Based on differences in cellular localization, the function of these proteins is thought to differ. TgCDC48Cy has been hypothesized to aid in the trafficking of proteins to the proteasome, and also in helping to bring proteins into the parasite from the host cell. TgCDC48Ap may play a role in trafficking nuclear-encoded proteins into the apicoplast (Agrawal et al. 2009). More studies are needed to confirm these hypotheses. Protein alignments comparing each *T. gondii* isoform (TgCDC48Cy: TGME49_273090 and TgCDC48Ap: TGME49_321640) with the *P. falciparum* ortholog (PlasmoDB: PF3D7_1133400) reveal 76 and 37% identity, respectively. This led us to hypothesize that MMV006169 may be working through inhibition of TgCDC48Cy and perhaps also TgCDC48Ap.

To test this hypothesis we utilized a targeted yeast three-hybrid system. The system allows us to directly test small molecule-protein interactions by expressing bait and prey proteins fused to each half (DNA-binding domain (DBD) and activation domain (AD)) of a split transcription factor (Licitra and Liu 1996, Henthorn et al. 2002, Baker et al. 2003, Chidley et al. 2011, Odell et al. 2015). A bridging molecule, termed the chemical inducer of dimerization (CID), containing methotrexate, linker, and a small molecule of interest brings the bait/prey fusion proteins together in a functional ternary complex, which can activate the expression of different reporter genes (Chapter 2 – Figure 8A). We expressed the DBD of the GAL4 transcription factor as a fusion with dihydrofolate reductase (DHFR), and the AD as a fusion with each isoform of *T. gondii* CDC48. The CID, Mtx-MMV006169, was synthesized by our collaborators at the University of St. Andrews (Drs. Fanny Tran and Nicholas Westwood) using the previously described SAR analysis to determine the optimal position for linker attachment (Chapter 2 – Figure 8B). CID competition assays show that Mtx-MMV006169 can enter yeast and compete for binding with a positive control CID (Chapter 2 – Figure 9). Using this functional CID and the CDC48 fusion proteins, we found no direct interaction between either isoform, suggesting that CDC48 is not the target of MMV006169 in *T. gondii* (Chapter 2 – Figure 10 and 11).

2.4 Discussion

While the identification of lead compounds is of vital importance for drug development, if the protein targets of these drugs are not fully understood the potential

for unexplained side-effects increases. Since the parasite lytic cycle is necessary for proliferation and viability, understanding the cellular machinery involved in growth is vital to the development of more useful anti-parasitics. The MMV Open Access Malaria box presented itself as a unique tool for the identification of potential anti-*Toxoplasma* compounds since the compounds included in the Malaria box have already been shown to inhibit erythrocyte-stage *P. falciparum* (Gamo et al. 2010, Guiguemde et al. 2010, Meister et al. 2011, Spangenberg et al. 2013). Additionally, a number of the targets of these molecules have already been characterized in other systems, helping to focus future target identification efforts.

We have screened the 400 small molecules available in the MMV Open Access Malaria box using a high-throughput YFP-based growth assay for inhibition of *T. gondii* (Gubbels et al. 2003, Bessoff et al. 2014). Screening this collection at a single concentration resulted in the identification of 79 potential inhibitors for further analysis. This represents a 19.8% hit rate in our hands. Further examination of the synthetic accessibility of these analogs and comparison of potencies against other apicomplexans led us to focus on one compound, MMV006169. MMV006169 is a potent (1.15 μ M) inhibitor of *T. gondii* growth that we also showed inhibits both replication and invasion. The compound contains a 2,4-diaminoquinazoline scaffold, and while MMV006169 has a similar potency in *T. gondii* and *C. parvum*, other compounds containing this scaffold were previously found have different potencies between the two organisms. It has been suggested that these differences could be consequences of parasite divergence. For

example, *C. parvum* lacks an apicoplast and thus uses different biochemical mechanisms to generate isoprenoids than *T. gondii* (Bessoff et al. 2014).

Further structure activity relationship analyses confirmed the lack of correlation between *T. gondii* and *C. parvum* IC₅₀s for different analogs. However, these SAR analyses provided further insight into how the molecule may be working in *T. gondii*. Single modifications of R¹ and R³ result in molecules sufficient to inhibit invasion and replication, while these effects are lost if more than one modification of R¹ is present. Modifications to all three ring structures are not tolerated to maintain inhibition of invasion and replication. Interestingly, preliminary invasion assays with additional structural analogs suggest the substitution of methylamines to either end of the compound (R³ on C-10 and R¹ on C-2, data not shown) result in enhancement of invasion. This suggests that the availability of the free, unhindered amine groups plays a role in enhancement of invasion. This requires further analysis and confirmation using the more sensitive laser-scanning cytometry method of quantifying parasite invasion (Mital et al. 2006). However, The presence of a conserved aromatic amine playing a role in the enhancement of invasion was previously reported on a group of substituted chloroisocoumarins (Child et al. 2013). Synthesis of an analog of these enhancers lacking the amine resulted in lack of enhancement. These chloroisocoumarins were shown to target TgPP1, but lack of an impact on replication and structural differences led us to believe that MMV006169 is likely working on another target. Another enhancer of invasion found in a large-scale compound screen also contains an unhindered aromatic

amine (Carey et al. 2004). Further analysis of the role of this functional group on enhancement of invasion is needed.

A compound containing the 2,4-diaminoquinazoline scaffold, was previously presented as being a novel inhibitor of *T. gondii* motility, but not invasion (Kamau et al. 2012). This is an interesting phenotype since the machinery necessary for *T. gondii* motility is also essential for parasite invasion. We resynthesized this molecule (Chapter 2 – Table 3, FT14.116.2) to look more critically at both processes. The assays used by Kamau et al., were very general and only looked at changes in parasite trails and overall invasion after one hour. There is a possibility that the parasites are actually moving, just not in the canonical fashion observed by trail assays. We performed invasion assays using two concentrations of compound (5 and 10 μ M) and found an invasion defect at the higher concentration of 10 μ M (data not shown). Trail assays reveal that compound treated parasites were still able to move (i.e., generate trails) comparable to those of the DMSO control (data not shown). These discrepancies could be due to compound freeze thaws or impure commercially provided compound in their hands.

We used the previously discussed SAR analyses to generate a CID for use in yeast three-hybrid experiments. We chose EN01.065 (C-7) as the starting point for synthesis and generated a CID capable of passing the yeast cell membrane as demonstrated by CID competition assay. Using this CID, neither isoform of CDC48 induced the expression of reporter genes, suggesting there is no direct interaction between CDC48 and MMV006169. However, there are some limitations to the yeast three-hybrid system that may generate false negative results. First, the expression of *T.*

gondii genes in yeast may result in misfolded proteins. If the protein is not in its native confirmation, it will not interact with the small molecule correctly, and thus not induce reporter genes. It is also possible that the *T. gondii* CDC48 proteins are not being made or are being made and then degraded. Since the proteins have been cloned into the yeast vector with an HA-tag, their presence can be tested by western blot. Localization of the protein can also be examined using immunofluorescence. This would allow the confirmation of the nuclear localization of the protein, but it will not confirm functionality of the protein. If the protein is not functional, it may not be able to interact with MMV006169 to produce reporter activation. To test the functionality of the *T. gondii* isoforms in *S. cerevisiae* we could complement *CDC48* deficient yeast with each of the *T. gondii* isoforms. *S. cerevisiae* *CDC48* mutants are characterized by the presence of apoptotic markers and cell cycle arrest where large budded cells appear with the nucleus located in the neck between the mother and the daughter cell (Moir et al. 1982, Frohlich et al. 1991, Madeo et al. 1997). Should complementation rescue the cell cycle or apoptotic phenotypes, and yeast three-hybrid experiments fail, then we would move on to other target identification strategies for MMV006169. However, should complementation experiments fail, we could only conclude that the isoforms do not function analogously to that of yeast proteins in that specific environment. Confirmation of functionality would then require the expression of these proteins recombinantly and testing for the ability for the ATPase to function with more specifically designed assays.

Steric hindrance can also cause problems. In a yeast three-hybrid system prey proteins are fused to a transcription factor. It could be that generating fusions with the

amino terminus of each gene prevent proper small molecule binding. To counter this, the transcription factor could be fused to the carboxy terminus instead. CDC48 is thought to associate with Der1, a pore involved in the ERAD pathway (Agrawal et al. 2009). It is possible that CDC48 needs to be associated with Der1 for proper folding to occur, and as such will not occur in yeast. CDC48 orthologs are commonly transmembrane proteins, but there is no evidence of transmembrane domains in either *T. gondii* isoform. Lastly, addition of the methotrexate/linker portion of the CID to MMV006169 may preclude the compound from properly interacting with its target. Further analyses of these possibilities will be the subject of future studies. Nonetheless, this work has provided extensive SAR analyses of MMV006169, which may contribute to future, lead compound development and outlined the impact of a subset of analogs on invasion and replication.

Chapter 2 – Table 1: Summary of MMV box hits against *T. gondii*

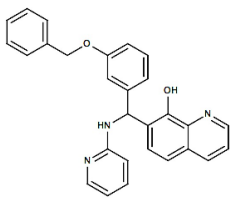
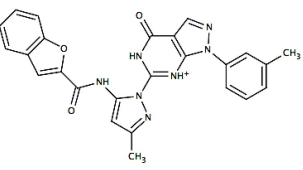
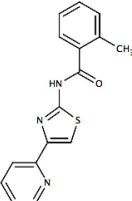
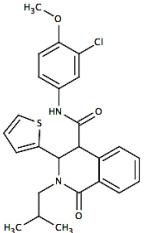
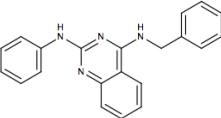
MMV box compounds found to inhibit *T. gondii* growth at 2.3 μM after two biological replicates. Smiles, source data, set, and plate locations provided by MMV.

HEOS COMPOUND ID	Smiles	Source	Set	PLATE March2012	WELL March2012	PLATE May2012	WELL May2012
MMV666601	CCOC(=O)C1=C(N=C2SC(=C3ccc(C)n(c3C)4ccc(F)cc4)C(=O)N2C1c5cccc(OC)c5OC)c6cccc6						
MMV007564	Cc1ccc(Cn2e(nc3cccc23)N4CCC(C)C4(=O)Nc5cccc5)cc1	GNF;GSK	Probe-like	A	F07	A	A05
MMV665917	Cc1ccc(NC(=O)N2CCN(CC2)3ccc4nnnc4n3)cc1	GNF	Drug-like	B	A03	B	A08
MMV000563	COc1ccc(cc1)C2Sc3cccc3N=C4C2=C(O)c5cccc45	GNF	Drug-like	B	G08	B	A09
MMV665891	c1cc(ccc1)c2ccc(cc2)c3nc4cccc4[nH]3	GSK	Drug-like	B	A08	B	B10
MMV665909	Br1cccc1C(=O)Nc2nc(cs2)c3cccc3	StJude	Drug-like	B	E02	B	B08
MMV000653	CCOc1cccc1CNC(=O)C2C(N(CC)C)C(=O)c3cccc23)c4cccc4	StJude	Drug-like	B	B11	B	B06
MMV020439	Cc1c(CN2CCN(Cc3cccc3)CC2)nc4ccc(NC(=O)c5cccc5)ccc14	GSK	Drug-like	A	H08	A	B06
MMV000570	Cc1ccc(Nc2cc(C)c3ccc(O)cc3n2)cc1	StJude	Probe-like	A	F08	A	B05
MMV665105	COCCN(C)C(=O)NCC1ccc(OC)cc1)c2ccc(cc2)C(C)C(=O)C3cccc3	GSK	Drug-like	B	E06	B	B04
MMV665977	CCOC(=O)C1=NC(C)C2cc(N(C)CC3ccc(OC)C(C)3)C(F)C2C1=O	GNF;GSK	Probe-like	A	H02	A	C03
MMV001246	CSc1cccc1C(=O)Nc2nc(cs2)c3cccc3	StJude	Drug-like	A	F09	A	C05
MMV665915	COc1ccc(cc1)c2nc(NC(=O)CS(=O)C(=O)c3ccc(F)cc3)sc2C	GNF;GSK	Drug-like	A	A02	A	C07
MMV665798	FC(F)F1ccc(Nc2nc(nc3cccc23)c4cccc4)c1	GSK	Drug-like	B	G03	B	D09
MMV665935	FC(F)F1ccc(Nc2nnnc3cccc23)cc1	GNF;GSK	Drug-like	B	C02	B	D03
MMV66596	CSC1=NC(=Nc2c(C)cccc2)C3(CCC(C)C)C(C)C(N)C4ccc(C)cc4	GNF	Probe-like	A	A07	A	D03
MMV000642	COc1ccc(NC(=O)C2(C)C(C)C(=O)c3cccc23)c4cccc4)cc1C1	GNF;StJude	Probe-like	A	A09	A	E03
MMV000960	CCN(CC)c1ccc(NC(=O)c2cccc2)cc1	GNF	Drug-like	B	A09	B	E04
MMV006309	CN(C)c1ccc(C=CC2=NC(=O)c3cccc3O2)cc1	GNF;GSK;GNF	Probe-like	A	A08	A	E06
MMV019758	COc1ccc(cc1OC)C(=O)Nc2ccc3nc(cc(C)C)3c2N4CCCCC4	GSK	Drug-like	B	D09	B	E06
MMV000498	CCN(C)C1cc(C)C2cc(NC(=O)c3cccc(OC)c3)ccc2n1	StJude	Drug-like	B	F09	B	E07
MMV011944	n1c(NCCO)c2c(ccc2)nc1Nc3cccc(OC)c3	GNF;GSK	Drug-like	B	H11	B	F08
MMV006937	Cc1ccc(cc1)c2cc3nc4CCCCc4(O)n3n2	GNF	Drug-like	A	C05	A	F08
MMV019064	COc1cccc(c1)c2nn(C)c3sc(cc23)C(=O)NCCN4CCN(C4)c5cccc5F	GSK	Drug-like	B	G09	B	F07
MMV007160	Cc1ccc(cc1)N2C3N(c4cccc4C2N(c5cccc35)S(=O)(=O)c6ccc(C)cc6)S(=O)(=O)c7ccc(C)cc7	GNF	Probe-like	A	G07	A	F05
MMV665827	CCOC(=O)C1=NC(C)C2cc(N3CCCC3)C(F)C2C1=O	GNF;GSK	Probe-like	A	G03	A	G10
MMV007907	Cc1ccc(Nc2nc(cs2)c3cccc3)cc1	GNF	Drug-like	A	F06	A	H09
MMV000788	CC(C)OCc1cc(CN2CCN(CC2)3ccc(C)C)3)c(O)c4ncccc14	StJude	Drug-like	B	E10	B	H06
MMV142383	CC(C)C1ccc(cc1)C(=O)Nc2nc3cccc3c2	StJude	Drug-like	B	B09	B	H05
MMV006861	C1CN(CCO1)c2ccc(Nc3ccc4cc5cccc5ccc34)cc2	GNF	Probe-like	A	H06	A	H05
MMV007839	C1(O)(CC(=O)c(ccc(OC)c2)c2O1)C(F)F(C)F(F)F	GNF	Drug-like	A	C10	A	H02
MMV403679	c1(c(cnn1c2cccc(C)c2)C(=O)N3=C3n4nc(C)cc4NC(=O)c5cccc6)c6o5	Commercial	Drug-like	C	C08	C	A04
MMV019670	O=C(Nc1ccc(cc1)N2CCN(Cc3cccc3)CC2)c4cccc4	GSK	Drug-like	C	B06	C	A07
MMV396669	n1c(cc(C)nc1Nc(cc2)ccc2NC(Cc3cccc3)=O)N4CCCC4	Commercial	Drug-like	C	G09	C	H03
MMV020654	CC(O)C1ccc(Br)cc1NC(=O)c2ccc(C)C2	GSK	Drug-like	C	H02	C	D10
MMV306025	C1(=NC(N)C2=O)C2=NC(=NN1CC)c3ccc(C(=O)OC)cc3	Commercial	Drug-like	C	B08	C	D03
MMV000963	n1c(NC2cccc2)c3c(ccc3)nc1Nc(cc4)ccc4OC	GNF;StJude	Drug-like	C	F11	C	E04
MMV006319	Cc1ccc(Nc2cccc(F)c2)nc(NC3cccc3)n1	GNF	Drug-like	C	G11	C	E05
MMV001318	Cc1ccc(NC(=O)Nc2ccc(Br)cc2)c1	StJude	Drug-like	C	E05	C	E08
MMV020660	COc1ccc(cc1OC)c2nonc2NC(=O)c3cccc(C)C3	GSK	Drug-like	C	H03	C	E10
MMV019266	Cc1sc2nnc(Sc3nc4cccc4[nH]3)c2c1C	GSK	Drug-like	C	G02	C	F09
MMV073843	CN(C)c1ccc(cc1)N=Cc2ccc(cc2)N3CCOCC3	GNF	Probe-like	E	A06	E	A02
MMV000445	CCCCCN1C(=N)N(C)C(O)COc2cccc(C)c2)c3cccc13	StJude	Probe-like	D	D09	D	A07
MMV006882	CCOC(=O)C1cnc2ccc(C)cc2c1NCCCN(C)C	GNF	Probe-like	D	G08	D	A08
MMV020403	COc1ccc(cc1)c2cn3c(C(=O)Nc4cccc4C)c(c5CCCCn2c35)c6cccc6	GSK	Probe-like	E	F05	E	A08
MMV007127	OC1=C2C(Sc3cccc3N=C2c4cccc14)c5ccc(Br)cc5	GNF	Probe-like	D	B08	D	A09
MMV666123	CC(C)C1c1ccc(cc1)C(=O)Nc2c3CSc3nn2c4cccc(C)C4	StJude	Probe-like	D	A03	D	A10
MMV665886	CC(Oc1ccc(NC(=O)c2cccc2)cc1)C(=O)c3ccc(C)cc3	GSK	Probe-like	E	H03	E	A11
MMV084434	COc1ccc(C=C2SC(=NC2=O)Nc3ccc(F)cc3)C(O)C1	GNF;GNF;GNF	Probe-like	E	D07	E	B07
MMV007577	Cc1cccc1OCCSc2nc3ccc(NC(=O)c4cccc4)cc3c2	GNF	Probe-like	D	B11	D	B06
MMV666109	CCOC(=O)C1(Cc2cccc2)CCN(Cc3ccc(OC)c3O)CC1	StJude	Probe-like	D	D05	D	C02
MMV007020	CCOc1ccc2nc(C)cc(Nc3ccc(cc3)N(C)C)C2c1	GNF	Probe-like	E	A09	E	C02
MMV665936	Cc1ccc(cc1)S(=O)(=O)c2c(COC(=O)c3ccc(C)C3)c(nn2)c4cccc4	GNF	Probe-like	D	E02	D	C03
MMV006656	CCOC(=O)C1=NC(C)C=C(C1c2cc(Br)C(OCC)C(O)C2)C(=O)OCC	GNF	Probe-like	E	H07	E	C03
MMV006522	CCOc1ccc2nc(C)cc(Nc3ccc(Br)cc3)c2c1	GNF	Probe-like	E	F11	E	C05
MMV000720	Cc1cnc(NC2c2ccc(OCc3cccc3)c2)c4ccc5ccnc5c4O)c1	GSK;StJude	Probe-like	D	E08	D	C07
MMV000619	CCCC(O)C(CN1COCC1)c2ccc(C)cc2)c3ccc(C)cc3	StJude	Probe-like	D	G10	D	C08

MMV000699	Cc1ccc(cc1)C2CC(n3nc(cc3N2)C(=O)N4CCN(CC4)C(c5ccccc5)c6ccccc6)C(F)(F)F	StJude	Probe-like	D	E07	D	D09
MMV000326	Cc1ccc2nc(C)cc(Nc3cccc(c3)C(F)(F)F)c2c1	StJude	Probe-like	D	C08	D	D06
MMV007574	O=C(Nc1ccc(cc1)C23CC4CC(CC(C4)C2)c5ccccc5)C3)c6cccs6	GNF	Probe-like	D	A07	D	D05
MMV665987	CCCCCc1cc(O)c2C3=C(CCC(C)C3)C(=O)Oc2c1	GNF	Probe-like	D	C04	D	D04
MMV006825	n1c(Nc(cc2)ccc2OC)cc(C)nc1NCc3ccccc3	GNF	Probe-like	E	H11	E	E05
MMV008455	COc1ccc(cc1)C2C(C(=O)Nc3cccc(OC)c3)c4cccc4C(=O)N2C5CCCCC5	GNF	Probe-like	D	H09	D	E08
MMV007199	COc1cccc1N2C(=N)SC(=C3ccc(OC4cccc4F)cc3)C2=O	GNF;GNF	Probe-like	D	E09	D	E09
MMV396717	c([nH]nc1c2c(O)cc(C)c(C)2)(C3=O)c1C(c4cccc4F)N3CCc(cc5)ccc5OC	Commercial	Probe-like	E	E10	E	E10
MMV665898	COc1cc(cc(OC)c1OC)C(=O)Nc2ccc(cc2)c3nc4cccc4[nH]3	GSK	Probe-like	E	B03	E	F09
MMV000621	CCCCCCC(O)C(CN1CCOCC1)c2cccc2)c3ccc(F)cc3	StJude	Probe-like	D	H10	D	F08
MMV019741	Cc1ccc(C)c(Cn2c(nc3cccc23)N4CC(C)C4)C(=O)NCc5cccs5)c1	GSK	Probe-like	D	C10	D	F06
MMV007654	Cc1ccc(C)c(c1)c2csc(Nc3cccc(C)c(C)c3)n2	GNF	Probe-like	E	A05	E	F05
MMV666095	CCCc1c(C)nc2ccc(Br)cc2c1O	GNF	Probe-like	D	G05	D	F03
MMV396594	c12c(nc(c3ccc(O)cc3)nc1N4CCN(C(=O)C5CCCC5)CC4)sc(CCCC6)c26	Commercial	Probe-like	E	F08	E	F02
MMV666106	O=C(NC1CCCC1)C(N(Cc2cccc2)C(=O)c3occc3)c4cccs4	GSK	Probe-like	D	H05	D	G03
MMV396663	c1(C(c(ccn2)c2)N3CC(C)C3)Cc4cccc4)c(C)C(NC(=O)c5cccs5)	Commercial	Probe-like	E	B08	E	G03
MMV007396	Cc1cccc1OCCSc2nc3ccc(NC(=O)c4cccs4)cc3s2	GNF	Probe-like	D	C11	D	G06
MMV000617	COc1ccc(cc1)C(O)(CC(C)C)C(N2CCOCC2)c3ccc(C)cc3	StJude	Probe-like	D	F10	D	G07
MMV011522	Cc1ccc(Nc2nc(N)c3cccc3n2)cc1Cl	GNF;StJude	Probe-like	E	G10	E	G11
MMV007113	c1ccc(cc1)C2=Nc3cccc3N=C(c4cccc4)c5ccccc25	GNF	Probe-like	D	G07	D	H09
MMV667489	N1C(c2cccc(ccc3)c23)C(CC=C4)C4c5c1c(Cl)ccc5C(OC)=O	Commercial	Probe-like	E	B10	E	H03
MMV006169	C(Nc1nc(Nc2cccc2)nc3cccc13)c4ccccc4	GNF	Probe-like	E	E09	E	B05

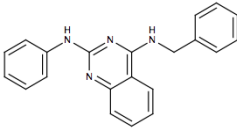
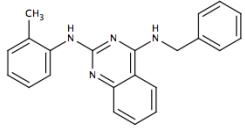
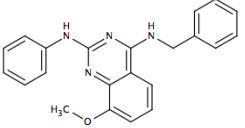
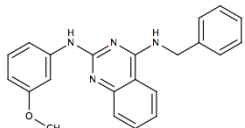
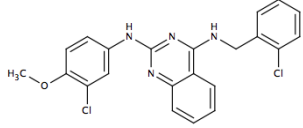
Chapter 2 – Table 2: Subset of MMV Malaria box molecules of interest

Five compounds chosen from the MMV Malaria box based on potency and similar efficacies against *C. parvum*.

Name	Structure	IC ₅₀ (μM) vs <i>T. gondii</i> (95% CI)
MMV000720		0.44 (0.30-0.66)
MMV403679		0.13 (0.11-0.14)
MMV001246		0.55 (0.44-0.70)
MMV000642		6.31 (4.25-9.36)
MMV006169		1.15 (0.74-1.79)

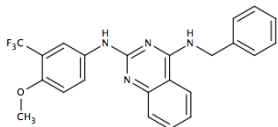
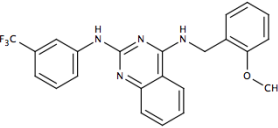
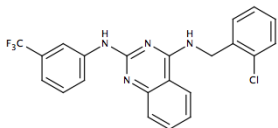
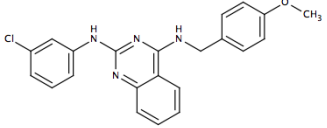
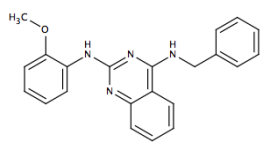
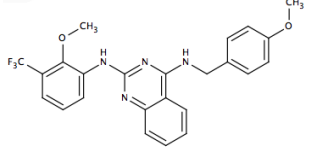
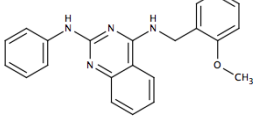
Chapter 2 – Table 3: MMV006169 structural analogs

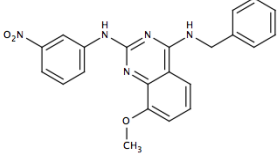
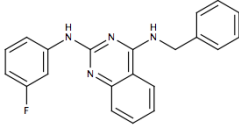
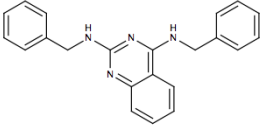
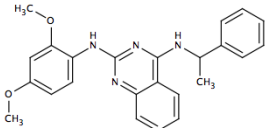
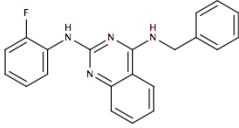
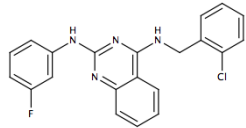
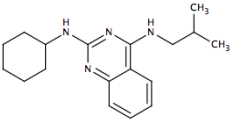
Seventy-four structural analogs of MMV006169 were ordered or synthesized (by Drs. Fanny Tran and Nicholas Westwood at the University of St. Andrews), all containing a conserved 2,4-diaminoquinazoline chemical scaffold. Calculated IC₅₀ values for each analog and corresponding 95% confidence intervals are reported. Excessively wide confidence intervals are reported as “n/a”.

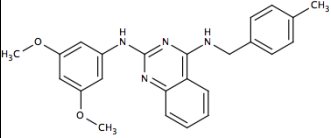
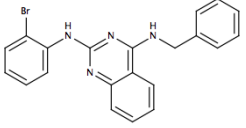
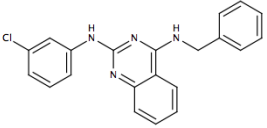
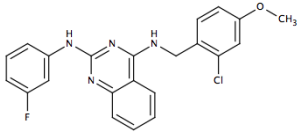
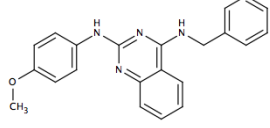
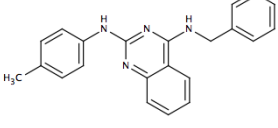
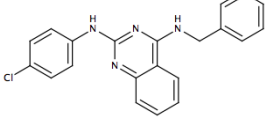
	Structure	<i>T. gondii</i> IC ₅₀ (μM) (95% CI)	<i>C. parvum</i> IC ₅₀ (μM) (95% CI)
MMV006169		1.15 (0.74-1.79)	1.5 (1.16-1.94)
FT14.116.2		0.26 (0.17-0.39)	2.83 (2.36-3.40)
EN01.068.2.3		0.44 (0.34-0.58)	4.09 (2.34-7.15)
EN01.042		0.46 (0.35-0.60)	0.87 (0.62-1.23)
OSSL_723641		0.55 (0.38-0.80)	0.44 (0.38-0.52)

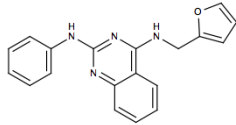
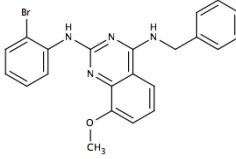
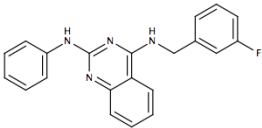
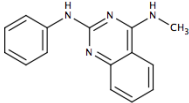
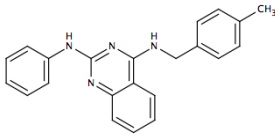
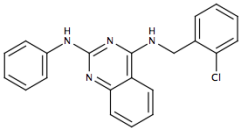
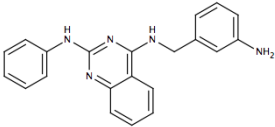
EN01.068.2.5		0.58 (0.31-1.09)	1.08 (0.64-1.80)
OSSL_324342		0.58 (0.46-0.75)	6.19 (2.80-13.69)
PA-Br		0.59 (0.16-2.19)	2.65 (2.30-3.05)
HG014		0.70 (0.25-1.94)	3.45 (3.10-3.84)
PA-01-22		0.74 (0.37-1.49)	>10 (n/a)
FT14.025.2		0.78 (0.52-1.17)	6.58 (4.63-9.36)
FT14.079.2		0.82 (0.34-1.99)	>10 (n/a)

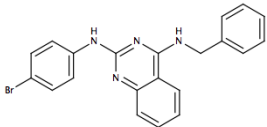
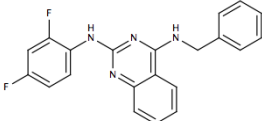
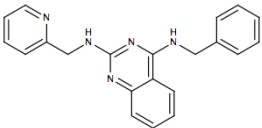
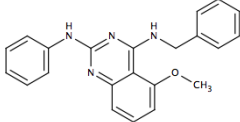
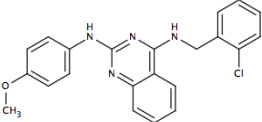
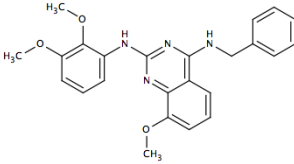
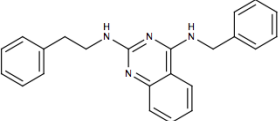
EN01.031		0.88 (0.32-2.41)	0.64 (0.48-0.87)
OSSL_324319		0.93 (0.71-1.20)	8.89 (6.35-12.45)
FT07.032.2		0.96 (0.80-1.16)	>10 (n/a)
CP01009		1.05 (0.58-1.91)	6.62 (6.08-7.22)
PA-01-09		1.06 (0.22-5.01)	5.82 (5.05-6.70)
FT07.031.7		1.01 (0.78-1.31)	>10 (n/a)
HG021		1.03 (0.78-1.36)	>10 (n/a)

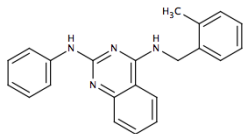
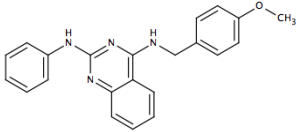
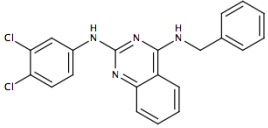
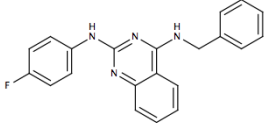
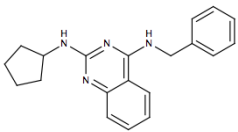
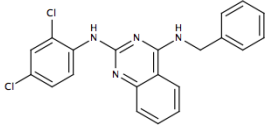
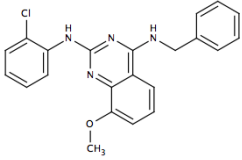
FT14.006.2		1.11 (0.74-1.68)	1.33 (1.00-1.76)
FT14.007.2		1.124 (0.70-1.80)	9.93 (n/a)
OSSL_723668		1.13 (0.57-2.25)	1.74 (1.29-2.39)
OSSL_723788		1.19 (0.89-1.60)	3.92 (1.25-12.32)
OSSL_102463		1.21 (0.81-1.80)	9.50 (n/a)
FT07.031.1		1.26 (1.08-1.47)	>10 (n/a)
EN01.065		1.27 (0.94-1.71)	0.37 (0.26-0.53)

PA-01-20		1.33 (0.72-2.47)	5.35 (4.86-5.88)
OSSL_102470		1.34 (1.07-1.67)	0.93 (0.64-1.40)
OSSL_324373		1.42 (1.04-1.92)	4.73 (3.37-6.62)
OSSL_325124		1.43 (0.96-2.12)	5.50 (4.02-7.53)
OSSL_102466		1.45 (1.07-1.96)	5.60 (2.97-10.58)
FT07.031.6		1.45 (1.01-2.08)	1.03 (0.83-1.29)
FT14.084.1		1.59 (0.94-2.68)	4.63 (3.88-5.53)

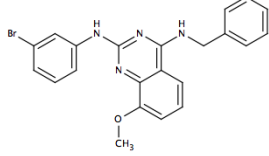
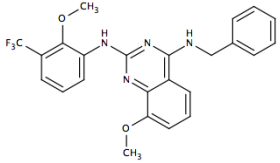
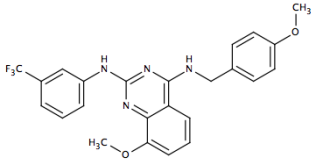
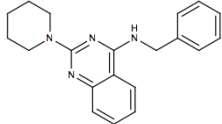
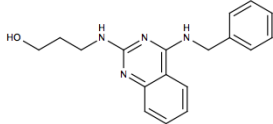
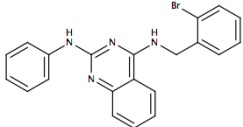
OSSL_723748		1.60 (0.90-2.84)	4.54 (3.23-6.36)
HG009		1.62 (1.13-2.32)	4.35 (3.92-4.83)
OSSL_102469		1.66 (1.29-2.14)	4.12 (1.62-10.47)
FT07.033.2		1.72 (1.55-1.91)	1.03 (0.18-6.08)
AP005		1.79 (0.68-4.71)	1.01 (0.77-1.32)
EN01.098		1.81 (1.34-2.45)	0.98 (0.85-1.14)
OSSL_102476		1.87 (1.55-2.26)	2.69 (1.66-4.37)

EN01.096		1.97 (1.65-2.35)	1.37 (1.15-1.63)
CP01007		1.98 (1.40-2.80)	6.44 (6.06-6.84)
HG019		2.00 (1.48-2.72)	1.41 (1.13-1.75)
FT14.078.4		2.09 (1.78-2.44)	>10 (n/a)
OSSL_723692		2.12 (1.83-2.46)	0.93 (0.77-1.12)
AP002		2.24 (1.26-3.97)	0.46 (0.35-0.61)
HG015		2.31 (1.85-2.89)	2.74 (2.31-3.25)

EN01.115		2.48 (1.68-3.67)	2.41 (2.13-2.72)
OSSL_324325		2.50 (1.63-3.86)	3.40 (1.97-5.85)
OSSL_324381		2.51 (2.07-3.04)	>10 (n/a)
EN01.134		2.55 (2.13-3.05)	1.45 (1.20-1.77)
AP003		2.56 (0.93-7.05)	0.69 (0.54-0.89)
PA-01-26		2.81 (n/a)	3.85 (3.31-4.47)
OSSL_324383		3.09 (2.49-3.83)	3.92 (2.64-5.80)

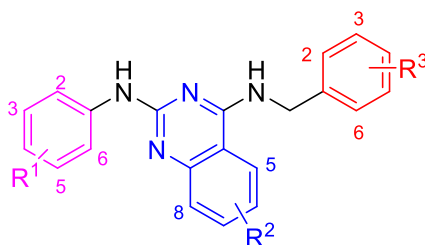
EN01.131		3.10 (2.45-3.91)	0.34 (0.27-0.43)
OSSL_723780		3.22 (2.50-4.15)	1.15 (0.94-1.40)
OSSL_324318		3.30 (2.42-4.50)	4.24 (3.41-5.27)
OSSL_102478		3.33 (2.56-4.33)	1.25 (0.91-1.62)
OSSL_324399		3.36 (2.40-4.72)	1.99 (1.51-2.63)
OSSL_324316		3.69 (3.17-4.29)	>10 (n/a)
CP01004		3.94 (n/a)	4.48 (3.95-5.08)

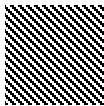

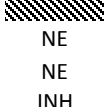


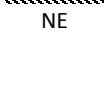
EN01.132		4.69 (4.03-5.46)	0.78 (0.67-0.91)
FT14.095.2		5.69 (3.89-8.33)	0.82 (0.65-1.03)
EN01.095		5.71 (3.95-8.25)	1.68 (1.51-1.87)
PA-01-21		5.96 (n/a)	4.31 (3.66-5.07)
FT14.026.2		6.57 (n/a)	2.33 (1.90-2.87)
OSSL_723607		7.28 (n/a)	>10 (n/a)
PA-01-11		11.54 (n/a)	8.12 (5.32-12.40)

PA-01-12		>18.18 (n/a)	3.76 (3.16-4.47)
PA-01-27		>18.18 (n/a)	9.46 (8.68-10.30)
FT14.027.2		>18.18 (n/a)	>10 (n/a)
OSSL_324334		>18.18 (n/a)	>10 (n/a)
OSSL_324392		>18.18 (n/a)	>10 (n/a)
FT14.092.2		>18.18 (n/a)	0.69 (0.58-0.83)

Chapter 2 – Table 4: SAR for phenotypic separation

Eleven structural analogs of MMV006169 were chosen based on similarities and differences in potency between *T. gondii* and *C. parvum* and/or inclusion of major modifications to the MMV006169 backbone. Analogs are listed from most to least potent against *T. gondii*. INH=inhibitor, NE=no effect, PAR INH=partial inhibition.

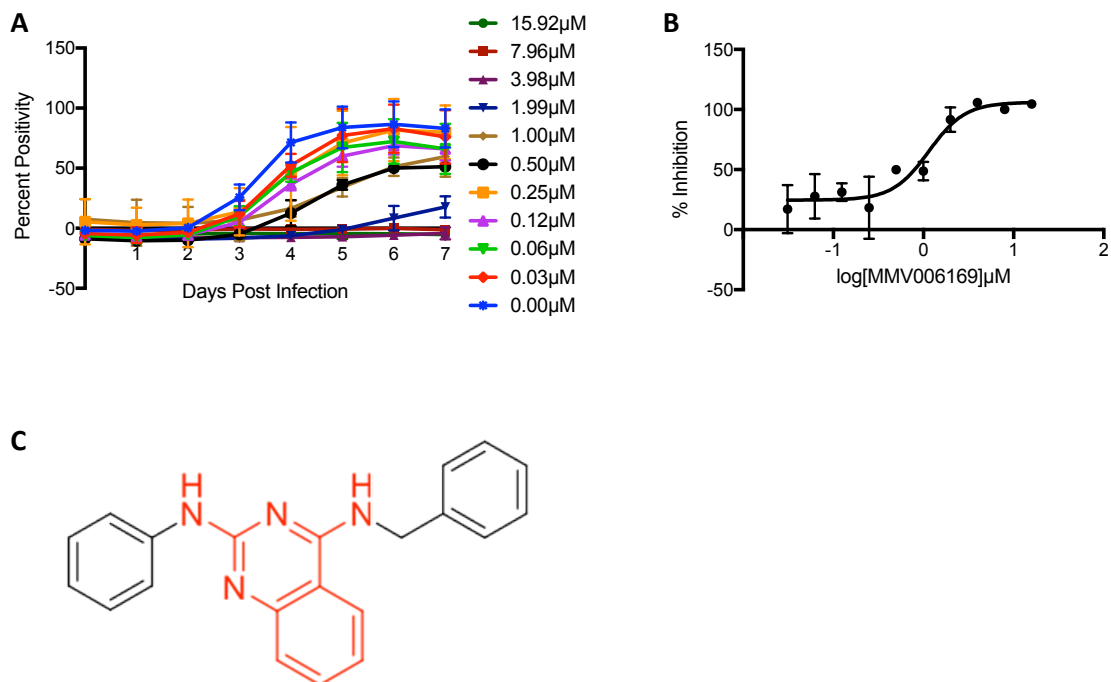


Analog Number	Compound	R ¹	R ²	R ³	IC ₅₀ (μM)		Replication	Invasion
					<i>T. gondii</i>	<i>C. parvum</i>		
-	MMV006169	H	H	H	1.15	1.5	INH	INH
C-1	OSSL_324342	3-CF ₃	H	H	0.58	6.19	INH	INH
C-2	FT14.079.2	NHCH ₃	H	CH ₂ Ph	0.82	>10	INH	
C-3	EN01.031	H	H	3-OMe	0.88	0.64	INH	
C-4	FT07.032.2	3-CF ₃	H	4-OMe	0.96	>10	INH	
C-5	FT07.031.7	2-OMe, 3-CF ₃	H	H	1.01	>10	INH	NE
C-6	FT07.031.1	2-OMe, 3-CF ₃	H	4-OMe	1.26	>10	PAR INH	NE
C-7	EN01.065	H	H	2-OMe	1.27	0.37	INH	INH
C-8	FT14.084.1	Cyclohexane	H	NHCH(CH ₃) ₂	1.59	4.63	INH	
C-9	AP005	4-OMe	H	H	1.79	1.01	INH	
C-10	FT14.078.4	Ph	H	NHCH ₃	2.09	>10	PAR INH	
C-11	FT14.027.2	3-CF ₃	8-OMe	4-OMe	>18.18	>10	NE	NE

Chapter 2 – Table 5: Primers for cloning *T. gondii* CDC48Ap and CDC48Cy

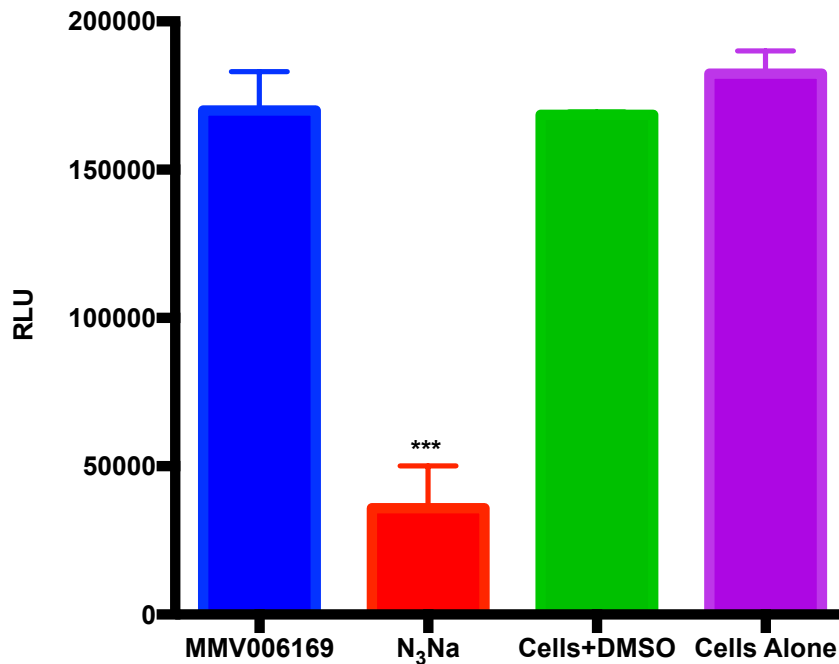
All primers were synthesized by Sigma Aldrich (The Woodlands, TX) with no special modifications. Sequences homologous to pGADT7 are underlined and were used for cloning in yeast.

Primer	Name	Sequence (5'→3'); Sequence homologous to pGADT7 is underlined
1	CDC48ApFw	GAGTACCCATACGACGTACCAGATTACGCTATGGGGACTGCGTGGTGCCC
2	CDC48ApRev	<u>ACAAGCCGACAACCTTGATTGGAGACTTGATC</u> ACTTTGTTTCCTTCGCCG
3	CDC48Ap480Fw	CGATCTATCGACCCAC
4	CDC48Ap978Fw	ATCAAAGTCACCCACAG
5	CDC48Ap1489Fw	GCGTATTGCTTCACGGTT
6	CDC48Ap2007Fw	CAGCTCTGTCTGGAAGCC
7	CDC48Ap2504Fw	AATGGACTCGATCGCGAA
8	CDC48CyFw	<u>GAGTACCCATACGACGTACCAGATTACGCTATGGCCGGCGGCATT</u> CGCAG
9	CDC48CyRev	<u>ACAAGCCGACAACCTTGATTGGAGACTTGACTACGAGTAGAGGTCAT</u> CGT
10	CDC48Cy498Fwd	CGTCCTGTAGAATTCAAG
11	CDC48Cy1018Fwd	TCCTTACCCTCATGGACG
12	CDC48Cy1518Fwd	TACCCTATCGACCATCCT
13	CDC48Cy2002Fwd	TTCTCCAGGCAACGTTGA



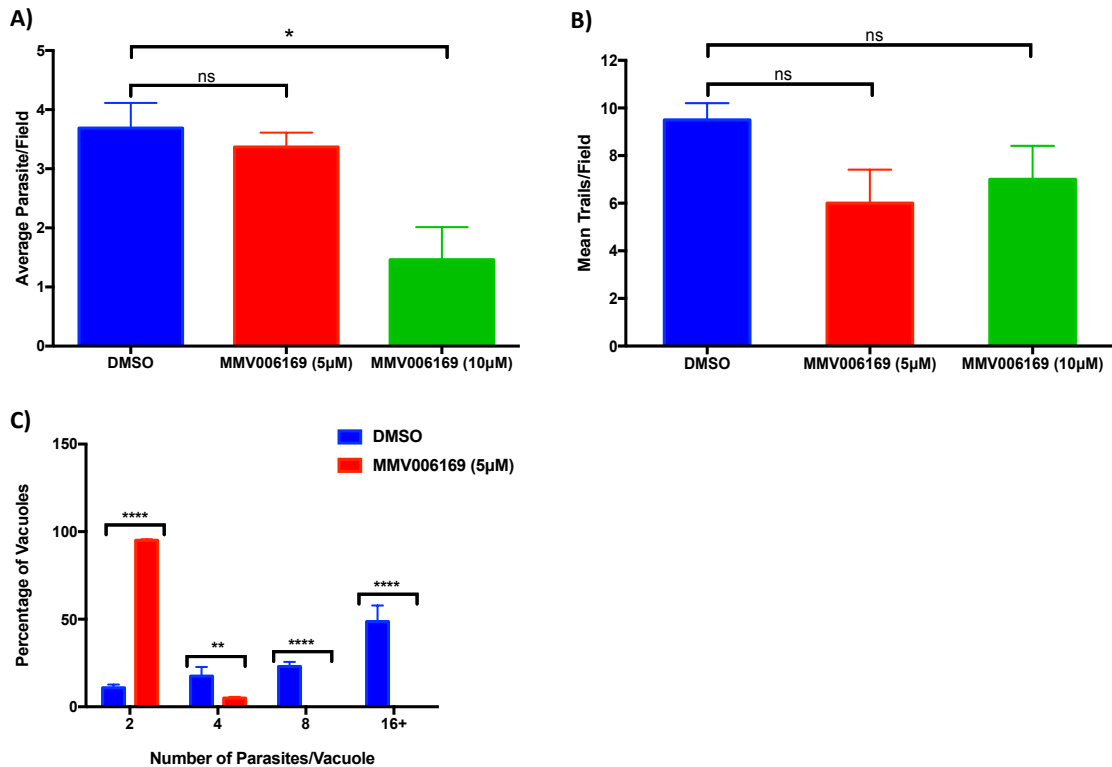
Chapter 2 – Figure 1: Effect of MMV006169 on *T. gondii* growth kinetics

A) YFP-based growth assay using varying concentrations of MMV006169. Values are represented as percent positivity over time. The highest fluorescence reading obtained during screening is assigned 100%, while blank wells containing cells and media are set to 0%. All other values are assigned between those points. B) IC₅₀ curve extrapolated from YFP-based growth assay data. The concentration of MMV006169 necessary to inhibit 50% of parasites is 1.15 μM (95% confidence interval: 0.74-1.79). Error bars represent standard deviation (n=3). C) Structure of MMV006169 with 2,4-diaminoquinazoline scaffold highlighted in red.



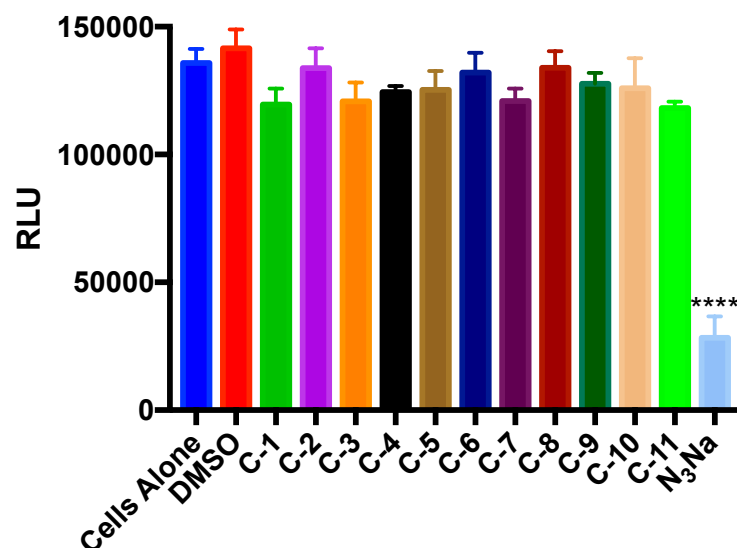
Chapter 2 – Figure 2: MMV006169 is not toxic to HFFs

Viability of host cells was determined via ATPase assay. HFFs were exposed to MMV006169 for 24-hours before host cell lysis and quantification of ATP levels by luminescence. Luminescence is reported as relative luminescence units (RLU). All wells were normalized to a control of HFFs and media with no CellTiter-Glo reagent. Sodium azide was included to represent a “kill control” in which we know the cells are no longer generating ATP. Bars represent mean +/- standard deviation, n=3. Data were analyzed using a one-way ANOVA (**p≤0.001).



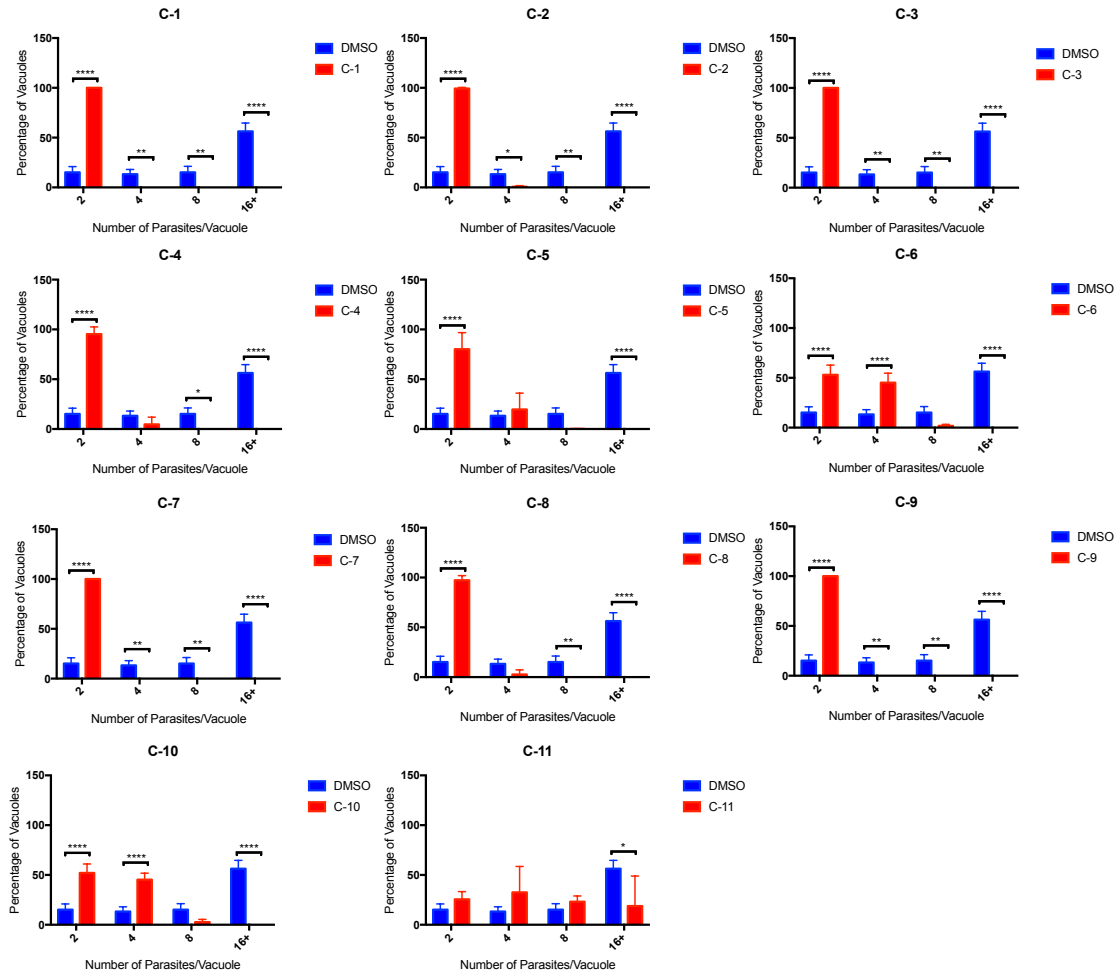
Chapter 2 – Figure 3: MMV006169 inhibits *T. gondii* invasion and replication, not motility.

Effect of MMV006169 on *T. gondii* invasion, motility, and replication. A) MMV006169 inhibits *T. gondii* invasion at 10 μ M. Two color invasion assays were scored blindly by immunofluorescence. (n=3, *p \leq 0.05 as determined by one-way ANOVA). B) MMV006169 does not inhibit *T. gondii* motility. Parasite trails were stained with α -SAG1 antibody and quantified by immunofluorescence (n=3, results analyzed by one-way ANOVA). C) MMV006169 inhibits *T. gondii* replication at 5 μ M. HFFs were infected with 2F1 YFP₂ strain *T. gondii* and grown in the presence (red) or absence (blue) of compound for 36 hours. The average number of parasites per vacuole in vacuoles containing two or more parasites was determined by immunofluorescence (n=3, *p \leq 0.05, **p \leq 0.01, ***p \leq 0.001, **** p \leq 0.0001 as determined by two-way ANOVA).



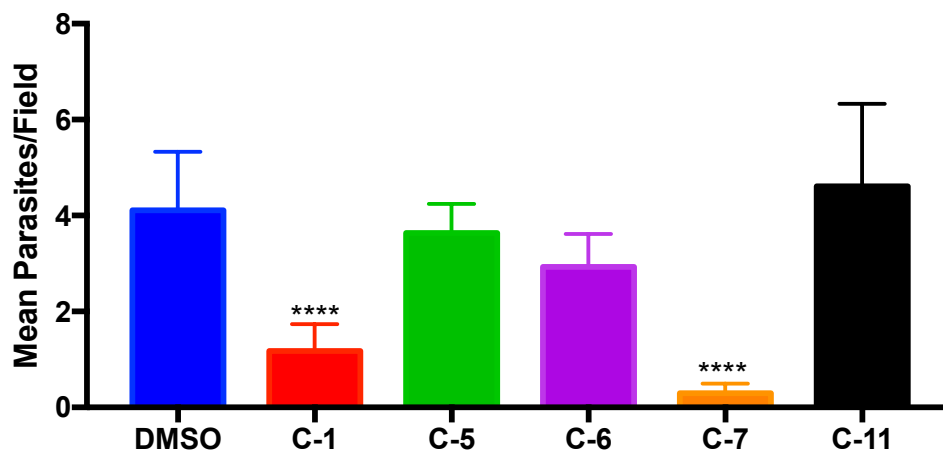
Chapter 2 – Figure 4: MMV006169 analogs are not toxic to host cells after 24 hours

Viability of host cells was determined via ATPase assay. HFFs were exposed to 10 μ M of each analog for 24-hours before host cell lysis and quantification of ATP levels by luminescence. Luminescence is reported as relative luminescence units (RLU). All wells were normalized to a control with no CellTiter-Glo reagent. Sodium azide was included to represent a “kill control” in which we know the cells are no longer generating ATP. Bars represent mean \pm standard deviation, n=3. Data were analyzed using a one-way ANOVA (****p \leq 0.0001).



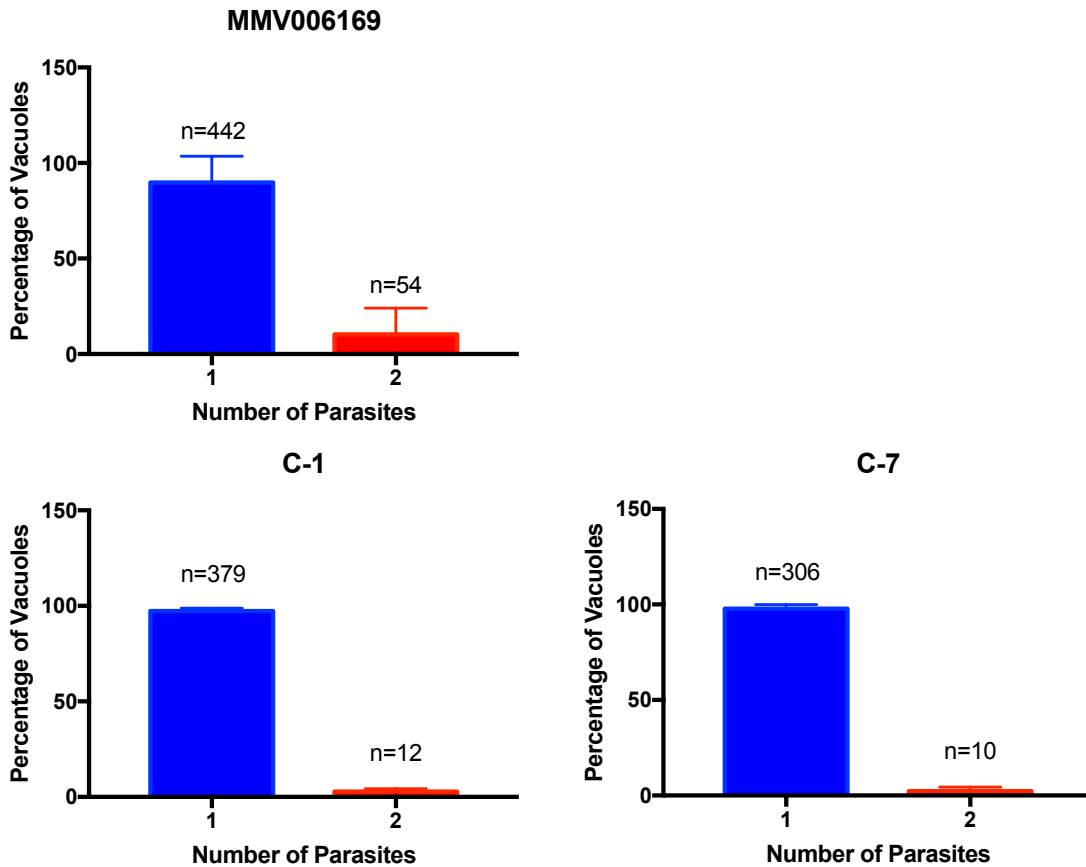
Chapter 2 – Figure 5: Effect of MMV006169 structural analogs on replication

Quantification of *T. gondii* replication after 36 hours. Eleven compounds from the SAR screen were assayed at 5 μ M. The number of parasites per vacuole (in vacuoles containing two or more parasites) was determined at each time point and compared to DMSO-treated controls. (n=3; , * $p \leq 0.05$, ** $p \leq 0.01$, *** $p \leq 0.001$, **** $p \leq 0.0001$ as determined by two-way ANOVA).



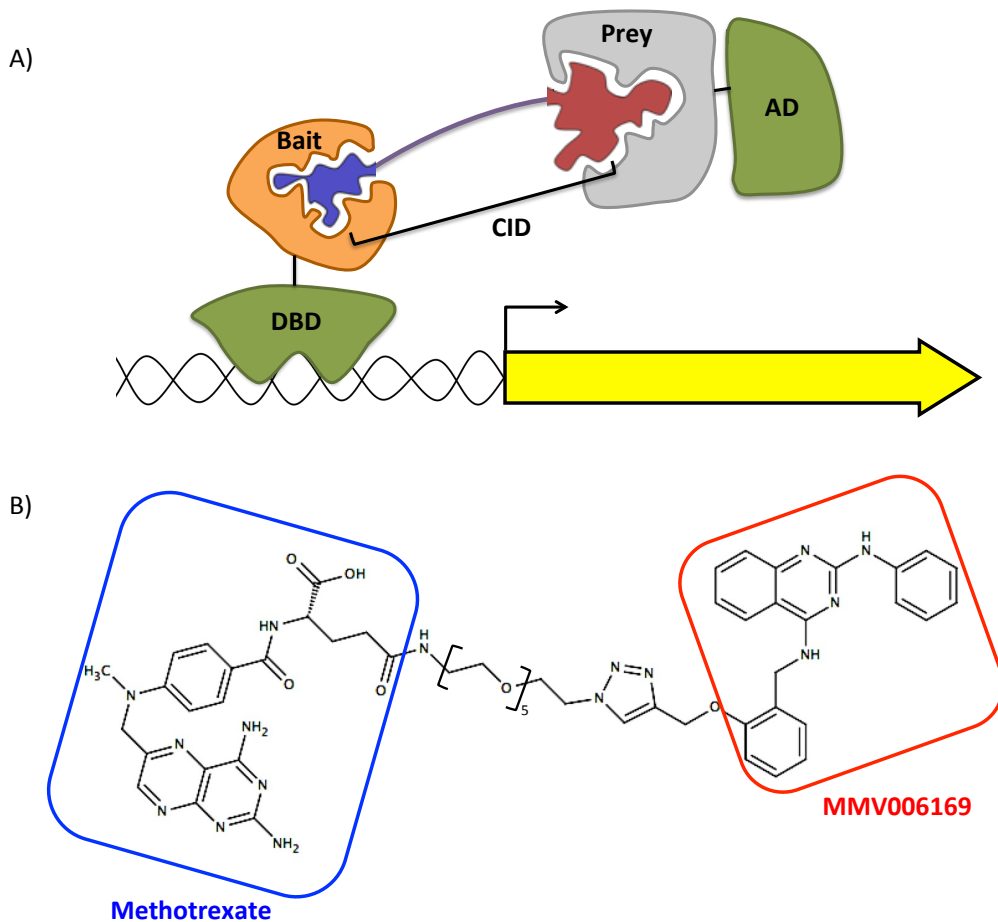
Chapter 2 – Figure 6: Effect of MMV006169 structural analogs on *T. gondii* invasion

Quantification of the ability of *T. gondii* tachyzoites to invade HFFs. Five compounds from the SAR screen were assayed at 10 μ M and scored blindly by immunofluorescence. (n=3; ****p \leq 0.0001 as determined by one-way ANOVA).



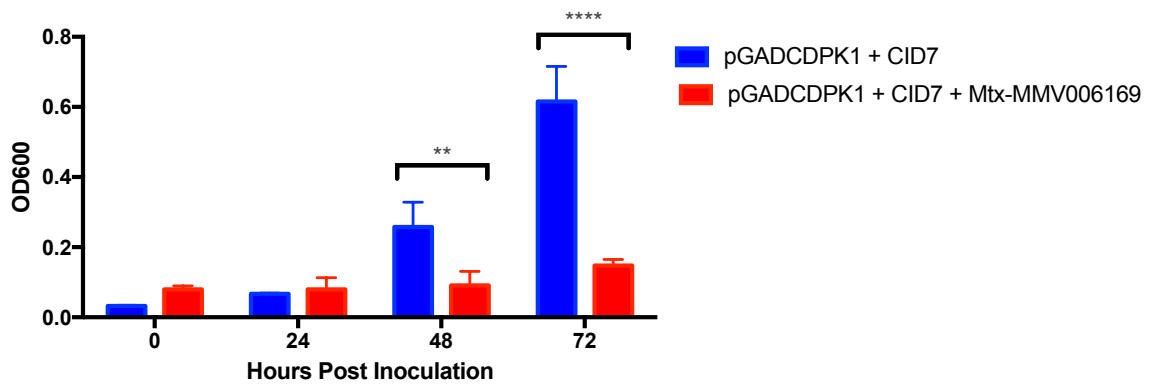
Chapter 2 – Figure 7: MMV006169 structural analogs cannot initiate replication

Quantification of the number of two-parasite containing vacuoles for analogs with the most severe invasion defects. Replication assays were differentially stained for intracellular and extracellular parasites at 36 hours using a standard two-color invasion assay protocol. (n=3, 100 fields per coverslip).



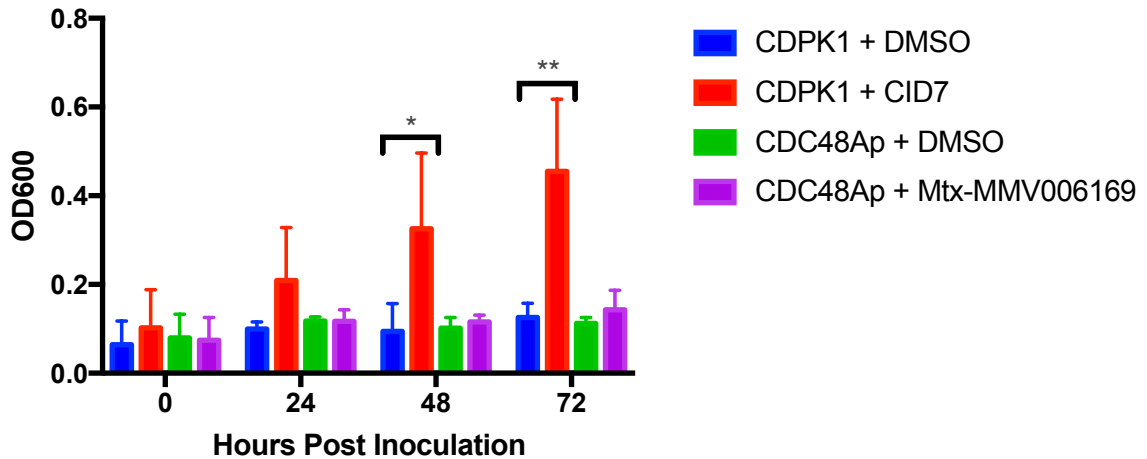
Chapter 2 – Figure 8: Targeted yeast three-hybrid and structure of Mtx-MMV006169

A) Schematic of targeted yeast three-hybrid ternary complex containing the DNA-binding (DBD) and activation domains (AD) of the GAL4 transcription factor (green) and the CID. The CID is comprised of methotrexate (blue) fused to MMV006169 (red) by a flexible linker (purple). The methotrexate moiety of the CID interacts with DHFR and if MMV006169 interacts with either isoform of CDC48, reporter activation will occur. B) Structure of MMV006169-based CID. Methotrexate is outlined in blue, MMV0006169 in red, and the linker is found between the two.



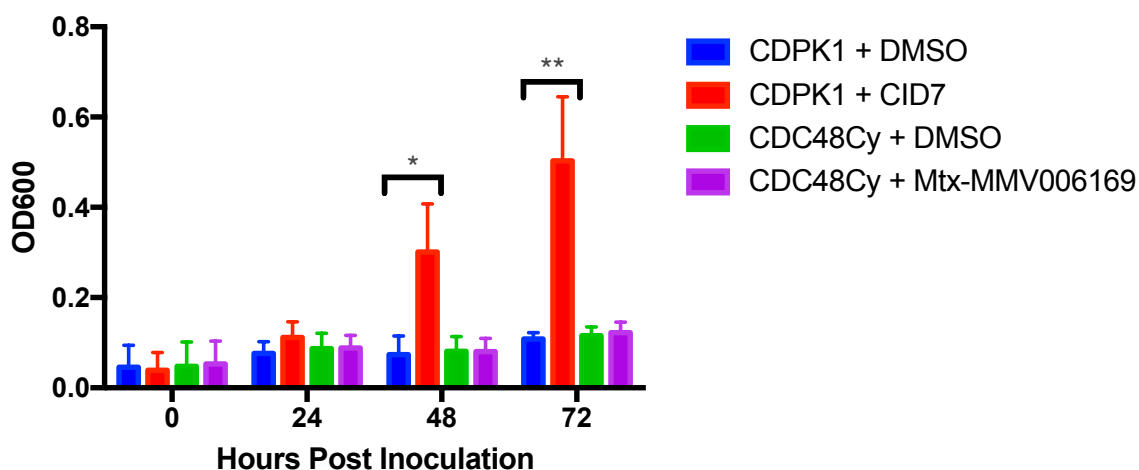
Chapter 2 – Figure 9: CID Competition Assay with Mtx-MMV006169

pGADCDPK1-containing yeast can activate reporter genes and grow in histidine lacking media upon the addition of 25 μ M CID7 (blue bars). The addition of 25 μ M Mtx-MMV006169 to this functioning positive control (red bars) inhibited reporter activation. This implies that Mtx-MMV006169 can enter yeast and compete for binding with CID7. Bars represent mean \pm standard deviation; n=2. Data were analyzed using paired t-tests (** $p \leq 0.01$, **** $p \leq 0.0001$).



Chapter 2 – Figure 10: Targeted yeast three-hybrid liquid growth assay suggests MMV006169 does not interact with CDC48Ap.

Growth of yeast in media lacking histidine is a reflection of reporter activation. The positive control, CDPK1, is able to grow more robustly in the presence of CID7 than in DMSO (red versus blue bars), implying a direct interaction between the CID and CDPK1. CDC48Ap grows to the same level in the presence of Mtx-MMV006169 (purple) and DMSO (green), meaning the histidine reporter gene has not been activated. Bars represent mean \pm standard deviation; $n=3$. Data were analyzed using paired t-tests ($*p \leq 0.05$, $**p \leq 0.01$).



Chapter 2 – Figure 11: Targeted yeast three-hybrid liquid growth assay suggests MMV006169 does not interact with CDC48Cy.

Growth of yeast in media lacking histidine is a reflection of reporter activation. The positive control, pGADCDPK1, is able to grow more robustly in the presence of CID7 than in DMSO (red versus blue bars), implying a direct interaction between the CID and CDPK1. pGADCDC48Cy grows to a similar level in the presence of Mtx-MMV006169 and DMSO (green and purple bars), meaning the histidine reporter gene has not been activated. Bars represent mean \pm standard deviation; $n=3$. Data were analyzed using paired t-tests (* $p \leq 0.05$, ** $p \leq 0.01$).

CHAPTER 3: APPROACHES TO IDENTIFYING THE TARGET(S) OF

MMV006169

3.1 Introduction

Studies aimed at identifying the target of small molecules face a variety of challenges. 1) Is the putative target identified the biologically relevant target? 2) Does the molecule have multiple targets? 3) Is the compound working through the organism of interest or through environmental/host cell mechanisms? To ensure these questions are answered adequately, multiple strategies for target identification are commonly used in parallel. Recent advances in high-throughput screening (Farrell et al. 2012), CID development (Tran et al. 2013), and the CRISPR/Cas9 system for gene deletions (Shen et al. 2014, Sidik et al. 2014, Sidik et al. 2016) have assuaged the process of target confirmation.

Full genome mutagenesis-based approaches for initial target identification have been successful in the study of *T. gondii* using several mutagens (Pfefferkorn and Pfefferkorn 1979, Morrissette et al. 2004, Gubbels et al. 2008, Coleman and Gubbels 2012, Farrell et al. 2014) and have led to the isolation of mutants resistant to varying levels of compound. However, if the target of these molecules is essential, the resistant mutants often have mutations in drug transporters, which render the parasite resistant without providing direct target information. This approach is also less informative if the compound has more than one target, as one may not be able to distinguish between partial compound resistance in phenotypic assays.

We have recently shown that a yeast three-hybrid approach to target identification can be useful for probing the *T. gondii* genome (Odell et al. 2015). Yeast three-hybrid has the advantage of examining protein-small molecule interactions without directly inhibiting the parasite life cycle. The interaction is first identified in yeast, and can then be brought back into the parasite for target confirmation. This approach is beneficial in that it allows one to look at essential genes and to identify more than one target at a time.

Here, we present approaches towards the identification of target(s) of the Medicines for Malaria Venture compound MMV006169. We have previously shown that MMV006169 inhibits the growth of both *T. gondii* and *C. parvum* (Bessoff et al. 2014), and specifically reduces *T. gondii* invasion and replication, with no effect on motility (Chapter 2). We examined the possibility of MMV006169 interacting with TgCDC48Cy or TgCDC48Ap based on structural similarities between MMV006169 and a known p97 inhibitor (Chapter 2) (Chou et al. 2011). Targeted yeast three-hybrid experiments to determine if MMV006169 could interact with TgCDC48Cy or TgCDC48Ap came up negative, suggesting the compound is working through an interaction with a different parasite and/or host cell protein target. The work in this chapter describes whole genome mutagenesis attempts to generate parasites resistant to MMV006169 and its analogs. Yeast three-hybrid library screens are performed identifying a putative host cell protein target for MMV006169, whose *T. gondii* isoforms show no interaction with MMV006169 by targeted yeast three-hybrid.

3.2 Materials and Methods

3.2.1 Parasite culture

T. gondii RH $\Delta h x g p r t \Delta k u 8 0$ and 2F1 YFP₂ tachyzoites (Gubbels et al. 2003), kindly provided by Dr. Marc-Jan Gubbels, were passaged serially in confluent monolayers of human foreskin fibroblasts (HFFs) maintained at 37°C (5% CO₂ and constant humidity) in Dulbecco's Modified Eagle's Medium (DMEM), supplemented with 10mM HEPES, pH 7.2, 10 units/mL penicillin G sodium salt, 10 units/mL streptomycin sulfate, and containing 1% heat-inactivated fetal bovine serum as previously described (Roos et al. 1994).

3.2.2 N-ethyl-N-nitrosourea titration and plaque assay

Titration of N-ethyl-N-nitrosourea (ENU) was performed as previously described with the following modifications (Coleman and Gubbels 2012, Farrell et al. 2014). Upon fresh lysis, 1 mL of 2F1 YFP₂ tachyzoite were plated on a confluent T25 tissue culture flask of HFFs and incubated at 37°C for 24 hours in Ed1 medium. Medium was replaced with 10 mL of Ed1 diluted (1:10) in DMEM and incubated at 37°C for 10 minutes. ENU was added in 0, 14.6, 29.3, 58.6, or 117 μ L volumes (0.85M stock in DMSO) per flask (working dilutions of ENU will be 1.25, 2.5, 5, and 10 mM, respectively) and DMSO such that total is 117 μ L for each flask. Flasks were incubated for 4 hours in at 37 °C and then washed with cold sterile PBS before harvesting by syringe release, passage through a 3- μ m Nuclepore filter (Whatman, Piscataway, NJ), and gently pelleting for 4 minutes at 1,100 x g. 10,000 parasites in 3 mL of Ed1 media were

added to one well in a 6-well plate. Parasites were serially diluted 10-fold across the remaining wells. Plates were incubated at 37°C for 7 days to allow plaques to form. After incubation, medium was aspirated and cell monolayers were fixed with 100% ethanol. Monolayers were stained using crystal violet solution containing 2% w/v crystal violet and 0.8% w/v oxaloacetate in ethanol, washed with PBS, and then air dried at room temperature.

3.2.3 ENU mutagenesis

Mutagenesis was performed as previously described with a few modifications (Coleman and Gubbels 2012, Farrell et al. 2014). One milliliter of freshly lysed 2F1 YFP₂ parasites (in Ed1 media) were seeded onto a confluent monolayer of HFFs in a T25 tissue culture flask and incubated at 37°C for 24 hours. Medium was replaced with 10 mL of Ed1 diluted 1:10 in DMEM and placed at 37°C for 10 minutes. Flasks were treated with 72.7 µL ENU (100 mg/mL stock in DMSO) for 4 hours at 37°C. Each flask was washed three times with cold filter sterilized PBS. Monolayers were harvested by syringe release, passed through a 3-µm Nuclepore filter (Whatman, Piscataway, NJ) to eliminate host cell debris, and gently pelleted (1,100 x g) for 4 minutes. The entire pellet was added to a single T25 tissue culture flask and allowed to lyse naturally. Mutagenized parasites were then passaged in media containing the EC₉₀ of each compound of interest.

3.2.4 Compound-induced cyst staining

HFFs were grown to confluence on 12 mm circular coverslips in 12-well plates. MMV006169 resistant parasites were harvested by syringe release, passed through a 3- μ m Nuclepore filter (Whatman, Piscataway, NJ) to eliminate host cell debris, and gently pelleted (1,100 x g, 4 minutes). Parasites were added to each coverslip at a multiplicity of infection of 4×10^5 in the presence of 3 μ M MMV006169. After 7 days, coverslips were incubated in fixative solution (1X PBS + 4% v/v paraformaldehyde) for 20 minutes, permeabilized (1X PBS + 0.25% v/v Triton X-100) for 15 minutes, and blocked for 30 minutes in 1X PBS + 1% w/v bovine serum albumin. Coverslips were incubated for 30 minutes in rabbit polyclonal anti-*Toxoplasma* (1:2000, catalog #90700556; AbD Serotec, Raleigh, NC) and then with goat anti-rabbit IgG conjugated to Alexa 488 (Invitrogen, 2mg/mL) at a 1:500 dilution together with TRITC-conjugated *Dolichos biflorus* lectin (Sigma-Aldrich, St. Louis MO) at a dilution of 1:100 for 60 min. 2F1 YFP₂ parasites treated with DMSO for 24 hours were included as a control. Coverslips were sealed to the surface of glass slides using nail polish and visualized at 100X on a Nikon Eclipse TE300 epifluorescence microscope.

3.2.5 YFP-based growth assay

Growth of *T. gondii* strain 2F1 YFP₂ parasites was monitored as described previously (Gubbels et al. 2003) with several modifications. Both parasites and HFFs were continuously cultured in HyClone DMEM/high modified medium without phenol red (Thermo Fisher Scientific) containing 1 or 10% v/v heat-inactivated fetal bovine serum (FBS). Medium was supplemented with 10 units/mL penicillin G sodium salt, 10

units/mL streptomycin sulfate, 10 mM HEPES, pH 7.2. Special Optics black/clear 384-well tissue culture-treated plate (BD Falcon) were seeded with 5×10^3 HFFs (in 50 μ L medium containing 10% v/v FBS) and grown at 37°C (5% CO₂ with constant humidity). Upon confluence, wells were washed with culture medium containing 1% v/v FBS. Thirty microliters of culture medium containing 1% v/v FBS was added to each well. 2F1 YFP₂ tachyzoites were syringe released, passed through a 3- μ m Nuclepore filter (Whatman, Piscataway, NJ), and gently pelleted (1,100 x g) for 4 minutes. Parasites were resuspended in culture medium supplemented with 1% v/v FBS and diluted to 1×10^5 parasites/mL. Twenty microliters of medium containing 2,000 parasites was added to each test well. Serially diluted test compounds were added to each well in a 5 μ L volume. Plates were incubated at 37°C in 5% CO₂ (constant humidity) and fluorescence was read daily for 8 days from the bottom of the plate with the lid in place using a Synergy 2 microplate reader (BioTek, Winooski, VT; excitation 485/20 and emission 528/20). Pyrimethamine was included as a positive control in each plate. The IC₅₀ of each compound was determined as described previously (Bessoff et al. 2014).

3.2.6 cDNA library preparation and negative selection

A previously generated *T. gondii* oligo-dT primed cDNA library containing 2.4×10^6 total CFU with an average insert size of 1.65 kb in the vector pGADT7 (generously provided by Dr. Michael White, University of South Florida) and the vector pGBKeDHFR was used to transform competent BAPJ69-4A yeast cells as described (Kvaal et al. 2002, Baker et al. 2003, Clontech 2007, Shaffer et al. 2012). The resulting

transformed yeast culture was plated on 50 x 150 mm diameter yeast drop out media plates containing 2% w/v glucose and lacking leucine and tryptophan (SC +Glu –trp –leu) and incubated at 30°C for 5 days. Plates were then placed at 4°C overnight to harden the media. Transformants were pooled by flooding each plate with 3 mL 1xTE buffer and scraped with a rubber policeman. All yeast was pooled, resuspended in glycerol solution, and frozen in aliquots containing 4.35×10^7 CFU/mL.

Negative selection was performed on a freshly thawed aliquot of pre-transformed yeast (containing library and pGBKeDHFR) by plating it on 20 x 150 mm plates of drop out media (SC +Glu –trp –leu) containing 0.5 g/L 5-fluoroorotic acid (5-FOA, Zymo Research) similar to that previously described (Chidley et al. 2011). The surviving yeast transformants were pooled and aliquoted at 2×10^7 CFU/mL. A single aliquot of yeast is thawed for each library screen.

3.2.7 Titering 3-Amino-1, 2, 4-triazole (3-AT) for library screens

A 5M solution of 3-AT (MP Biomedicals) was two-fold serially diluted and plated (SC +Glu –trp –leu) such that final concentrations of 5 mM, 2.5 mM, 1.25 mM, 0.63 mM, and 0.31 mM were obtained. The positive control CID7 (or DMSO) was spread onto each plate at a final concentration of 5 μ M. Plates were allowed to incubate at room temperature overnight in the dark. Library containing yeast was then plated at 7×10^7 CFU/mL and incubated at 30°C for 7 days. Colonies on each plate were marked and recorded daily until a lawn was seen on plates containing CID7 with no 3-AT. The

concentration of 3-AT in which no growth was seen on DMSO control plates, but was seen upon CID treatment was used in all future experiments.

3.2.8 Yeast three-hybrid library screens

On the day prior to each library screen, CID was spread onto yeast drop out media containing 2% w/v glucose selective for the cDNA library (leucine), DNA-binding domain (pGBKeDHFR, tryptophan), and the histidine reporter gene (SC +Glu –trp –leu –his) at a chosen concentration (25 mM for Mtx-MMV006169). 3-AT was also spread on each plate at a final concentration of 1.25 mM. These plates were left at room temperature overnight to allow the CID and compound to absorb into the yeast media. A negative control plate was set up in parallel containing DMSO in place of CID. A library aliquot was removed from -80°C, diluted, counted, and plated at 5×10^7 CFU/mL (20x library coverage). Plates were incubated at 30°C and monitored daily until growth was seen on negative control (DMSO + 3-AT) plates.

3.2.9 Yeast three-hybrid reporter confirmation

Confirmation of reporter gene activation was done similarly to that previously published with several modifications (Odell et al. 2015). A single colony of yeast isolated from a yeast three-hybrid library screen was used to inoculate 3 mL of synthetic complete media supplemented with glucose lacking tryptophan and leucine (SC +Glu –trp –leu) and incubated with shaking for 48 hours. On the day of the assay, 200 µL of yeast was sub-cultured into 4 mL of SC +Glu –trp –leu and incubated for 4 hours until the yeast

reached log phase. The yeast was counted and diluted to 2×10^5 cells/mL and 25 μ L was used to inoculate the wells of a 96-well plate (BD Falcon) containing 125 μ L SC +Glu – trp –leu –his. Wells were also treated with 1.5 μ L of 2.5 mM CID (or DMSO) and 1.5 μ L of 50 mM 3-AT to reduce background growth. Media alone (150 μ L) with 1.5 μ L DMSO and 1.5 μ L 3-AT were included as negative control. A positive control including 125 μ L media, 1.5 μ L 2.5 mM CID7, 1.5 μ L 50 mM 3-AT, and 25 μ L (2×10^5) yeast expressing pGBKeDHFR and pGADBRADIN were included in each assay plate. Plates were parafilmmed and incubated with shaking (200 rpm). The OD₆₀₀ for each well was recorded daily from the bottom of the plate with the lid in place using a Synergy 2 microplate reader (BioTek, Winooski, VT). The assay was terminated with robust growth was observed in positive control wells.

3.2.10 Construction of pGADNDH2-1 and pGADNDH2-2

Plasmid construction was completed using restriction enzymes and Phusion high fidelity polymerase purchased from New England BioLabs (Ipswich, MA). All primers were synthesized by Sigma Aldrich (The Woodlands, TX). To construct pGADNDH2-1, pGADT7 (Clontech Laboratories, Mountain View, CA), was digested with SacI and NdeI. TgNDH2-1 was amplified from RH Δ *hxgprt* Δ *ku80* cDNA using primers 14 and 15 (Chapter 3 – Table 3). Gel extracted digested plasmid and the TgNDH2-1 PCR product were co-transformed into competent AH109 yeast as previously described (Gietz and Schiestl 2007). Transformants were selected on yeast drop out plates (SC +Glu –leu) and incubated at 30°C for 48 hours. The resulting plasmid was screened by restriction digest

and sequenced using primers 16 and 17 (Chapter 3 – Table 3). pGADNDH2-2 was cloned as described above using primers 18-22.

3.2.11 Targeted yeast three-hybrid liquid assay

To perform targeted yeast three-hybrid assays a plasmid containing the hypothesized MMV006169 target (pGADNDH2-1 or pGADNDH2-2) and a plasmid encoding *E. coli* dihydrofolate reductase fused to the Gal4 DNA-binding domain (pGBKeDHFR) was co-transformed into competent BAPJ69-4A yeast cells (a generous gift from Dr. Donald Doyle, Georgia Institute of Technology), plated on yeast drop out plates (SC +Glu –trp –leu) and grown at 30°C. A single colony of the resulting co-transformants was grown overnight in 3 mL of synthetic complete liquid media (SC +Glu –trp –leu). After 24 hours, 200 µL of the yeast culture was used to inoculate 4 mL of SC +Glu –trp –leu and incubated for 4 hours with shaking (200 rpm). Log phase cells (determined by OD₆₀₀) were counted and diluted to 2x10⁵ cells/mL. 25 µL was used to inoculate each test well in a 96-well plate (BD Falcon) containing 125 µL SC +Glu –trp –leu –his. CID (1.5 µL of 2.5 mM or DMSO) and 3-AT (1.5 µL of 50 mM) were added to test wells. As a negative control, 1.5 µL DMSO and 1.5 µL 3-AT were added to well containing 150 µL of media alone. BAPJ69-4A strain yeast expressing pGBKeDHFR and a plasmid encoding the Gal4 activation domain fused to TgBRADIN (Odell et al. 2015) were used as a positive control (125 µL media, 1.5 µL 2.5 mM CID7, 1.5 µL 50 mM 3-AT, and 25 µL yeast). Plates were sealed with parafilm and incubated with shaking (200 rpm) at 30°C. With the lid in place, the OD₆₀₀ for each well was recorded from the

bottom of the plate using a Synergy 2 microplate reader (BioTek, Winooski, VT). Plates were read daily and the assay was terminated when robust growth was observed in positive control wells.

3.3 Results

3.3.1 Isolation of MMV006169 resistant mutants

In an attempt to identify the target(s) of MMV006169, we implemented a whole genome mutagenesis approach that has previously proven successful in the study of *T. gondii* (Pfefferkorn and Pfefferkorn 1979, Morrissette et al. 2004, Gubbels et al. 2008, Coleman and Gubbels 2012, Farrell et al. 2014). We used N-ethyl-N-nitrosourea (ENU), a DNA alkylating agent, which works primarily by nucleotide substitution with a preference for A-T to T-A transversions or A-T to G-C transitions (Acevedo-Arozena et al. 2008, Farrell et al. 2014). This approach allows us to interrogate the entire genome, including essential genes, which is not possible using other deletion or gene interruption-based techniques. It was previously shown that by inducing 70% killing of parasites, one could generate a parasite line with 10-100 mutations per genome (Pfefferkorn and Pfefferkorn 1979, Farrell et al. 2014). Since ENU is unstable in liquid stocks, we began by titering and pre-aliquoting our mutagen to avoid further freeze thaw cycles. By exposing parasites to varying concentrations of mutagen and performing plaque assays on each population, we determined that treating parasites at a final concentration of 6.31 mM of ENU was adequate to induce 70% killing (Chapter 3 – Figure 1).

Using this concentration of mutagen we performed upwards of 20 attempts to generate parasite lines resistant to the parent compound (MMV006169), OSSL_324342 ($IC_{50}=0.58 \mu\text{M}$), OSSL_732641 ($IC_{50}=0.55 \mu\text{M}$), and with OSSL_324373 (DBeQ, $IC_{50}=1.42 \mu\text{M}$) (Chapter 2 – Table 3). These analogs were chosen based on potency. Despite changing the mutagenesis protocol, varying compound concentrations, and long-term culturing in compound, we were unable to generate resistant parasite lines to any compound other than MMV006169. We isolated nine clones with some level of resistance to MMV006169, and saw a maximum shift in IC_{50} of 3.6-fold above the non-mutagenized control (Clone 3, $4.41 \mu\text{M}$, Chapter 3 – Table 1). However, we noted that these resistant parasites were never able to naturally egress from host cells. Instead, they stained positively with *Dolichos biflorus* lectin indicative of tissue cyst formation (Chapter 3 – Figure 2). This suggests that prolonged exposure to compound or the mutations created during ENU exposure resulted in differentiation into bradyzoites. Based on the lack of a robust shift in IC_{50} and the knowledge that other groups have been unable to isolate resistant mutants against related analogs (Jon Boyle, personal correspondence), we decided to implement an alternate strategy for target identification.

3.3.2 Yeast three-hybrid system optimization

As an alternate approach to identifying the target(s) of MMV006169, we performed library-scale yeast three-hybrid experiments to examine its target profile. As false-positives are a common constraint in yeast three-hybrid experiments, we implemented a negative selection step to minimize these interactions (Chapter 1 – Figure

5). We used the yeast strain BAPJ69-4A, which was generated such that the reporter *URA3* was inserted into the HO locus under the control of a GAL4 inducible promoter, and media containing 5-fluoroorotic acid (5-FOA) for this selection (Chidley et al. 2011, Shaffer et al. 2012). In yeast without functional *URA3*, which encodes OMP decarboxylase, 5-FOA is converted to 5-fluorooritidine monophosphate (5-FOMP), which is not harmful to the cell. However, in the presence of functional OMP decarboxylase, 5-FOMP is converted to 5-fluorouridine monophosphate, a competitive inhibitor of thymidylate synthase, and is thus toxic to the cell. This means that anything expressing *URA3* in the absence of a functional transcription factor will be killed. Yeast that survives this selection is pooled and used in conjunction with CID to perform our full-scale library screens.

Titering of 3-amino-1, 2, 4-triazole (3-AT) also proved important in our library screens. 3-AT is a competitive inhibitor of the *HIS3* gene, which encodes imidazoleglycerol-phosphate dehydratase. The *HIS3* reporter has been shown to be leaky, meaning that low levels of the gene product are expressed in the absence of CID (Van Criekeing and Beyaert 1999). To counter this leakiness, 3-AT can be added to kill anything expressing low levels of *HIS3* (Durfee et al. 1993, Fields 1993, Clontech 2007). We spread concentrations of 3-AT ranging from 0.31 μM – 5 μM and either DMSO or a positive control CID7 onto each plate. Library-containing yeast was then plated and the number of yeast colonies present on each plate was recorded daily for seven days (Chapter 3 – Table 2). We chose to use 3-AT at 1.25 μM , which inhibited background growth (DMSO plates) but allowed growth of yeast in the presence of CID.

3.3.3 A host cell target for MMV006169

Screening of the negatively selected cDNA library with Mtx-MMV006169 presented 18 clones encoding a potential CID-interacting protein. Each clone was analyzed in a reporter activation assay, where yeast growth is dependent on its ability to synthesize histidine. We isolated a single clone (#14) capable of growing robustly in media lacking histidine (Chapter 3 – Figure 3). Sequencing analysis revealed that this clone contained the C-terminal 867 base pairs of the gene encoding human NADH dehydrogenase subunit 2 (ND2; accession: P03891). ND2 is a component of complex 1 of the electron transport chain, which plays a role in oxidation of NADH to NAD, proton pumping, and the shuttling of electrons to ubiquinone (Kerscher et al. 2008). It has been previously shown that both quinolones and quinazolines can inhibit complex 1 function, but inhibition is typically toxic to the host cell (Degli Esposti 1998, Li et al. 2003). Our initial analysis of toxicity at 24 hours showed no evidence of host cell toxicity (Chapter 2 – Figure 4), however, upon extension of our toxicity analysis we found EN01.065 is toxic to host cells after longer periods of exposure (Chapter 3 – Figure 4). This suggests that EN01.065 may be working by inhibiting ATP production.

In contrast to the proton-pumping NADH dehydrogenase (complex 1) found in mammalian cells, *T. gondii* has 2 isoforms of type II, non-proton pumping NADH dehydrogenases (TgNDH2-1 and TgNDH2-2) (Saleh et al. 2007). It has been previously shown that HDQ, a quinolone, can directly inhibit TgNDH2-1 resulting in a defect in parasite replication (Lin et al. 2008). Since it is known that both quinolones and

quinazolines can inhibit mammalian complex I, we hypothesized that quinazolines may also be able to inhibit *T. gondii* NADH dehydrogenases. To test this, we cloned both isoforms (TgNDH2-1 and TgNDH2-2) into our yeast expression vectors and performed targeted yeast three-hybrid experiments using Mtx-MMV006169. Neither isoform resulted in reporter activation in this system, suggesting that MMV006169 does not interact with TgNDH2-1 or TgNDH2-2, but may actually be working through host cell ND2 (Chapter 3 – Figure 5).

3.4 Discussion

Small molecule target identification has been performed using a broad range of approaches, including affinity chromatography, phage-display libraries, whole genome mutagenesis, and yeast three-hybrid experiments (see Chapter 1 for comprehensive review). We recently screened the Medicines for Malaria Venture Open Access Malaria box (Chapter 2) (Bessoff et al. 2014). In that work, we show that MMV006169 is a potent inhibitor of *T. gondii* growth, more specifically invasion and replication. In this study, we present the results of *T. gondii* whole genome mutagenesis to attempt to identify the target(s) of MMV006169. We attempted to generate mutants against MMV006169 and three structural analogs (OSSL_324342, OSSL_732641, and OSSL_324373), both at the IC₅₀ and EC₉₀ of each compound as determined by YFP-based growth assay (see Chapter 2 for further detail). We were only able to generate mutants resistant to MMV006169 at its EC₉₀ (3.2 μM). Of the 9 clones isolated, only a maximum of 3.6-fold increase in the IC₅₀ of MMV006169 was observed. Previous work

with other compounds has shown that resistance is not always associated with large changes in the IC_{50} . For example, Morrissette et al. isolated several different mutations in α -tubulin that conferred oryzalin resistance, but were associated with different changes in the IC_{50} (2 μ M or 25 μ M) compared with the original IC_{50} of oryzalin (Morrissette et al. 2004). The same phenomenon was reported by Nagamune et al. who saw a 2 to 3-fold increases in the IC_{50} of artemisinin in resistant parasites compared to wild-type (Nagamune et al. 2007). However, the fact that we also could not generate mutants resistant to additional structural analogs, and the failure of other labs to do so (Jon Boyle, personal correspondance), led us to suspect that the molecule has more than one parasite target or it is working exclusively on host cells. The former hypothesis is supported by the fact that structural analogs of MMV006169 show varying effects on *T. gondii* invasion and replication (Chapter 2). Additionally, work on a related analog (resynthesized and screened as FT14.116.2, Chapter 2 – Table 3) shows C5 inhibits *T. gondii* motility, but not invasion (Kamau et al. 2012), further suggesting the likelihood of the analogs hitting multiple targets.

In this chapter, we presented preliminary data suggesting that an MMV006169-resistant parasite line differentiates into bradyzoites when grown in the presence of compound. Since the genome of these parasites was never sequenced, we cannot confirm that they contained any point mutations rendering them truly resistant. This implies that treating tachyzoites with MMV006169 for prolonged periods of time results in their differentiation to bradyzoites. It is known that parasites will undergo differentiation as part of a stress response when exposed to different pharmacological and physical triggers

(Sullivan and Jeffers 2012). Interestingly, it has also been shown that bradyzoites continue to replicate within tissue cysts at a rate much slower than tachyzoites (Watts et al. 2015). This led us to wonder if the parasites quantified in our replication assays were, in fact, bradyzoites and not tachyzoites. To test for a heightened stress response we can expose parasites to media of varying alkalinity (7.2-8.2) and look for differences in their ability to differentiate (Hong et al. 2016). If MMV006169 does cause a heightened stress response, compound exposure at pH 8.2 will result in a greater level of differentiation compared to untreated parasites. The same may hold true for lower pH (7.4 or 7.8) media, which doesn't normally stimulate differentiation of wild-type parasites. Determination of the exact step in which stage conversion occurs will be the subject of future studies.

In an attempt to identify the target(s) of MMV006169, we implemented a yeast three-hybrid approach, with which we have been successful in the past (Odell et al. 2015). Our screening attempts suggest that MMV006169 may function by inhibiting human NADH dehydrogenase subunit 2 (ND2), a critical part of complex 1 of the electron transport chain. Complex 1 is comprised of 46 different subunits, 7 of which (ND1-6 and ND4L) are mitochondrially encoded (Chomyn et al. 1985, Attardi et al. 1986, Chomyn et al. 1986, Voet et al. 2008). The complex is divided into three functional units, a dehydrogenase, hydrogenase-like, and transport unit (Friedrich and Scheide 2000, Mathiesen and Hagerhall 2002). ND2 is part of the dehydrogenase unit, responsible for oxidizing NADH to NAD. ND2 is also thought to be necessary for proper complex 1 assembly (Ugalde et al. 2007). ND2 is comprised of 9 transmembrane domains, 5 of which were present in the fragment recovered in our yeast three-hybrid screen. Typically,

transmembrane domain containing proteins are not recovered in yeast three-hybrid screens as they must be present in the yeast nucleus for an interaction to occur. However, since we are expressing only a fragment of a human gene in yeast, we cannot eliminate the possibility that the protein is misfolding or not being properly trafficked. The misfolded/improperly trafficked protein would be retained in the endoplasmic reticulum, and since the endoplasmic reticulum is contiguous with the nucleus these proteins could still interact with a CID.

Over 60 different compound families have been shown to inhibit complex 1. They are divided into three different classes: A) quinones, B) semiquinones, and C) quinols (Degli Esposti 1998). Interestingly, no specific binding sites have been defined for these compound classes; they are all believed to bind the same hydrophobic pocket (Okun et al. 1999). MMV006169 contains a 2,4-diaminoquinazoline scaffold, which belongs with the class B inhibitors of ND2. Interesting, Mtx-MMV006169 was designed using EN01.065, an analog differing from the parent only in the addition of a methoxy group, as a starting point. EN01.065 shows the most dramatic impact on host cell ATP levels after 8 days, which further strengthens the hypothesis that MMV006169 analogs may work by inhibiting host cell enzymes.

T. gondii isoforms of ND2 (TgNDH2-1 and TgNDH2-1) are considered alternative type II dehydrogenases. Their active sites face the mitochondrial matrix and they are individually non-essential (Lin et al. 2011). Like *P. falciparum* and most other type II NADH dehydrogenases, TgNDH2-1 and 2-2 are thought to interact with membranes through the aid of amphipathic α -helices, but possess no transmembrane

domains (Melo et al. 2004, Fisher et al. 2007, Lin et al. 2011). Individual deletions of either isoform result in replication defects (Lin et al. 2011) as does treatment of parasites with the TgNDH2-1 inhibitor 1-Hydroxy-2-Dodecyl-4(1H)Quinolone (HDQ). Since treatment with MMV006169 matches the phenotype seen with HDQ, and the compounds both fit class B inhibitors of human ND2, we tested the hypothesis that MMV006169 inhibits TgNDH2-1 and/or TgNDH2-2, but saw no positive interactions with either isoform by yeast three-hybrid. Taken together, these experiments suggest that MMV006169 may be working primarily through interactions with host cell NADH dehydrogenase, although we cannot eliminate the possibility that attaching a linker to MMV006169 prevents it from interacting from another relevant target.

Chapter 3 – Table 1: IC₅₀ values for MMV006169 resistant parasite clones

IC₅₀ values extrapolated from YFP-based growth assays performed on MMV006169 resistant clones. Clones were continuously cultured in 1% DMEM containing 3 μM (EC₉₀) MMV006169. To conserve compound, clones were only assayed until a clean IC₅₀ curve was obtained with clones 1, 2, 8, and 9 being screened once, clones 3, 4, 6, and 7 screened twice, and non-mutagenized screened in triplicate. Clone 5 did not recover after freeze thaw.

Clone #	IC ₅₀ (μM)
1	3.35
2	2.13
3	4.41
4	3.39
6	4.06
7	1.80
8	3.42
9	2.30
Non-mutagenized	1.22

Chapter 3 – Table 2: Titering 3-AT

3-AT was plated at the concentration indicated onto SC + Glu – trp – leu media. One hour later, CID7 (5 μ M, A) or DMSO (B) were spread onto each plate. The next day, 7×10^7 yeast cells were plated, plates were parafilmed and stored at 30°C for 7 days. The number of colonies per plate was recorded daily.

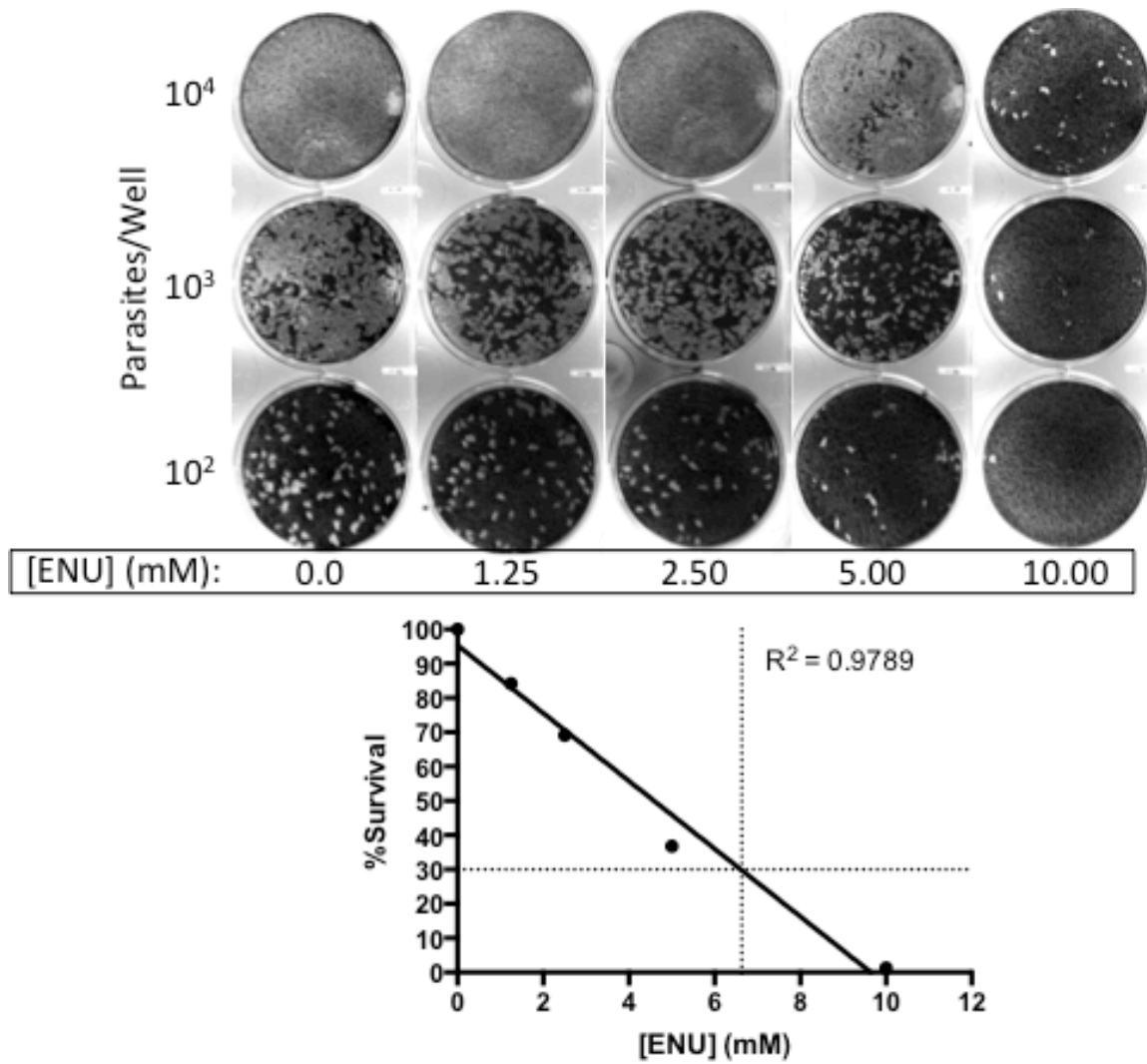
		CID7					
		[3-AT] μ M					
		5.00	2.50	1.25	0.63	0.31	0.00
Days Post Plating	0	0	0	0	0	0	0
	1	0	0	0	0	0	0
	2	0	0	0	0	0	0
	3	0	0	0	0	0	6
	4	0	0	2	4	0	7
	5	0	3	3	9	13	12
	6	0	4	5	24	41	41
	7	2	5	10	37	64	lawn

		DMSO					
		[3-AT] μ M					
		5.00	2.50	1.25	0.63	0.31	0.00
Days Post Plating	0	0	0	0	0	0	0
	1	0	0	0	0	0	0
	2	0	0	0	0	0	0
	3	0	0	0	0	0	0
	4	0	0	0	0	0	0
	5	1	0	0	9	11	lawn
	6	2	0	0	24	22	lawn
	7	2	0	0	47	38	lawn

Chapter 3 – Table 3: Primers for cloning *T. gondii* NDH2-1 and NDH2-2

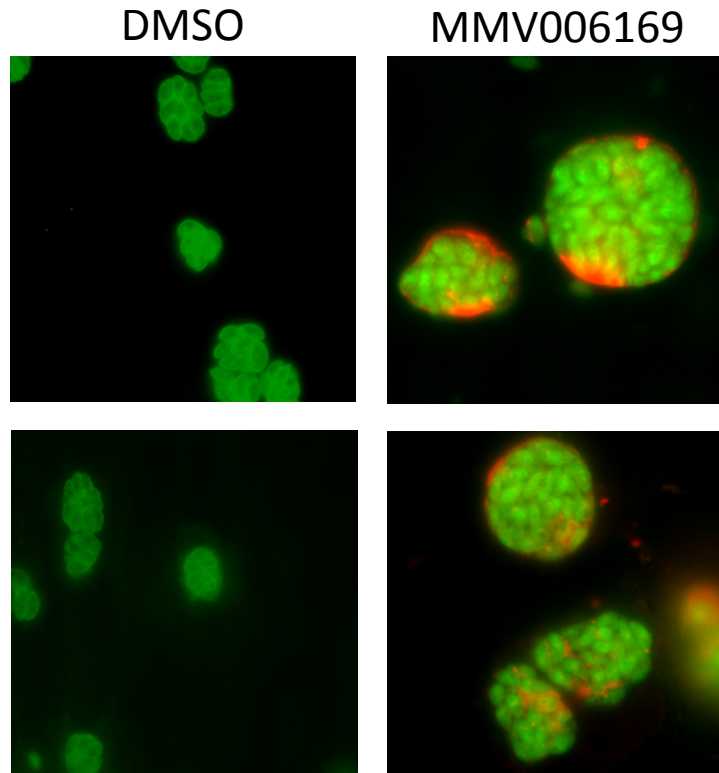
All primers were synthesized by Sigma Aldrich (The Woodlands, TX) with no special modifications. Sequences homologous to pGADT7 are underlined and were used for cloning in yeast.

Primer	Name	Sequence (5'→3'); Sequence homologous to pGADT7 is underlined
14	NDH1IVCFw	GAGTACCCATACGACGTACCAGATTACGCTATGGCAGGGCAGTGGCTGCG
15	NDH1IVCRev	<u>ACAAGCCGACAACCTTGATTGGAGACTTGATCACTTGCCTCGGTCGCCGT</u>
16	NDH1-500Fw	CGGAAGTTTCTACGAAGGC
17	NDH1-1000Fw	GTCGACCTTTGCCTTCAGTC
18	NDH2IVCFw	GAGTACCCATACGACGTACCAGATTACGCTATGGCGATGCTCTTCTCCAG
19	NDH2IVCRev	<u>ACAAGCCGACAACCTTGATTGGAGACTTGATCAGTGGTTGTAATATTCG</u>
20	NDH2-500Fw	CCGACACCTTGACCCAAAC
21	NDH2-1000Fw	CAAAGAGGACATGAGCAAG
22	NDH2-1500Fw	GGCCGACACGCACCGACCC



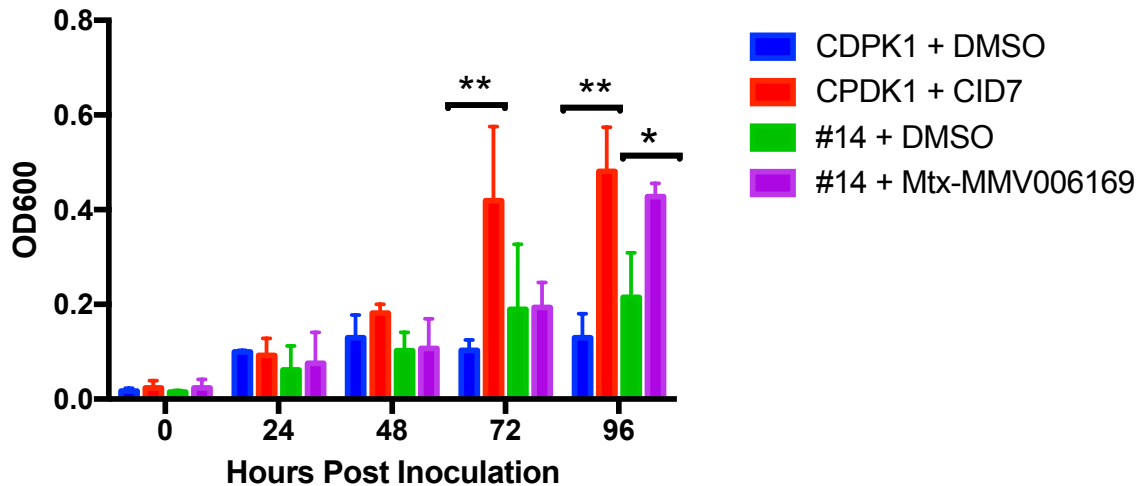
Chapter 3 – Figure 1: Titration of ENU

Plaque assay performed plating varying numbers of 2F1 YFP₂ parasites (indicated left) exposed to varying concentrations of ENU (indicated bottom). Below is the standard survival curve for percent parasite survival versus concentration of ENU. Optimal concentration of ENU determined to be 6.31 mM.



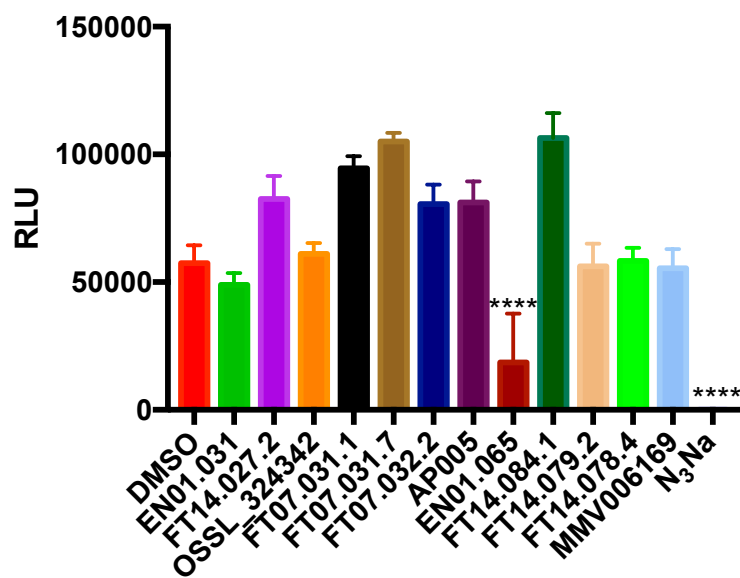
Chapter 3 – Figure 2: MMV006169 resistant clone forms cysts after compound treatment

2F1 YFP₂ parasites were continuously cultured in 1% DMEM containing 3 μ M MMV006169 for seven days prior to fixation (3 μ M corresponds to the EC₉₀ with non-mutagenized parasites). DMSO control parasites were fixed after 24 hours. The cyst wall was stained with TRITC-conjugated *Dolichos biflorus* lectin and parasites with an anti-*Toxoplasma* antibody.



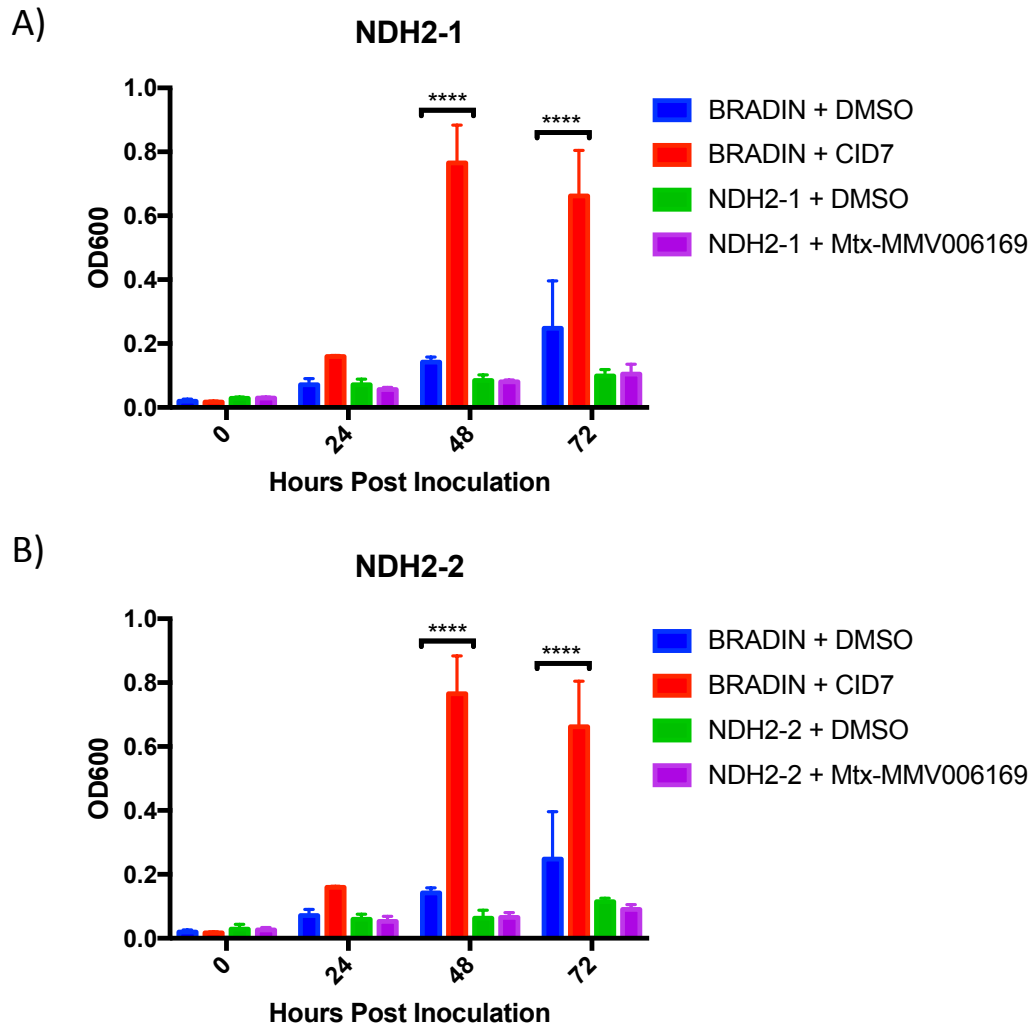
Chapter 3 – Figure 3: Clone 14 interacts with Mtx-MMV006169

Targeted yeast three-hybrid assay where growth of yeast in media lacking histidine is a reflection of reporter activation. The positive control, CDPK1, is able to grow more robustly in the presence of CID7 than in DMSO (red versus blue bars), implying a direct interaction between CID7 and CDPK1. Clone #14 grows more robustly in the presence of Mtx-MMV006169 (purple, $p \leq 0.05$) than DMSO (green) suggesting the gene-product of clone #14 is a target of MMV006169. Bars represent mean \pm standard deviation; $n=3$. Data were analyzed using paired t-tests ($*p \leq 0.05$, $**p \leq 0.01$).



Chapter 3 – Figure 4: MMV006169 analog toxicity after 8 days

Viability of host cells was determined via ATPase assay. HFFs were exposed to 10 μ M analogs for 8-days prior to host cell lysis and quantification of ATP levels by luminescence. Luminescence is reported as relative luminescence units (RLU). All wells were normalized to a control with no CellTiter-Glo reagent. Sodium azide was included to represent a “kill control” in which we know the cells are no longer generating ATP. Bars represent mean \pm standard deviation, n=4. Data were analyzed using a one-way ANOVA (**** $p \leq 0.0001$).



Chapter 3 – Figure 5: MMV006169 does not interact with TgNDHs by yeast three-hybrid

Targeted yeast three-hybrid experiments quantifying growth of yeast in media lacking histidine as a reflection of reporter activation. The positive control, BRADIN, is able to grow more robustly in the presence of CID7 than in DMSO (red versus blue bars), implying a direct interaction between the CID and TgBRADIN. NDH2-1 and NDH2-2 grow to similar levels in the presence of Mtx-MMV006169 (purple) and DMSO (green), meaning the histidine reporter gene has not been activated. Bars represent mean +/- standard deviation; n=3. Data were analyzed using paired t-tests (****p≤0.0001).

CHAPTER 4: DISCUSSION AND FUTURE DIRECTIONS

Small molecule target identification is a lengthy process limited first by the identification of potent compounds of interest. Historically, large compound libraries have been screened with a low percentage of promising hits being identified (Carey et al. 2004, Dittmar et al. 2016). It is impossible to know what the expected success rate of for target identification projects such as this should be, as most groups only document successes and not failures. It is even difficult to correlate successful target identification with compound potency. While it is true that increased potency may increase the specificity of a compound for its protein target(s), target identification has been successful using compounds with varying degrees of potency. For example, Compound 1 was shown to specifically inhibit TgPKG with an IC_{50} 1 nM (Donald et al. 2002), while atorvastatin inhibits the human quinone reductase, NQO2, with an IC_{50} of 50 μ M (Chidley et al. 2011). This means that every target identification endeavor is unique and will come with its own set of challenges.

Screening of the MMV Open Access Malaria box provided us with a novel starting point for compound discovery as the 400 compounds included in this collection were already shown to inhibit growth of the related apicomplexan, *P. falciparum*. Similarities between apicomplexans include a conserved intracellular life cycle involving invasion of host cells, modification of a parasitophorous vacuole, secretion from specialized organelles, and egress from host cells (Cowman and Crabb 2006, Boothroyd and Dubremetz 2008, Treeck et al. 2011). This study identified 79 inhibitors of *T. gondii*

growth, many of which were not identified in previous MMV box screens against *T. gondii* (Boyom et al. 2014). Boyom et al. reported 7 inhibitors of *T. gondii* growth with potencies ranging between 0.19-4.54 μ M. Of these 11, only two, MMV666095 and MMV085203, were also found in our screen. The lack of overlap between MMV box screens could be a functional consequence of the screening assays chosen. The screen used by Boyom et al. involved incubation of parasites with compound for 24 hours followed by treatment with 3-(4,5-dimethylthiazol-2-yl)-5-(3-carboxymethoxyphenyl)-2-(4-sulfophenyl)-2H-tetrazolium, inner salt (MTS) and the electron coupling reagent phenazine methosulfate (PMS). MTS is converted to formazan, which can be read at 490 nm absorbance. This means our assay runs for 7 days longer, has 8 times as many time points, and is read based on fluorescence instead of absorbance. Of the 79 molecules we identified, MMV006169 was shown to be an inhibitor of replication and invasion with no quantifiable difference seen in two-dimensional motility.

Our targeted yeast three-hybrid experiments using TgCDC48Cy and TgCDC48Ap were unsuccessful, however, they only included the genes cloned into the yeast vector such that the GAL4-AD was fused to the amino-terminus of each protein. It would be interesting to examine the effect of carboxy-terminal fusions. If these proteins generated a functional yeast three-hybrid complex, it would suggest the previous amino-terminal fusion was preventing proper CID-target protein interaction. Both isoforms of TgCDC48 have been shown to retain localization upon carboxy-terminal tagging, but no attempts have been made to alter the amino terminus (Agrawal et al. 2009). Additionally, it is known that CDC48 associates with Der1, a pore involved in the ERAD pathway. It is

possible that CDC48 needs to be associated with this pore for proper folding or activity to occur. *T. gondii* has 3 isoforms (2 localized to the endoplasmic reticulum, 1 localized to the apicoplast) of the *S. cerevisiae* Der1, the most similar localizing to the endoplasmic reticulum and having 20% identity. Rather than using yeast three-hybrid, precursor molecules synthesized during CID generation can be immobilized to a column and used for affinity purification experiments with either recombinantly expressed CDC48 isoforms in the presence and absence of Der1, or with whole parasite lysates to determine if the presence of Der1 reveals an active site for MMV006169 on CDC48.

Interestingly, there is a third form of TgCDC48 (TgME49_230710) annotated in the *Toxoplasma* database (www.toxodb.org, release 29). This gene has never been studied, with very limited proteomics data available to confirm the suggested sequence. This isoform shares 17% identity with the *S. cerevisiae* CDC48, which is predicted to interact with DBeQ, 17% identity with TgCDC48Cy, and 19% identity with TgCDC48Ap. This lack of homology suggests that this third “isoform” of TgCDC48 will not interact with DBeQ, and thus also not MMV006169. However, it would be easy to assess this by cloning TgME49_230710 into our yeast expression vectors and performing targeted yeast three-hybrid analyses as previously described.

Our library scale yeast three-hybrid experiments suggest that the target of MMV006169 may be the host cell mitochondrially-encoded NADH dehydrogenase subunit 2. The fragment pulled from the library encodes 739 base pairs of ND2 equivalent to 5 transmembrane domains. Yeast three-hybrid systems are notoriously poor at detecting transmembrane domain containing proteins, as they must be retained in the

nucleus to activate the expression of reporter genes. However, the system has worked in some cases to isolate transmembrane domain-containing proteins (Young and Ozenberger 1995, Kajkowski et al. 1997). Since the fragment of ND2 isolated in our screen is typically encoded on the human mitochondrial genome, it does not contain a mitochondrial localization sequence. So, while the protein has transmembrane domains, it does not have a targeting sequence to shuttle it away from the endoplasmic reticulum after folding. Additionally, the yeast expression vector used in our experiments contains a nuclear localization sequence. That sequence in conjunction with the fact that the nucleus is contiguous with the endoplasmic reticulum might explain why this transmembrane domain containing protein was identified in our yeast three-hybrid experiments (Laba et al. 2014). However, it is equally likely that this interaction is the artifact of improper protein folding or the consequence of having expressed only a fragment of the protein. We can directly test the inhibition of ND2 by MMV006169 by performing a mitochondrial *in vitro* activity assay. This works by isolating mitochondria from lysed host cells with differential centrifugation. Mitochondria are solubilized with digitonin or maltocide and complex 1 is immunocaptured. Substrates are mixed with MMV006169 and changes in NADH are measured spectrophotometrically (Janssen et al. 2007, Spinazzi et al. 2012). If NADH levels are reduced we will know that ND2 is a target of MMV006169.

The same logic described above also pertains to the targeted yeast three-hybrid experiments performed with TgNDH2-1 and TgNDH2-2. Both were cloned as amino-terminal fusions with the GAL4-AD. It would be interesting to see if the results of the

assay were to differ had the activation domain been fused in a different position. Additionally, it has been previously shown that TgNDH2-1 can be functionally expressed in *Yarrowia lipolytica*, which expresses a single, non-essential NDH2 and as such is the model organism for the study of alternative NADH dehydrogenases (Kerscher 2000). This model was used to confirm that TgNDH2-1 is the target of HDQ (Lin et al. 2008). It would be interesting to determine if MMV006169 works on TgNDH2-1 using the same system. It would also be useful to optimize the system such that TgNDH2-2 can be used. Initial attempts to express TgNDH2-2 in *Y. lipolytica* demonstrated oxidoreductase activity equivalent to that of having no dehydrogenase present (Lin et al. 2008). We suspect the primary reason for this is the improper identification of mature protein start positions. The *T. gondii* mitochondrial localization sequence is insufficient to target these isoforms to the *Y. lipolytica* mitochondria (Lin et al. 2008). To aid in this process, the mitochondrial NUAM protein localization sequence was fused to the predicted mature protein start site and full length start positions of each protein. For TgNDH2-1, only the fusion to the predicted mature start position allowed oxidoreductase activity (Lin et al. 2008). By troubleshooting the mature protein start position of TgNDH2-2, we may be able to generate an enzyme that functions more efficiently in *Y. lipolytica* and as such can be used to directly test if MMV006169 can inhibit its activity.

The most direct set of experiments to test the hypothesis that MMV006169 interacts with TgNDHs would be to generate clean TgNDH2-1 and TgNDH2-2 gene deletions and look for a change in parasite sensitivity to compound. Proof of concept experiments have already been performed on parasites lacking these genes in the

presence of HDQ (Lin et al. 2011). Using CRISPR technology, we would individually delete each isoform of the NADH dehydrogenase and replace it with a selectable marker (Shen et al. 2014, Sidik et al. 2014). Upon confirmation of the proper genotype, we would perform replication assays (see Chapter 2 – Materials and Methods) and look for a change in the number of parasites present per vacuole. If we see an increase in the number of parasites per vacuole upon compound treatment in one (or both) knockout parasite lines, we will know that we have isolated a relevant target. If we do not, then TgNDHs do not interact with MMV006169.

Throughout the course of this project a major problem has been trying to determine if we have identified an inhibitor of the parasite or host cell. While the above experiments are elegant and informative, they are also work and resource intensive. To easily distinguish between a host cell and parasite target, we could perform experiments where human ND2 activity is measured in the presence of MMV006169 as described above to determine if the compound has any impact on the host enzyme (Janssen et al. 2007, Spinazzi et al. 2012). Measurements of parasite ATP levels would then be performed in the presence of MMV006169 and other known complex 1 inhibitors such as piericidin A and capsaicin to see if similar effects are noted on parasite ATP levels (Degli Esposti 1998, Carey et al. 2004). These experiments would quickly tell us if the genetic approaches described above would be worth pursuing.

The yeast strain used in this work, BAPI69-4A, was chosen for the presence of the negatively selectable marker, *URA3*, and three additional reporters *ADE2*, *HIS3*, and *lacZ* under the control of galactose inducible promoters (Shaffer et al. 2012). We had

hoped that using this strain would allow us to significantly reduce the number of false positive clones obtained during screening to streamline the target identification process. However, while the negative selection did prevent a large number of yeast from growing on selective plates in the absence of CID, even our positive control experiments using TgBRADIN and TgCDPK1 resulted only in the activation of the histidine reporter in the presence of CID. This means that even with verified small molecule-protein interactions, three of the reporters in this strain were non-responsive. Since the arduous processes of SAR analysis and CID synthesis have already been completed, it would be interesting to screen different *T. gondii* cDNA libraries with these MMV006169-based CIDs to see what putative targets are identified. We currently have two different libraries in hand and several yeast strains that can be used with different reporters for testing CID-dependent reporter activation. Moreover, we have received a number of *P. falciparum*, *P. yoelii*, and *P. vivax* cDNA libraries (generous gifts of Drs. Douglas LaCount, Purdue University, and Lawrence Bergman, Drexel University), and we have synthesized our own *C. parvum* cDNA library. All of these libraries would be of interest to screen against our current CIDs. It would also be imperative to include human cDNA libraries in future screens to address the possibility that the compounds are binding to host cell targets.

While yeast three-hybrid approaches have been used successfully for target identification in *T. gondii* (Odell et al. 2015) and other systems (Licitra and Liu 1996, Chidley et al. 2011) the work presented here highlights some of the complications associated with the technology. The best possible cDNA library, most potent compound, and well-designed CID should be in place before attempting these experiments and even

then the target(s) of the compound of interest may not be identified. Amongst other reasons, this could be because (1) the phenotype in the initial screening assay is based on synergistic (multiple targets) effects of the compound, (2) the target is not present in the library, (3) the target is not properly folded or retained in the yeast nucleus, (4) or the target requires the presence of other proteins in a complex to maintain the conformation necessary to interact with the compound of interest. To increase the likelihood of success, multiple strategies for target identification should be used in parallel with yeast three-hybrid. Here we attempted to perform whole genome mutagenesis to identify the target of MMV006169, but were unsuccessful likely because the molecule is specific for the host cell or has multiple targets.

The modular approach to CID synthesis developed by our collaborators could, in principle, facilitate the use of other target identification approaches (Tran et al. 2013). The intermediate molecules derivatized to some length of linker can be attached to biotin and as such immobilized to streptavidin-coated beads for affinity chromatography or phage display approaches. Alternatively, the precursor molecule could be labeled with a fluorophore for use in a drug western blot. The recent advances in the field using CRISPR technology have simplified the follow-up required once a potential target has been identified (Shen et al. 2014, Sidik et al. 2014, Sidik et al. 2016). One can now determine if a gene is essential based on a literature search and then generate a gene deletion, disruption, or inducible down-regulation in one step. The resulting parasite line is then grown in the presence and absence of compound to confirm that the correct target was identified.

This work has contributed to the field of apicomplexan biology by identifying a number of potent inhibitors of *T. gondii* growth that could be used as biological probes to better aid in the understanding of apicomplexan biology. More specifically, it has outlined SAR leading to the identification of a number of replication and invasion inhibitors of *T. gondii*. It has also contributed by further outlining strengths and weaknesses of a variety of approaches to small-molecule target identification.

COMPREHENSIVE BIBIOLOGRAPHY

- Abida, W. M., et al. (2002). "Receptor-dependence of the transcription read-out in a small-molecule three-hybrid system." ChemBioChem **3**(9): 887-895.
- Acevedo-Arozena, A., et al. (2008). "ENU mutagenesis, a way forward to understand gene function." Annu Rev Genomics Hum Genet **9**: 49-69.
- Adl, S. M., et al. (2007). "Diversity, nomenclature, and taxonomy of protists." Syst Biol **56**(4): 684-689.
- Agrawal, S., et al. (2009). "Genetic evidence that an endosymbiont-derived endoplasmic reticulum-associated protein degradation (ERAD) system functions in import of apicoplast proteins." J Biol Chem **284**(48): 33683-33691.
- Aho, S., et al. (1997). "A novel reporter gene MEL1 for the yeast two-hybrid system." Anal Biochem **253**(2): 270-272.
- Amara, J. F., et al. (1997). "A versatile synthetic dimerizer for the regulation of protein-protein interactions." Proc Natl Acad Sci U S A **94**(20): 10618-10623.
- Andenmatten, N., et al. (2012). "Conditional genome engineering in *Toxoplasma gondii* uncovers alternative invasion mechanisms." Nat Methods.
- Andrews, K. T., et al. (2014). "Drug repurposing and human parasitic protozoan diseases." Int J Parasitol Drugs Drug Resist **4**(2): 95-111.
- Attardi, G., et al. (1986). "Seven unidentified reading frames of human mitochondrial DNA encode subunits of the respiratory chain NADH dehydrogenase." Cold Spring Harb Symp Quant Biol **51 Pt 1**: 103-114.
- Baker, K., et al. (2003). "An optimized dexamethasone-methotrexate yeast 3-hybrid system for high-throughput screening of small molecule-protein interactions." Anal Biochem **315**(1): 134-137.
- Bessoff, K., et al. (2013). "Drug repurposing screen reveals FDA-approved inhibitors of human HMG-CoA reductase and isoprenoid synthesis that block *Cryptosporidium parvum* growth." Antimicrob Agents Chemother **57**(4): 1804-1814.
- Bessoff, K., et al. (2014). "Identification of *Cryptosporidium parvum* active chemical series by Repurposing the open access malaria box." Antimicrob Agents Chemother **58**(5): 2731-2739.
- Bhutta, Z. A. and R. E. Black (2013). "Global maternal, newborn, and child health--so near and yet so far." N Engl J Med **369**(23): 2226-2235.
- Black, M. W. and J. C. Boothroyd (2000). "Lytic cycle of *Toxoplasma gondii*." Microbiol Mol Biol Rev **64**(3): 607-623.
- Bookwalter, C. S., et al. (2014). "A *Toxoplasma gondii* Class XIV Myosin, Expressed in Sf9 Cells with a Parasite Co-chaperone, Requires Two Light Chains for Fast Motility." J Biol Chem.
- Boothroyd, J. C. and J. F. Dubremetz (2008). "Kiss and spit: the dual roles of *Toxoplasma* rhoptries." Nat Rev Microbiol **6**(1): 79-88.
- Borges-Pereira, L., et al. (2015). "Calcium Signaling throughout the *Toxoplasma gondii* Lytic Cycle: A Study using Genetically Encoded Calcium Indicators." J Biol Chem **290**(45): 26914-26926.

- Boyom, F. F., et al. (2014). "Repurposing the open access malaria box to discover potent inhibitors of *Toxoplasma gondii* and *Entamoeba histolytica*." Antimicrob Agents Chemother **58**(10): 5848-5854.
- Braun, L., et al. (2013). "A *Toxoplasma* dense granule protein, GRA24, modulates the early immune response to infection by promoting a direct and sustained host p38 MAPK activation." J Exp Med **210**(10): 2071-2086.
- Bruckner, A., et al. (2009). "Yeast two-hybrid, a powerful tool for systems biology." Int J Mol Sci **10**(6): 2763-2788.
- Burdine, L. and T. Kodadek (2004). "Target identification in chemical genetics: the (often) missing link." Chem Biol **11**(5): 593-597.
- Carey, K. L., et al. (2004). "A small-molecule approach to studying invasive mechanisms of *Toxoplasma gondii*." Proc Natl Acad Sci U S A **101**(19): 7433-7438.
- Carruthers, V. B., et al. (1999). "Ethanol and acetaldehyde elevate intracellular [Ca²⁺] and stimulate microneme discharge in *Toxoplasma gondii*." Biochem J **342** (Pt 2): 379-386.
- Carruthers, V. B. and L. D. Sibley (1999). "Mobilization of intracellular calcium stimulates microneme discharge in *Toxoplasma gondii*." Mol Microbiol **31**(2): 421-428.
- Carvalho, L. J. M. (2010). "Murine cerebral malaria: how far from human cerebral malaria?" Trends Parasitol **26**(6): 271-272.
- Chidley, C., et al. (2011). "A yeast-based screen reveals that sulfasalazine inhibits tetrahydrobiopterin biosynthesis." Nat Chem Biol **7**(6): 375-383.
- Chien, C. T., et al. (1991). "The two-hybrid system: a method to identify and clone genes for proteins that interact with a protein of interest." Proc Natl Acad Sci U S A **88**(21): 9578-9582.
- Child, M. A., et al. (2013). "Small-molecule inhibition of a depalmitoylase enhances *Toxoplasma* host-cell invasion." Nat Chem Biol **9**(10): 651-656.
- Chomyn, A., et al. (1986). "URF6, last unidentified reading frame of human mtDNA, codes for an NADH dehydrogenase subunit." Science **234**(4776): 614-618.
- Chomyn, A., et al. (1985). "Six unidentified reading frames of human mitochondrial DNA encode components of the respiratory-chain NADH dehydrogenase." Nature **314**(6012): 592-597.
- Chou, T. F., et al. (2011). "Reversible inhibitor of p97, DBeQ, impairs both ubiquitin-dependent and autophagic protein clearance pathways." Proc Natl Acad Sci U S A **108**(12): 4834-4839.
- Clontech (2007). "Matchmaker GAL4 Two-Hybrid System 3 & Libraries User Manual."
- Coleman, B. I. and M. J. Gubbels (2012). "A genetic screen to isolate *Toxoplasma gondii* host-cell egress mutants." J Vis Exp(60).
- Cowman, A. F. and B. S. Crabb (2006). "Invasion of red blood cells by malaria parasites." Cell **124**(4): 755-766.
- Crews, C. M., et al. (1994). "GTP-dependent binding of the antiproliferative agent didemnin to elongation factor 1 alpha." J Biol Chem **269**(22): 15411-15414.
- Degli Esposti, M. (1998). "Inhibitors of NADH-ubiquinone reductase: an overview." Biochim Biophys Acta **1364**(2): 222-235.

- Del Carmen, M. G., et al. (2009). "Induction and regulation of conoid extrusion in *Toxoplasma gondii*." Cell Microbiol **11**(6): 967-982.
- Derouin, F. and M. Santillana-Hayat (2000). "Anti-toxoplasma activities of antiretroviral drugs and interactions with pyrimethamine and sulfadiazine in vitro." Antimicrob Agents Chemother **44**(9): 2575-2577.
- Dittmar, A. J., et al. (2016). "Drug Repurposing Screening Identifies Novel Compounds That Effectively Inhibit *Toxoplasma gondii* Growth." mSphere **1**(2).
- Dobrowolski, J. M. and L. D. Sibley (1996). "*Toxoplasma* invasion of mammalian cells is powered by the actin cytoskeleton of the parasite." Cell **84**(6): 933-939.
- Donald, R. G., et al. (2002). "*Toxoplasma gondii* cyclic GMP-dependent kinase: chemotherapeutic targeting of an essential parasite protein kinase." Eukaryot Cell **1**(3): 317-328.
- Donald, R. G., et al. (2006). "Anticoccidial kinase inhibitors: identification of protein kinase targets secondary to cGMP-dependent protein kinase." Mol Biochem Parasitol **149**(1): 86-98.
- Dubey, J. P. (1994). "Toxoplasmosis." J Am Vet Med Assoc **205**(11): 1593-1598.
- Dubey, J. P. (1997). "Bradyzoite-induced murine toxoplasmosis: stage conversion, pathogenesis, and tissue cyst formation in mice fed bradyzoites of different strains of *Toxoplasma gondii*." J Eukaryot Microbiol **44**(6): 592-602.
- Dubey, J. P. (2014). The History and Life Cycle of *Toxoplasma gondii*. Toxoplasma gondii - The Model Apicomplexan: Perspectives and Methods. L. M. Weiss and K. Kim. London, UK, Academic Press: 1-17.
- Dubey, J. P. and J. L. Jones (2008). "*Toxoplasma gondii* infection in humans and animals in the United States." Int J Parasitol.
- Dubey, J. P., et al. (2007). "Epidemiology and control of neosporosis and *Neospora caninum*." Clin Microbiol Rev **20**(2): 323-367.
- Dubey, J. P., et al. (1997). "Oocyst-induced murine toxoplasmosis: life cycle, pathogenicity, and stage conversion in mice fed *Toxoplasma gondii* oocysts." J Parasitol **83**(5): 870-882.
- Durfee, T., et al. (1993). "The Retinoblastoma Protein Associates with the Protein Phosphatase Type-1 Catalytic Subunit." Genes & Development **7**(4): 555-569.
- Farrell, A., et al. (2014). "Whole genome profiling of spontaneous and chemically induced mutations in *Toxoplasma gondii*." BMC Genomics **15**: 354.
- Farrell, A., et al. (2012). "A DOC2 protein identified by mutational profiling is essential for apicomplexan parasite exocytosis." Science **335**(6065): 218-221.
- Fields, S. (1993). "The Two-Hybrid System to Detect Protein-Protein Interactions." Methods **5**(2): 116-124.
- Fields, S. and O. Song (1989). "A novel genetic system to detect protein-protein interactions." Nature **340**(6230): 245-246.
- Fisher, N., et al. (2007). "The malaria parasite type II NADH:quinone oxidoreductase: an alternative enzyme for an alternative lifestyle." Trends Parasitol **23**(7): 305-310.
- Fomovska, A., et al. (2012). "Novel N-benzoyl-2-hydroxybenzamide disrupts unique parasite secretory pathway." Antimicrob Agents Chemother **56**(5): 2666-2682.

- Fox, B. A., et al. (2009). "Efficient gene replacements in *Toxoplasma gondii* strains deficient for nonhomologous end joining." *Eukaryot Cell* **8**(4): 520-529.
- Franken, H., et al. (2015). "Thermal proteome profiling for unbiased identification of direct and indirect drug targets using multiplexed quantitative mass spectrometry." *Nat Protoc* **10**(10): 1567-1593.
- Friedrich, T. and D. Scheide (2000). "The respiratory complex I of bacteria, archaea and eukarya and its module common with membrane-bound multisubunit hydrogenases." *FEBS Lett* **479**(1-2): 1-5.
- Frohlich, K. U., et al. (1991). "Yeast cell cycle protein CDC48p shows full-length homology to the mammalian protein VCP and is a member of a protein family involved in secretion, peroxisome formation, and gene expression." *J Cell Biol* **114**(3): 443-453.
- Gajria, B., et al. (2008). "ToxoDB: an integrated *Toxoplasma gondii* database resource." *Nucleic Acids Res* **36**(Database issue): D553-556.
- Gamo, F. J., et al. (2010). "Thousands of chemical starting points for antimalarial lead identification." *Nature* **465**(7296): 305-310.
- Gietz, R. D. and R. H. Schiestl (2007). "Frozen competent yeast cells that can be transformed with high efficiency using the LiAc/SS carrier DNA/PEG method." *Nat Protoc* **2**(1): 1-4.
- Golemis, E. A. and R. Brent (1992). "Fused protein domains inhibit DNA binding by LexA." *Mol Cell Biol* **12**(7): 3006-3014.
- Graindorge, A., et al. (2015). "Functional Dissection of the Repertoire of Myosin Heavy Chains in *Toxoplasma gondii*." *MPM Annual Meeting XXVI, Poster, Abstract #160*.
- Gubbels, M. J., et al. (2008). "Forward genetic analysis of the apicomplexan cell division cycle in *Toxoplasma gondii*." *PLoS Pathog* **4**(2): e36.
- Gubbels, M. J., et al. (2003). "High-Throughput Growth Assay for *Toxoplasma gondii* Using Yellow Fluorescent Protein." *Antimicrob Agents Chemother* **47**(1): 309-316.
- Guiguemde, W. A., et al. (2010). "Chemical genetics of *Plasmodium falciparum*." *Nature* **465**(7296): 311-315.
- Gut, J. and R. G. Nelson (1999). "Cryptosporidium parvum: synchronized excystation in vitro and evaluation of sporozoite infectivity with a new lectin-based assay." *J Eukaryot Microbiol* **46**(5): 56S-57S.
- Gyuris, J., et al. (1993). "Cdi1, a human G1 and S phase protein phosphatase that associates with Cdk2." *Cell* **75**(4): 791-803.
- Hakes, T. B. and D. Armstrong (1983). "Toxoplasmosis. Problems in diagnosis and treatment." *Cancer* **52**(8): 1535-1540.
- Hall, C. I., et al. (2011). "Chemical genetic screen identifies *Toxoplasma* DJ-1 as a regulator of parasite secretion, attachment, and invasion." *Proc. Natl. Acad. Sci. U S A* **108**(26): 10568-10573.
- Harbut, M. B., et al. (2012). "Targeting the ERAD pathway via inhibition of signal peptide peptidase for antiparasitic therapeutic design." *Proc Natl Acad Sci U S A* **109**(52): 21486-21491.

- Heaslip, A. T., et al. (2010). "A small-molecule inhibitor of *T. gondii* motility induces the posttranslational modification of myosin light chain-1 and inhibits myosin motor activity." PLoS Pathog **6**(1): e1000720.
- Heery, D. M., et al. (1997). "A signature motif in transcriptional co-activators mediates binding to nuclear receptors." Nature **387**(6634): 733-736.
- Henthorn, D. C., et al. (2002). "A GAL4-based yeast three-hybrid system for the identification of small molecule-target protein interactions." Biochem Pharmacol **63**(9): 1619-1628.
- Hong, D., et al. (2016). "Opposing Transcriptional Mechanisms Regulate Toxoplasma Development." bioRxiv: doi:10.1101/094847.
- Hostettler, I., et al. (2016). "In Vitro Screening of the Open-Source Medicines for Malaria Venture Malaria Box Reveals Novel Compounds with Profound Activities against *Theileria annulata* Schizonts." Antimicrob Agents Chemother **60**(6): 3301-3308.
- Hotha, S., et al. (2003). "HR22C16: a potent small-molecule probe for the dynamics of cell division." Angew Chem Int Ed Engl **42**(21): 2379-2382.
- Hu, K., et al. (2002). "Daughter cell assembly in the protozoan parasite *Toxoplasma gondii*." Mol Biol Cell **13**(2): 593-606.
- Huang, W., et al. (2015). "SAR Studies of 5-Aminopyrazole-4-carboxamide Analogues as Potent and Selective Inhibitors of *Toxoplasma gondii* CDPK1." ACS Med Chem Lett **6**(12): 1184-1189.
- Huynh, M. H. and V. B. Carruthers (2009). "Tagging of endogenous genes in a *Toxoplasma gondii* strain lacking Ku80." Eukaryot Cell **8**(4): 530-539.
- Iltzsch, M. H. and K. O. Tankersley (1994). "Structure-activity relationship of ligands of uracil phosphoribosyltransferase from *Toxoplasma gondii*." Biochem Pharmacol **48**(4): 781-792.
- Israelski, D. M., et al. (1989). "Zidovudine antagonizes the action of pyrimethamine in experimental infection with *Toxoplasma gondii*." Antimicrob Agents Chemother **33**(1): 30-34.
- Ito, T., et al. (2001). "A comprehensive two-hybrid analysis to explore the yeast protein interactome." Proc Natl Acad Sci U S A **98**(8): 4569-4574.
- Janssen, A. J., et al. (2007). "Spectrophotometric assay for complex I of the respiratory chain in tissue samples and cultured fibroblasts." Clin Chem **53**(4): 729-734.
- Jones, J. L. and G. N. Holland (2010). "Annual burden of ocular toxoplasmosis in the US." Am J Trop Med Hyg **82**(3): 464-465.
- Jones, L. A., et al. (2006). "Ocular toxoplasmosis: in the storm of the eye." Parasite Immunol **28**(12): 635-642.
- Jung, H. J., et al. (2010). "Terpestacin inhibits tumor angiogenesis by targeting UQCRB of mitochondrial complex III and suppressing hypoxia-induced reactive oxygen species production and cellular oxygen sensing." J Biol Chem **285**(15): 11584-11595.
- Kafsack, B. F., et al. (2009). "Rapid membrane disruption by a perforin-like protein facilitates parasite exit from host cells." Science **323**(5913): 530-533.

- Kajkowski, E. M., et al. (1997). "Investigation of growth hormone releasing hormone receptor structure and activity using yeast expression technologies." J Recept Signal Transduct Res **17**(1-3): 293-303.
- Kamau, E. T., et al. (2012). "A focused small-molecule screen identifies 14 compounds with distinct effects on *Toxoplasma gondii*." Antimicrob Agents Chemother **56**(11): 5581-5590.
- Kerscher, S., et al. (2008). "The three families of respiratory NADH dehydrogenases." Results Probl Cell Differ **45**: 185-222.
- Kerscher, S. J. (2000). "Diversity and origin of alternative NADH:ubiquinone oxidoreductases." Biochim Biophys Acta **1459**(2-3): 274-283.
- Khurana, V., et al. (2015). "Toward stem cell-based phenotypic screens for neurodegenerative diseases." Nat Rev Neurol **11**(6): 339-350.
- Kortagere, S., et al. (2011). "Rapid discovery of inhibitors of *Toxoplasma gondii* using hybrid structure-based computational approach." J Comput Aided Mol Des **25**(5): 403-411.
- Kotz, J. (2012). "Phenotypic screening, take two." Science-Business eXchange **5**(15).
- Kvaal, C. A., et al. (2002). "Isolation of a *Toxoplasma gondii* cyclin by yeast two-hybrid interactive screen." Mol Biochem Parasitol **120**(2): 187-194.
- Laba, J. K., et al. (2014). "Traffic to the inner membrane of the nuclear envelope." Curr Opin Cell Biol **28**: 36-45.
- Langhorne, J., et al. (2011). "The relevance of non-human primate and rodent malaria models for humans." Malar J **10**: 23.
- Lee, V. H. L. (1991). Peptide and protein drug delivery. New York, M. Dekker.
- Leeson, P. (2012). "Drug discovery: Chemical beauty contest." Nature **481**(7382): 455-456.
- Leung, J. M., et al. (2014). "Disruption of TgPHIL1 alters specific parameters of *Toxoplasma gondii* motility measured in a quantitative, three-dimensional live motility assay." PLoS One **9**(1): e85763.
- Leung, J. M., et al. (2014). "Identification of *T. gondii* myosin light chain-1 as a direct target of TachypleginA-2, a small-molecule inhibitor of parasite motility and invasion." PLoS One **9**(6): e98056.
- Li, N., et al. (2003). "Mitochondrial complex I inhibitor rotenone induces apoptosis through enhancing mitochondrial reactive oxygen species production." J Biol Chem **278**(10): 8516-8525.
- Licitra, E. J. and J. O. Liu (1996). "A three-hybrid system for detecting small ligand-protein receptor interactions." Proc Natl Acad Sci U S A **93**(23): 12817-12821.
- Lien, E. J. (1981). "Structure-activity relationships and drug disposition." Annu Rev Pharmacol Toxicol **21**: 31-61.
- Lin, H., et al. (2000). "Dexamethasone-Methotrexate: An Efficient Chemical Inducer of Protein Dimerization *In Vivo*." J Am Chem Soc **122**: 4247-4248.
- Lin, S. S., et al. (2011). "Two internal type II NADH dehydrogenases of *Toxoplasma gondii* are both required for optimal tachyzoite growth." Mol Microbiol **82**(1): 209-221.

- Lin, S. S., et al. (2008). "The *Toxoplasma gondii* type-II NADH dehydrogenase TgNDH2-I is inhibited by 1-hydroxy-2-alkyl-4(1H)quinolones." Biochim Biophys Acta **1777**(11): 1455-1462.
- Lomenick, B., et al. (2009). "Target identification using drug affinity responsive target stability (DARTS)." Proc Natl Acad Sci U S A **106**(51): 21984-21989.
- Lomenick, B., et al. (2011). "Identification of direct protein targets of small molecules." ACS Chem Biol **6**(1): 34-46.
- Lovett, J. L. and L. D. Sibley (2003). "Intracellular calcium stores in *Toxoplasma gondii* govern invasion of host cells." J Cell Sci **116**(Pt 14): 3009-3016.
- Luder, C. G., et al. (2014). *Toxoplasma* Animal Models and Therapeutics. *Toxoplasma gondii* - The Model Apicomplexan: Perspectives and Methods. L. M. Weiss and K. Kim. London, UK, Academic Press: 217-255.
- Luft, B. J. and J. S. Remington (1992). "Toxoplasmic Encephalitis in AIDS." Clin. Infect. Diseases **15**: 211-222.
- MacBeath, G. and S. L. Schreiber (2000). "Printing proteins as microarrays for high-throughput function determination." Science **289**(5485): 1760-1763.
- Madeo, F., et al. (1997). "A yeast mutant showing diagnostic markers of early and late apoptosis." J Cell Biol **139**(3): 729-734.
- Manjunatha, U. H., et al. (2016). "Cryptosporidiosis Drug Discovery: Opportunities and Challenges." ACS Infect Dis **2**(8): 530-537.
- Mathiesen, C. and C. Hagerhall (2002). "Transmembrane topology of the NuoL, M and N subunits of NADH:quinone oxidoreductase and their homologues among membrane-bound hydrogenases and bona fide antiporters." Biochim Biophys Acta **1556**(2-3): 121-132.
- Meister, S., et al. (2011). "Imaging of *Plasmodium* liver stages to drive next-generation antimalarial drug discovery." Science **334**(6061): 1372-1377.
- Melo, A. M., et al. (2004). "New insights into type II NAD(P)H:quinone oxidoreductases." Microbiol Mol Biol Rev **68**(4): 603-616.
- Meng, L., et al. (1999). "Epoxomicin, a potent and selective proteasome inhibitor, exhibits in vivo antiinflammatory activity." Proc Natl Acad Sci U S A **96**(18): 10403-10408.
- Mital, J., et al. (2005). "Conditional expression of *Toxoplasma gondii* apical membrane antigen-1 (TgAMA1) demonstrates that TgAMA1 plays a critical role in host cell invasion." Mol Biol Cell **16**(9): 4341-4349.
- Mital, J., et al. (2006). "Laser scanning cytometer-based assays for measuring host cell attachment and invasion by the human pathogen *Toxoplasma gondii*." Cytometry A **69**(1): 13-19.
- Moir, D., et al. (1982). "Cold-sensitive cell-division-cycle mutants of yeast: isolation, properties, and pseudoreversion studies." Genetics **100**(4): 547-563.
- Montoya, J. G. and O. Liesenfeld (2004). "Toxoplasmosis." Lancet **363**(9425): 1965-1976.
- Montoya, J. G. and J. S. Remington (2008). "Management of *Toxoplasma gondii* infection during pregnancy." Clin Infect Dis **47**(4): 554-566.

- Morrison, D. A. (2009). "Evolution of the Apicomplexa: where are we now?" Trends Parasitol **25**(8): 375-382.
- Morrisette, N. S., et al. (2004). "Dinitroanilines bind alpha-tubulin to disrupt microtubules." Mol Biol Cell **15**(4): 1960-1968.
- Mosqueda, J., et al. (2012). "Current advances in detection and treatment of babesiosis." Curr Med Chem **19**(10): 1504-1518.
- Murphy, R. C., et al. (2010). "Discovery of Potent and Selective Inhibitors of Calcium-Dependent Protein Kinase 1 (CDPK1) from *C. parvum* and *T. gondii*." ACS Med Chem Lett **1**(7): 331-335.
- Nagamune, K., et al. (2007). "Artemisinin induces calcium-dependent protein secretion in the protozoan parasite *Toxoplasma gondii*." Eukaryot Cell **6**(11): 2147-2156.
- Odell, A. V., et al. (2015). "Yeast three-hybrid screen identifies TgBRADIN/GRA24 as a negative regulator of *Toxoplasma gondii* bradyzoite differentiation." PLoS One **10**(3): e0120331.
- Ojo, K. K., et al. (2010). "*Toxoplasma gondii* calcium-dependent protein kinase 1 is a target for selective kinase inhibitors." Nat Struct Mol Biol **17**(5): 602-607.
- Okun, J. G., et al. (1999). "Three classes of inhibitors share a common binding domain in mitochondrial complex I (NADH:ubiquinone oxidoreductase)." J Biol Chem **274**(5): 2625-2630.
- Osborne, M. A., et al. (1996). "The inositol 5'-phosphatase SHIP binds to immunoreceptor signaling motifs and responds to high affinity IgE receptor aggregation." J Biol Chem **271**(46): 29271-29278.
- Pai, M. Y., et al. (2015). "Drug affinity responsive target stability (DARTS) for small-molecule target identification." Methods Mol Biol **1263**: 287-298.
- Pappas, G., et al. (2009). "Toxoplasmosis snapshots: global status of *Toxoplasma gondii* seroprevalence and implications for pregnancy and congenital toxoplasmosis." Int J Parasitol **39**(12): 1385-1394.
- Pfefferkorn, E. R. and L. C. Pfefferkorn (1979). "Quantitative studies of the mutagenesis of *Toxoplasma gondii*." J Parasitol **65**(3): 364-370.
- Plavec, I., et al. (2004). "Method for analyzing signaling networks in complex cellular systems." Proc Natl Acad Sci U S A **101**(5): 1223-1228.
- Porter, S. B. and M. A. Sande (1992). "Toxoplasmosis of the central nervous system in the acquired immunodeficiency syndrome." N Engl J Med **327**(23): 1643-1648.
- Portman, N. and J. Slapeta (2014). "The flagellar contribution to the apical complex: a new tool for the eukaryotic Swiss Army knife?" Trends Parasitol **30**(2): 58-64.
- Qureshi, S. A. (2010). "In Vitro-In Vivo Correlation (IVIVC) and Determining Drug Concentrations in Blood from Dissolution Testing – A Simple and Practical Approach." The Open Drug Delivery Journal **4**: 38-47.
- Remington, J. S., et al. (1995). Toxoplasmosis. Infectious Diseases of the Fetus and the Newborn Infant. J. S. Remington and J. O. Klein. Philadelphia, W. B. Saunders Company: 140-267.
- Roos, D. S., et al. (1994). Molecular tools for genetic dissection of the protozoan parasite *Toxoplasma gondii*. Methods in Cell Biology. **45**: 27-63.

- Ruden, D. M., et al. (1991). "Generating yeast transcriptional activators containing no yeast protein sequences." *Nature* **350**(6315): 250-252.
- Saleh, A., et al. (2007). "Growth inhibition of *Toxoplasma gondii* and *Plasmodium falciparum* by nanomolar concentrations of 1-hydroxy-2-dodecyl-4(1H)quinolone, a high-affinity inhibitor of alternative (type II) NADH dehydrogenases." *Antimicrob Agents Chemother* **51**(4): 1217-1222.
- Savitski, M. M., et al. (2014). "Tracking cancer drugs in living cells by thermal profiling of the proteome." *Science* **346**(6205): 1255784.
- Scherf, U., et al. (2000). "A gene expression database for the molecular pharmacology of cancer." *Nat Genet* **24**(3): 236-244.
- SenGupta, D. J., et al. (1996). "A three-hybrid system to detect RNA-protein interactions in vivo." *Proc Natl Acad Sci U S A* **93**(16): 8496-8501.
- Shaffer, H. A., et al. (2012). "BAPJ69-4A: A yeast two-hybrid strain for both positive and negative genetic selection." *Journal of Microbiological Methods* **91**(1): 22-29.
- Sheffield, H. G. and M. L. Melton (1968). "The fine structure and reproduction of *Toxoplasma gondii*." *J Parasitol* **54**(2): 209-226.
- Sheiner, L., et al. (2011). "A systematic screen to discover and analyze apicoplast proteins identifies a conserved and essential protein import factor." *PLoS Pathog* **7**(12): e1002392.
- Shen, B., et al. (2014). "Efficient gene disruption in diverse strains of *Toxoplasma gondii* using CRISPR/CAS9." *MBio* **5**(3): e01114-01114.
- Sidik, S. M., et al. (2014). "Efficient genome engineering of *Toxoplasma gondii* using CRISPR/Cas9." *PLoS One* **9**(6): e100450.
- Sidik, S. M., et al. (2016). "A Genome-wide CRISPR Screen in *Toxoplasma* Identifies Essential Apicomplexan Genes." *Cell* **166**(6): 1423-1435 e1412.
- Sousa, T., et al. (2008). "The gastrointestinal microbiota as a site for the biotransformation of drugs." *Int J Pharm* **363**(1-2): 1-25.
- Spangenberg, T., et al. (2013). "The open access malaria box: a drug discovery catalyst for neglected diseases." *PLoS One* **8**(6): e62906.
- Speer, C. A., et al. (1995). "Sporozoites of *Toxoplasma gondii* lack dense-granule protein GRA3 and form a unique parasitophorous vacuole." *Mol Biochem Parasitol* **75**(1): 75-86.
- Spencer, D. M., et al. (1993). "Controlling signal transduction with synthetic ligands." *Science* **262**(5136): 1019-1024.
- Spinazzi, M., et al. (2012). "Assessment of mitochondrial respiratory chain enzymatic activities on tissues and cultured cells." *Nat Protoc* **7**(6): 1235-1246.
- Subauste, C. (2012). "Animal models for *Toxoplasma gondii* infection." *Curr Protoc Immunol* **Chapter 19**: Unit 19 13 11-23.
- Sullivan, W. J., Jr. and V. Jeffers (2012). "Mechanisms of *Toxoplasma gondii* persistence and latency." *FEMS Microbiol Rev* **36**(3): 717-733.
- Taunton, J., et al. (1996). "A mammalian histone deacetylase related to the yeast transcriptional regulator Rpd3p." *Science* **272**(5260): 408-411.
- Tenter, A. M., et al. (2000). "*Toxoplasma gondii*: from animals to humans." *Int J Parasitol* **30**(12-13): 1217-1258.

- Tomavo, S. and J. C. Boothroyd (1995). "Interconnection between organellar functions, development and drug resistance in the protozoan parasite, *Toxoplasma gondii*." Int J Parasitol **25**(11): 1293-1299.
- Tran, F., et al. (2013). "A modular approach to triazole-containing chemical inducers of dimerisation for yeast three-hybrid screening." Molecules **18**(9): 11639-11657.
- Trecek, M., et al. (2011). "The phosphoproteomes of *Plasmodium falciparum* and *Toxoplasma gondii* reveal unusual adaptations within and beyond the parasites' boundaries." Cell Host Microbe **10**(4): 410-419.
- Triezenberg, S. J., et al. (1988). "Evidence of DNA: protein interactions that mediate HSV-1 immediate early gene activation by VP16." Genes Dev **2**(6): 730-742.
- Ugalde, C., et al. (2007). "Mutated ND2 impairs mitochondrial complex I assembly and leads to Leigh syndrome." Mol Genet Metab **90**(1): 10-14.
- Van Criekinge, W. and R. Beyaert (1999). "Yeast Two-Hybrid: State of the Art." Biol Proced Online **2**: 1-38.
- van der Ven, A. J., et al. (1996). "Anti-toxoplasma effect of pyrimethamine, trimethoprim and sulphonamides alone and in combination: implications for therapy." J Antimicrob Chemother **38**(1): 75-80.
- Van Voorhis, W. C., et al. (2016). "Open Source Drug Discovery with the Malaria Box Compound Collection for Neglected Diseases and Beyond." PLoS Pathog **12**(7): e1005763.
- Voet, D., et al. (2008). Fundamentals of biochemistry : life at the molecular level. Hoboken, NJ, Wiley.
- Vojtek, A. B., et al. (1993). "Mammalian Ras interacts directly with the serine/threonine kinase Raf." Cell **74**(1): 205-214.
- W.H.O. (2015). "World Health Organization: World malaria report 2015." 1–280.
- Walker, M. and J. R. Zunt (2005). "Parasitic central nervous system infections in immunocompromised hosts." Clin Infect Dis **40**(7): 1005-1015.
- Walton, J. A. G., et al. (2009). "Synthesis and biological evaluation of functionalised tetrahydro- β -carboline analogues as inhibitors of *Toxoplasma gondii* invasion." Org Biomol Chem **7**: 3049-3060.
- Watkins, S. M., et al. (2002). "Lipid metabolome-wide effects of the PPARgamma agonist rosiglitazone." J Lipid Res **43**(11): 1809-1817.
- Watts, E., et al. (2015). "Novel Approaches Reveal that *Toxoplasma gondii* Bradyzoites within Tissue Cysts Are Dynamic and Replicating Entities In Vivo." MBio **6**(5): e01155-01115.
- Weiss, L. M. and K. Kim (2000). "The development and biology of bradyzoites of *Toxoplasma gondii*." Front Biosci **5**: D391-405.
- Wetzel, D. M., et al. (2004). "Calcium-mediated protein secretion potentiates motility in *Toxoplasma gondii*." J Cell Sci **117**(Pt 24): 5739-5748.
- Young, K. H. (1998). "Yeast two-hybrid: so many interactions, (in) so little time." Biol Reprod **58**(2): 302-311.
- Young, K. H. and B. A. Ozenberger (1995). "Investigation of ligand binding to members of the cytokine receptor family within a microbial system." Ann N Y Acad Sci **766**: 279-281.

Zheng, W., et al. (2013). "Phenotypic screens as a renewed approach for drug discovery."
Drug Discov Today **18**(21-22): 1067-1073.

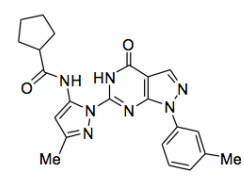
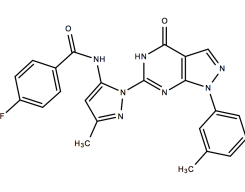
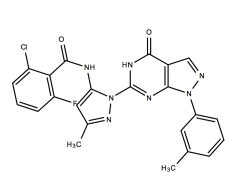
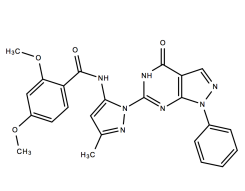
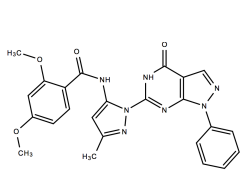
APPENDIX A: ANALYSIS OF THE REPLICATION INHIBITOR MMV403679

[N.B. Structural analogs synthesized for this work produced by Stephen Ojo (University of St. Andrews). C. parvum data presented here were generated by the joint effort of Kovi Bessoff and Rajiv Jumani (University of Vermont).]

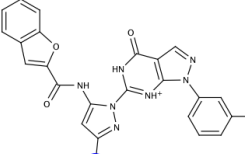
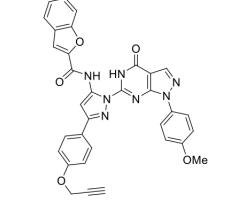
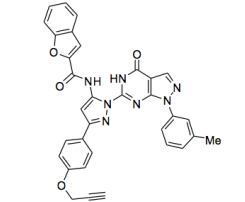
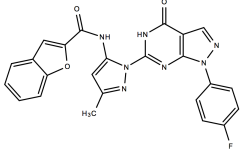
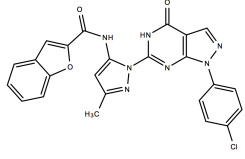
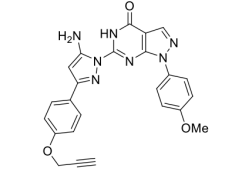
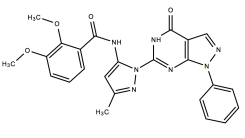
As mentioned in Chapter 2, our screens of the MMV Open Access Malaria box lead us to the identification of five small molecules of interest. MMV403679, is a potent, non-toxic inhibitor of both *T. gondii* and *C. parvum* growth (Appendix A – Figure 1; (Bessoff et al. 2014)). The compound also inhibits *T. gondii* replication (Appendix A – Figure 2). To better understand how MMV403679 inhibits *T. gondii* and *C. parvum*, we performed extensive structure-activity relationship analyses on this compound using 38 analogs either purchased (Life Chemicals, Ontario, Canada) or synthesized (Appendix A – Table 1). We had aimed to use this SAR to develop a novel CID for use in yeast three-hybrid experiments, but never reached that point with the project.

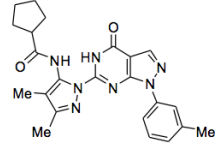
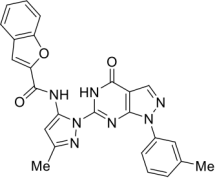
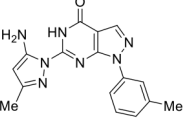
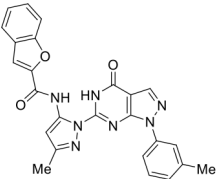
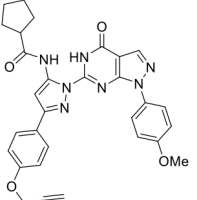
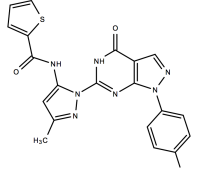
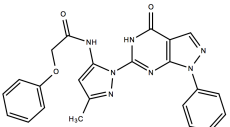
Appendix A – Table 1: MMV403679 structural analogs

Thirty-eight structural analogs of MMV403679 containing a conserved allopurinol chemical scaffold. Calculated IC₅₀ values for each analog and corresponding 95% confidence intervals are reported. Excessively wide confidence intervals are reported as “n/a”.

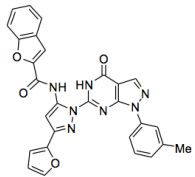
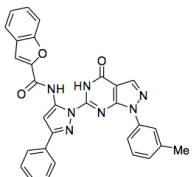
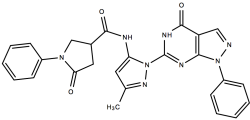
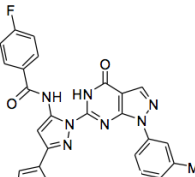
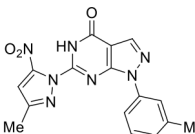
Name	Structure	<i>T. gondii</i> IC ₅₀ (μM)	<i>T. gondii</i> IC ₅₀ 95% CI	<i>C. parvum</i> IC ₅₀ (μM)	<i>C. parvum</i> IC ₅₀ 95% CI
F5091-0161		0.04	(0.03-0.05)	0.06	N/A
F5091-0196		0.04	(0.010-0.17)	0.12	(0.08-0.19)
F5091-0208		0.06	(0.05-0.06)	0.07	(0.06-0.09)
F5091-0573		0.06	N/A	0.18	N/A
F5091-0036		0.07	(0.06-0.08)	0.07	(0.04-0.10)

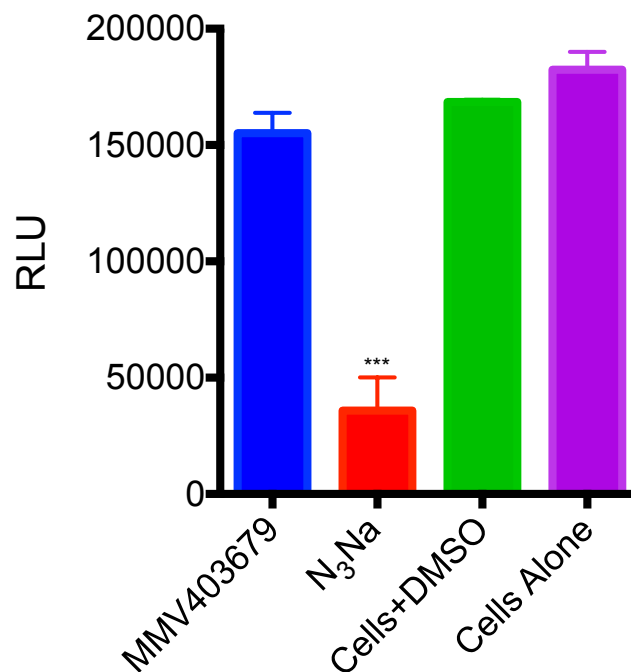
F5091-0230		0.09	(0.04-0.19)	0.15	(0.11-0.21)
F5091-0270		0.10	(0.08-0.12)	0.12	(0.07-0.21)
F5091-0204		0.10	(0.06-0.15)	0.08	(0.07-0.09)
F5091-0186		0.10	very wide	0.04	(0.03-0.05)
F5091-0123		0.10	(0.07-0.15)	0.08	(0.06-0.10)
SA006		0.10	(0.08-0.13)	Not screened	Not screened
F5091-0869		0.11	(0.01-2.61)	0.17	N/A

F5091-0273		0.13	(0.11-0.14)	0.12	(0.10-0.14)
SA001		0.14	(0.11-0.17)	1.4	(0.16-12.21)
SA010		0.14	(0.12-0.17)	Not screened	Not screened
F5091-0873		0.15	(0.11-0.21)	0.21	(0.10-0.45)
F5091-0723		0.18	(0.13-0.24)	0.41	(0.24-0.71)
SA004		0.21	(0.18-0.25)	1.17	(0.93-1.47)
F5091-0038		0.22	(0.17-0.30)	0.10	(0.07-0.16)

SA013		0.25	(0.21-0.29)	Not screened	Not screened
Reordered F5091-0273		0.26	(0.22-0.31)	Not screened	Not screened
SA003		0.31	(0.21-0.45)	0.32	(0.26-0.39)
Synthesized 403679		0.36	(0.30-0.45)	0.65	(0.60-0.71)
SA002		0.37	(0.24-0.58)	1.11	(0.94-1.31)
F5091-0871		~ 0.3806	very wide	0.14	(0.09-0.24)
F5091-0080		0.44	(0.38-0.51)	0.57	(0.39-0.83)

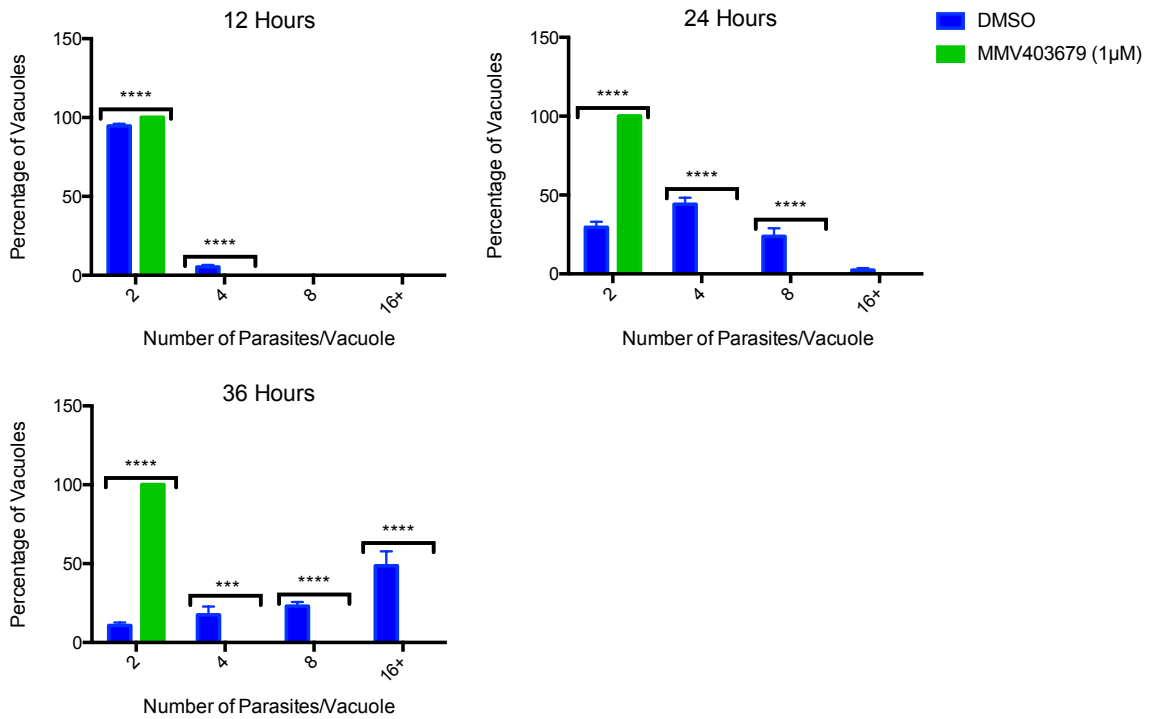
F5091-0655		0.49	(0.39-0.60)	0.20	(0.16-0.25)
SA011		0.66	(0.56-0.76)	Not screened	Not screened
F5091-0772		1.24	(0.68-2.23)	0.20	(0.17-0.24)
F2135-0883		1.21	(0.86-1.22)	0.9992	(0.91-1.10)
403679-4		1.31	(1.08-1.59)	1.032	(0.81-1.32)
SA005		1.38	(1.17-1.63)	2.24	(1.94-2.58)
F5091-0249		1.61	(1.19-2.17)	0.17	(0.14-0.21)

SA009		2.41	(1.83-3.18)	Not screened	Not screened
SA007		3.13	(2.84-3.44)	Not screened	Not screened
F5091-0127		4.57	(3.65-5.72)	0.69	(0.53-0.90)
SA016		>18.18	N/A	Not screened	Not screened
403679-1		>18.18	N/A	>10	N/A



Appendix A – Figure 1: MMV403679 is not toxic to human foreskin fibroblasts

Viability of host cells was determined using the Promega CellTiter-Glo ATPase assay per manufacturer's instructions (see Chapter 2 Materials and Methods). HFFs were exposed to 10 μ M MMV403679 for 24-hours followed by lysis of host cells and quantification of ATP levels by luminescence. Luminescence is reported as relative luminescence units (RLU). All samples were normalized to a control of HFFs and media with no CellTiter-Glo reagent. Sodium azide (N_3Na) was included as a control for host cell death where cells are no longer generating ATP. Bars represent mean \pm standard deviation, n=3. Data were analyzed using a one-way ANOVA (***) $p \leq 0.001$.



Appendix A – Figure 2: MMV403679 inhibits *T. gondii* replication

Human foreskin fibroblasts were infected with 2F1 YFP₂ strain *T. gondii* and grown in the presence (green) or absence (blue) of 1 μM MMV403679 for 12, 24, or 36 hours. The average number of parasites per vacuole at each time point was determined by immunofluorescence (n=3, ****p* ≤ 0.001, *****p* ≤ 0.0001 as determined by two-way ANOVA).

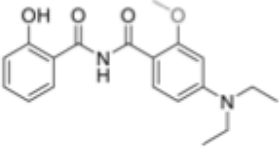
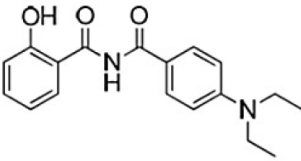
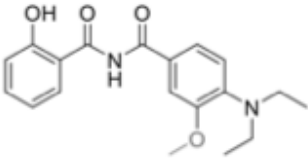
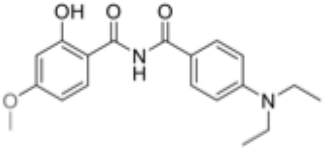
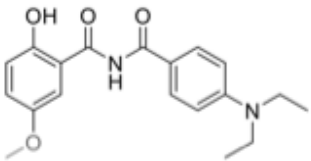
APPENDIX B: ATTEMPTS TO IDENTIFY THE TARGET(S) OF QQ-437

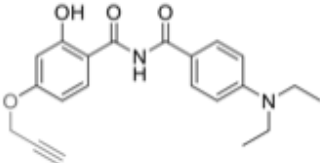
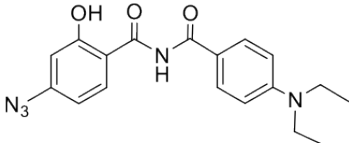
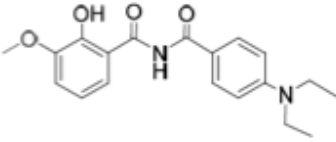
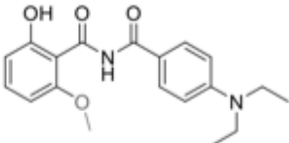
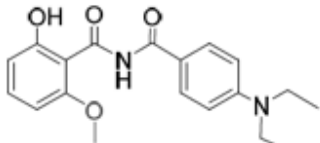
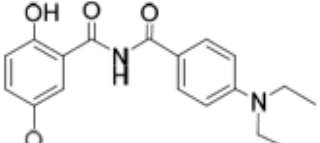
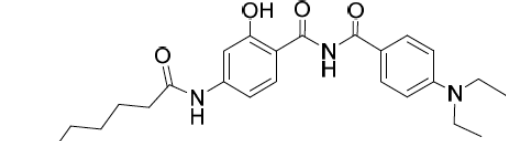
[N.B. Structural analogs synthesized for this work were produced by Fanny Tran (University of St. Andrews).]

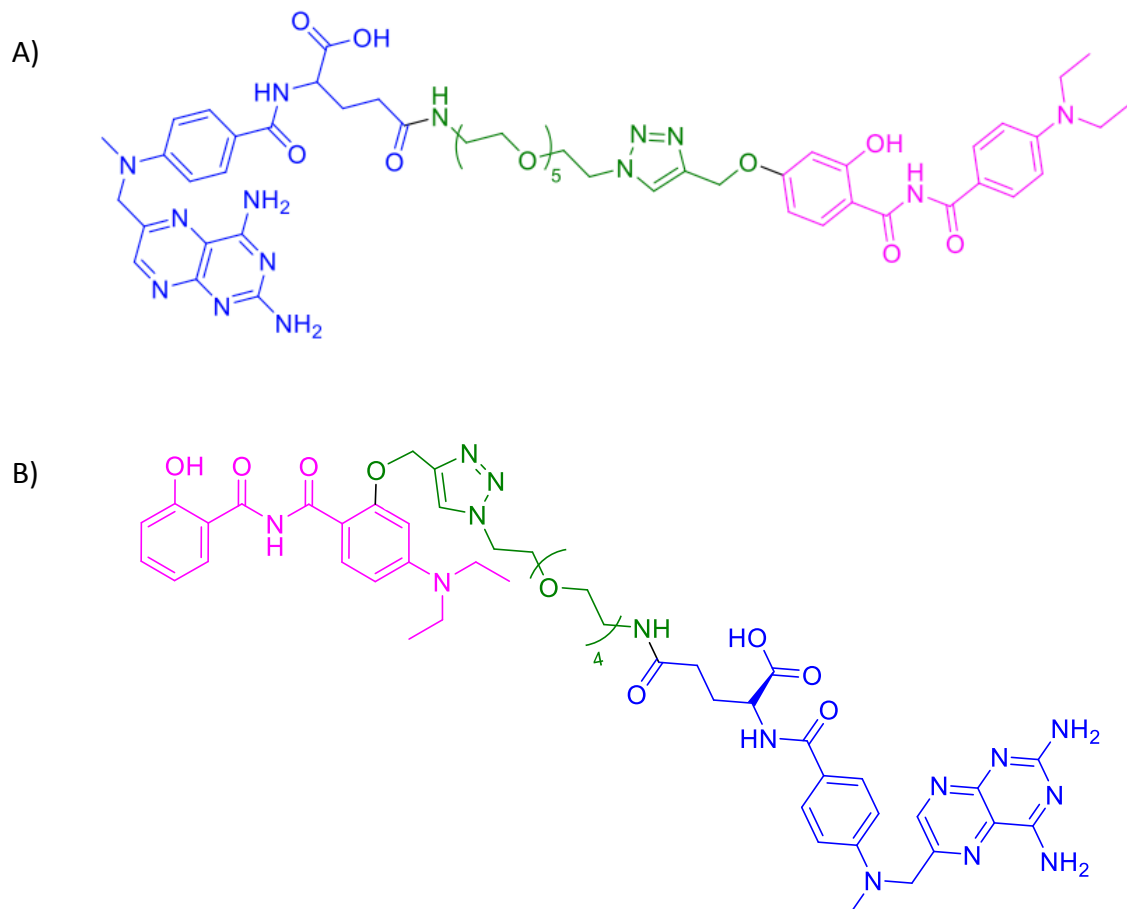
QQ-437 is a highly potent compound that has previously been shown to reduce *T. gondii* proliferation. Insertional mutagenesis has provided indirect evidence that the target of QQ-437 is adaptin 3-beta (AP3B) (Fomovska et al. 2012). We attempted to confirm this hypothesis by cloning TgAP3B into the yeast three-hybrid vector pGADT7 and have used two different QQ-437-based chemical inducers of dimerization (CIDs) (Appendix B – Figure 1) to screen for an interaction between QQ-437 and AP3B. These CIDs were synthesized based on data generated in a small-scale SAR screen (Appendix B – Table 1). Unfortunately, there was not a positive interaction between either of our CIDs and AP3B (Appendix B – Figure 2). This may be due to insufficient SAR leading to suboptimal positioning of linker attachment or because AP3B is not the biologically relevant target of QQ-437 in *T. gondii*. To test the latter hypothesis, I have screened both CIDs against our *T. gondii* cDNA library and was unable to isolate any true interactions via yeast three-hybrid.

Appendix B – Table 1: QQ-437 structural analogs

Structures of QQ-437 and 11 structural analogs. Calculated IC₅₀ values for each analog and corresponding 95% confidence intervals are reported. Excessively wide confidence intervals are reported as “n/a”.

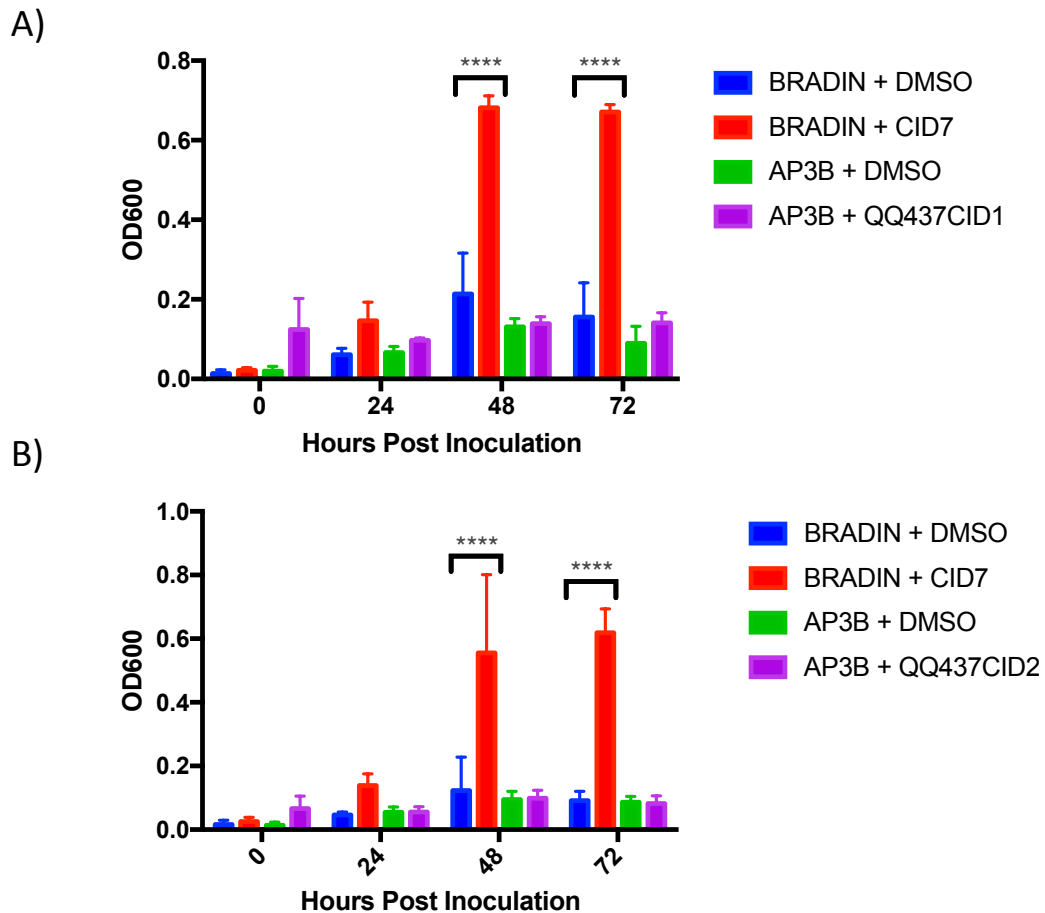
Name	Structure	<i>T. gondii</i> IC ₅₀ (uM)	<i>T. gondii</i> IC ₅₀ 95% CI
FT07.134.1		0.00009324	(0.00005-0.00015)
QQ437		0.004053	(0.002-0.006)
FT07.131.8a		0.005604	(0.004-0.007)
FT14.009.3		0.01622	(0.01-0.03)
FT07.168.3		0.07419	(0.06-0.10)

FT07.135.8		0.1591	(0.12-0.20)
QQ437-Azide		0.2764	(0.24-0.31)
FT07.059.3		0.3971	(0.20-0.79)
FT14.028.3		2.269	(2.09-2.47)
FT07.067.3		>18.18	N/A
FT07.068		>18.18	N/A
FT07.070.3		>18.18	N/A



Appendix B – Figure 1: Structures of QQ-437-based CIDs

A) Structure of QQ437CID1. B) Structure of QQ437CID2. QQ-437 structure is highlighted in pink, linker in green, and methotrexate is shown in blue.



Appendix B – Figure 2: Targeted yeast three-hybrid suggests QQ-437 does not interact with AP3B.

Growth of yeast in media lacking histidine is a reflection of reporter activation. The positive control, pGADBRADIN, is able to grow more robustly in the presence of CID7 than in DMSO (red versus blue bars), implying an interaction between CID7 and BRADIN. pGADAP3B grows to the same level in the presence of (A, purple) QQ437CID1, (B, purple) QQ437CID2, and DMSO (green), meaning no reporter activation is seen. Bars represent mean \pm standard deviation; $n=3$. Data were analyzed using paired t-tests (**** $p \leq 0.0001$).

APPENDIX C: SCREENING A SUBSET OF THE NIH CLINICAL COLLECTION

[N.B. The full NIH Clinical Collection screening against C. parvum and selection of this subset of molecules was performed by Kovi Bessoff (University of Vermont)]

As part of an effort to identify novel inhibitors of *T. gondii* growth, we received a subset of compounds taken from the NIH Clinical Collection (NCC) for screening. The NCC is comprised of 719 FDA-approved small molecules, classified as both drug and drug-like, with known mechanisms of action. Our collaborators screened the entire collection against the related apicomplexan *C. parvum* and a subset of molecules that showed inhibitory activity were provided for screening against *T. gondii* (Bessoff et al. 2013). Using the previously described YFP-based growth assay (Chapter 2 Materials and Methods) these compounds were screened in triplicate (Appendix C – Figure 1). The majority of the compounds inhibited *T. gondii* growth with sub-micromolar potency, and many of them have known targets in human cells or are likely working through inhibition of DNA replication. We aimed to determine if these compounds inhibit *T. gondii* in a manner similar to that of host cells. This would help identify conserved pathways and thus aid in the understanding of general parasite biology. Moreover, if compounds were found to work differently, they could be used to tease apart parasite biological mechanisms.

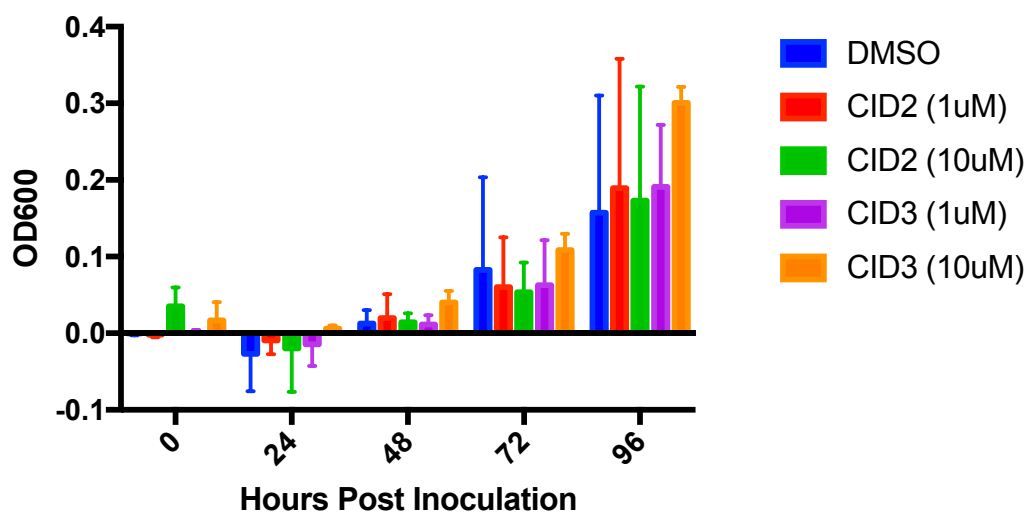
Appendix C – Table 1: Efficacy of NIH Clinical Collection compounds on *T. gondii* growth.

YFP-based growth assays were performed on 17 NCC compounds as previously described. Each compound was serially diluted to yield a total of 11 test concentrations that were screened in triplicate.

	<i>T. gondii</i> IC ₅₀ (μM)	<i>T. gondii</i> IC ₅₀ 95% CI
Homoharringtonine	0.03029	0.02048 to 0.04479
Docetaxel	0.03855	0.02866 to 0.05184
Digoxin	0.07251	0.06177 to 0.08512
Hexachlorophene	0.09068	0.06052 to 0.1359
Triptolide	0.1309	Very Wide
Minocycline	0.2278	0.09084 to 0.5713
5-Fluorouracil	0.2343	0.1968 to 0.2791
Oligomycin C	0.396	0.2277 to 0.6887
Floxuridine	0.4183	0.1770 to 0.9885
Chloroxine	0.5631	0.2798 to 1.133
Carmofur	0.8335	0.4586 to 1.515
Indomethacin	1.234	0.7927 to 1.920
Doxycycline	1.311	0.6706 to 2.565
Tegaserod Maelate	5.301	3.552 to 7.910
6-Azauridine	>18uM	N/A
Glipizide	>18uM	N/A
Mevastatin	>18uM	N/A

APPENDIX D: TARGETED YEAST THREE-HYBRID FOR INTERACTION BETWEEN 118793 AND EG5

During the original small-molecule screen performed in our lab, 118793 was identified as one of the more potent inhibitors of *T. gondii* invasion (Carey et al. 2004). In mammalian cells it has been shown that 118793 interacts with the mitotic kinesin Eg5 (Hotha et al. 2003). Preliminary structure-activity relationship (SAR) data suggest that the target in *T. gondii* is not likely a homolog of this mammalian protein. However, mammalian Eg5 represents an excellent positive control for drug-protein interaction studies involving 118793. To develop this positive control, we amplified full-length mammalian Eg5 from cDNA generated from human foreskin fibroblasts (HFFs) and cloned it into the yeast vector pGADT7. The resulting plasmid was then co-transformed into AH109 with pGBKeDHFR and used in targeted yeast three-hybrid experiments (Chapter 2 Materials and Methods) with the previously generated CIDs 2 (ST501611) and 3 (ST504011) at varying concentrations. At that point in our development of the yeast three-hybrid system, there was no positive control to use in these assays, so they were performed only with the addition of a DMSO control. No reporter activation was seen upon the addition of either CID (Appendix D – Figure 1). Without a positive control we cannot conclude that 118793 cannot interact with Eg5, but these experiments obtained negative results.



Appendix D – Figure 1: Targeted yeast three-hybrid suggests Eg5 does not interact with 118793.

Growth of yeast in media lacking adenine is a reflection of reporter activation. PGADFLeg5-containing yeast grows to the same level in the presence of CID2 (1 and 10 μ M, red and green), CID 3 (1 and 10 μ M, purple and orange), and DMSO (green), meaning no reporter activation occurred. Bars represent mean \pm standard deviation; n=3. Data were analyzed using paired t-tests.

APPENDIX E: GENERATING THE TgUNC ANTIBODY AND DEFINING CELLULAR LOCALIZATION

[N.B. The rabbit work including antigen injections and bleeds were done by Cocalico Biologicals (Stevens, PA). Testing of antibody against Sf9 cell samples was performed by Anne Kelsen (University of Vermont).]

TgUNC, a UCS-domain containing protein, has been shown to aid in TgMyoA folding, but the protein itself has never been characterized in *T. gondii* (Bookwalter et al. 2014). UCS-domain containing proteins historically interact with myosins and heat shock proteins and are found in many different organisms including a number of apicomplexan parasites. First attempts to characterize the gene involved localizing it in intact parasites. Using both FLAG- and 3xMyc-tagged TgUNC (RH $\Delta h x g p r t \Delta k u 8 0$) it was determined that the protein localizes in a punctate manner to the parasite cytosol (Appendix E – Figure 1).

To further characterize the protein, we attempted to generate a TgUNC antibody. The UCS domain (last 1327bp) of TgUNC was sub-cloned into pCR 2.1-Topo vector using TA cloning. The resulting plasmid was digested with HindIII and NdeI to excise the UCS domain. The 1.3kb fragment was then ligated into pre-digested (HindIII/NdeI) pET28a and sequenced to ensure proper insertion and the plasmid was renamed pETUCSDCln1. pETUCSDCln1 was transformed into *BL21-CodonPlus(DE3)-RIL* competent cells for bacterial expression. A negative control of pET28a transformed into

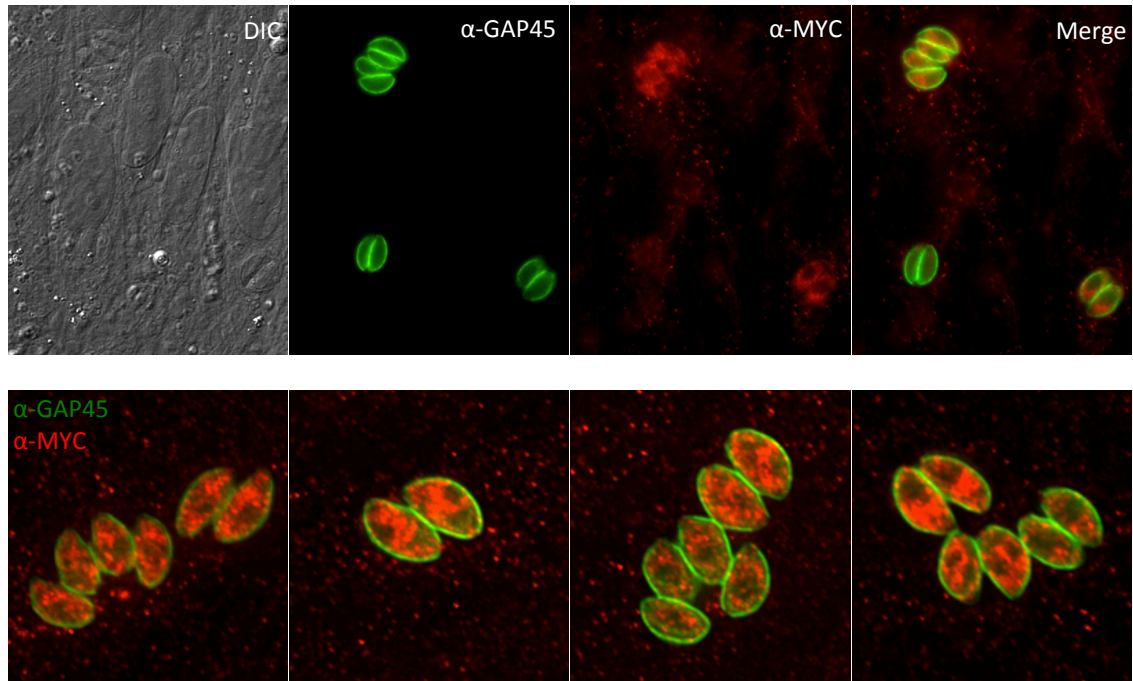
BL21-CodonPlus(DE3)-RIL competent cells was included in parallel in all induction experiments. A single colony of bacteria was used to inoculate 3 mL of LB supplemented with 50µg/mL kanamycin and incubated overnight at 37°C. The next day, the culture was diluted 1:20 and grown with shaking at 37°C for 2 hours. Uninduced samples (1 mL each) were removed and prepared for analysis on an SDS-PAGE gel. The remaining culture was induced by adding 1 mM IPTG and incubated with shaking at 37°C for 2 hours. Whole cell lysate samples were removed and prepared for loading on an SDS-PAGE gel. The remaining cells were pelleted, frozen, thawed, and resuspended in B-PER Bacterial Protein Extraction Reagent mixed with lysozyme and DNase. The large bands shown between 37 and 50 kDa show the bacterially expressed UCS domain (Appendix E – Figure 2, white box). These bands are notably absent from the empty vector control.

Ten pre-bleed samples were provided by Cocalico Biologicals (22-31) for examination. Western blots were performed on *T. gondii* RH lysate using pre-bleed anti-sera as primary antibody (1:500 and 1:2000) and goat anti-rabbit (1:20000) as secondary antibody (Appendix E – Figure 3). Anti-sera 30 and 31 were only screened at 1:500 due to lack of space on the SDS-PAGE gel. Pre-bleed anti-sera 24, 29, 30, and 31 were eliminated from further study due to excessive cross-reactivity between the anti-sera and RH lysate. Anti-sera samples 22, 23, 25, 26, 27, and 28 were screened by immunofluorescence to confirm lack of reactivity against *T. gondii* (Appendix E – Figure 4). From this subset, rabbits 22 and 26 (renamed UVT149 and UVT150 by Cocalico Biologicals) were injected with UCSD (UCS domain only) antigen to generate antibodies. Subsequent bleeds from each animal were screened by western blot for

reactivity against RH *ΔhxpprtΔku80*, 3xMYC- (UCS3xMYCln1), or FLAG-tagged (UCSFLAGln4) TgUNC lysates to confirm that TgUNC could be detected (Appendix E – Figure 5). UVT150 appears to be the stronger antibody by western blot, while UVT149 is stronger by immunofluorescence based on co-localization with 3xMYC-tagged parasites (Appendix E – Figure 6). Additionally, UVT150 was screened against baculovirus/Sf9 recombinantly expressed full-length TgUNC (FL TgUNC), TgUNC lacking the TRP domain (Δ TPR), and the UCS-domain (UCS only) of TgUNC alone (Bookwalter et al. 2014). All recombinantly expressed proteins were detected using UVT150 (Appendix E – Figure 7).

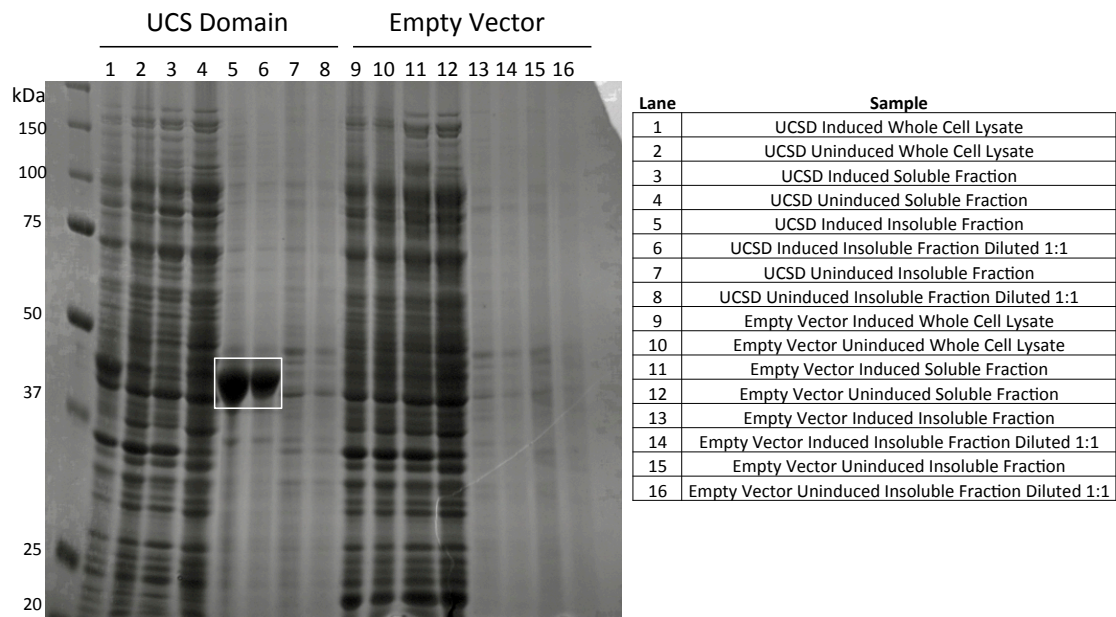
In addition to the generation of an antibody, parasites lacking TgUNC were generated using the DiCre system (Andenmatten et al. 2012). The conditional deletion will circumvent the potential issue of protein compensation, where a related protein takes the place of TgUNC. It also allows us to look at the phenotypic consequences of the gene deletion if TgUNC is essential. The DiCre system requires the use of MG311 parasites, which are RH *ΔhxpprtΔku80* strain parasites with multiple copies of dimerizable Cre recombinase randomly integrated into the genome. To use this strain, 3xMYC-tagged TgUNC was cloned into pG265, between two *loxP* sites. The 5' and 3'UTRs were also cloned into the vector to ensure proper targeting to the TgUNC locus. The resulting parasites were selected in 50 μ g/mL xanthine and 25 μ g/mL mycophenolic acid. To induce gene excision, parasites were incubated in 50 nM rapamycin for 3 hours followed by syringe release and plating on a fresh monolayer of HFFs. After 48 hours, parasite lysate was prepared. Evidence in the field suggests that a deletion of TgUNC results in

the loss of TgMyoA (along with all other myosins) (Graindorge et al. 2015). To confirm the excision of TgUNC, a quantitative western blot for TgMyoA normalized to GRA8 was performed. The addition of rapamycin resulted in the depletion of TgMyoA in two independent clones (D3 and D6), with no loss of signal seen in the non-*loxP* flanked 3xMYCUCSCln1 (Appendix E – Figure 8).



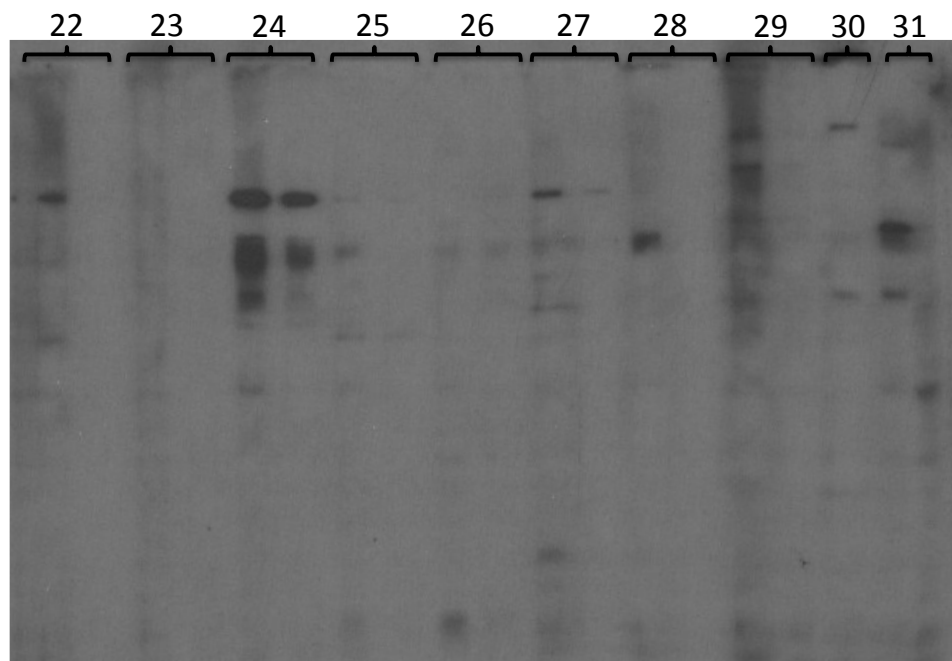
Appendix E – Figure 1: Subcellular localization of TgUNC

3xMYC-tagged TgUNC localizes to the *T. gondii* cytosol (red, top). DeltaVision deconvolution microscopy (bottom) shows that TgUNC has a punctate arrangement in the cytosol. A TgGAP45 antibody was used to outline the entire tachyzoite (green).



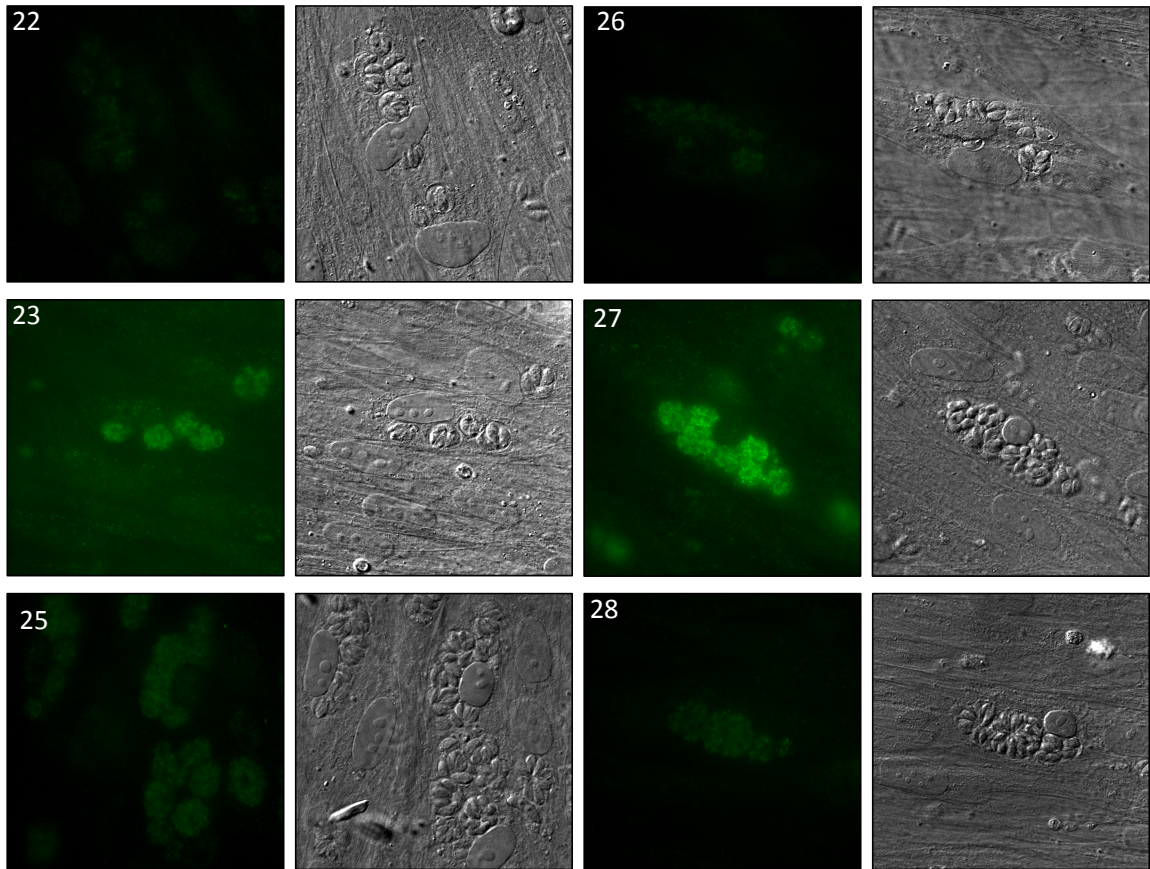
Appendix E – Figure 2: IPTG Induction of TgUNC UCS domain expression.

Induced and uninduced samples of BL21 bacteria containing pETUCSDCln1. Bacterially expressed UCSD is highlighted between 50 and 37 kDa in the induced insoluble fraction (white box, lanes 5 and 6), but is notably absent from the uninduced samples (lanes 13 and 14).



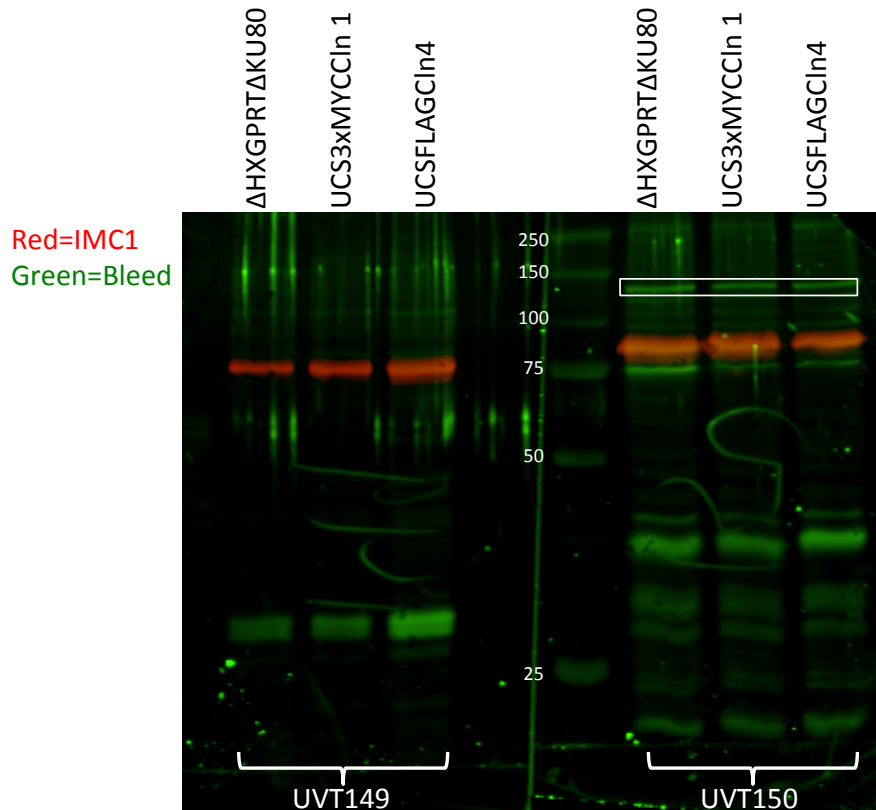
Appendix E – Figure 3: Screening pre-bleed samples against RH lysate

T. gondii RH lysate (equivalent of ½ of a T175 flask in large vacuoles) was run on small SDS-PAGE gel. Samples were probed using indicated pre-bleed at 1:500 and 1:2000 overnight (except 30 and 31, 1:500 only), followed by secondary probing with goat anti-rabbit antibody (1:20000). Robust cross-reactivity seen in pre-bleeds 24, 29, 30, and 31 resulted in their discontinuation from consideration for antibody generation.



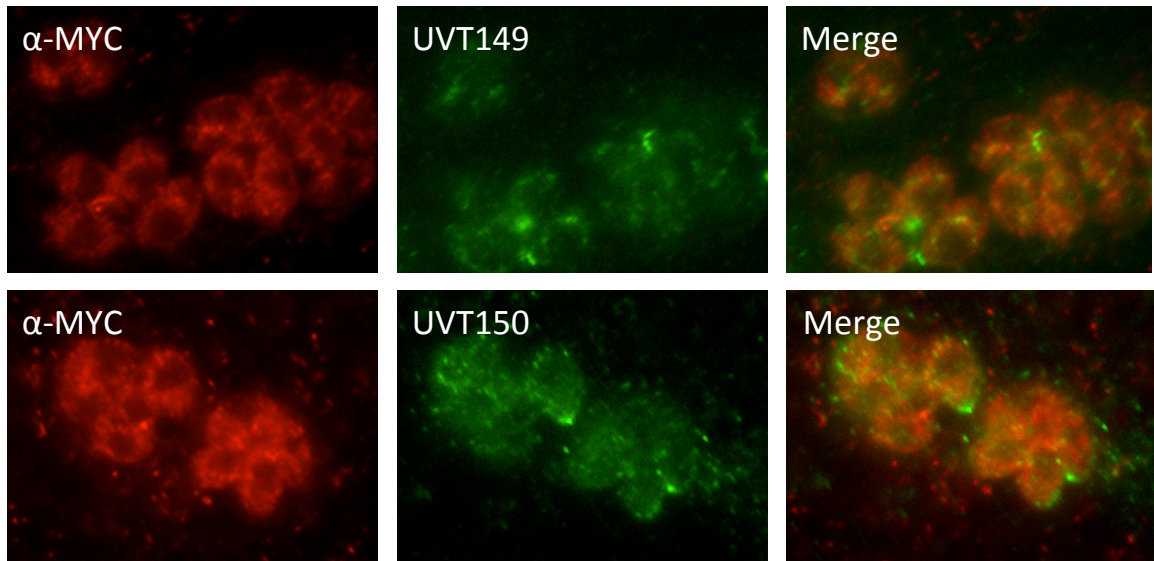
Appendix E – Figure 4: Immunofluorescence with pre-bleeds against *T. gondii*

RH strain *T. gondii* was probed with each pre-bleed (1:500) followed by goat anti-rabbit antibody (1:500). Pre-bleeds showing parasite fluorescence (23, 25, 27, and 28) were eliminated from further consideration.



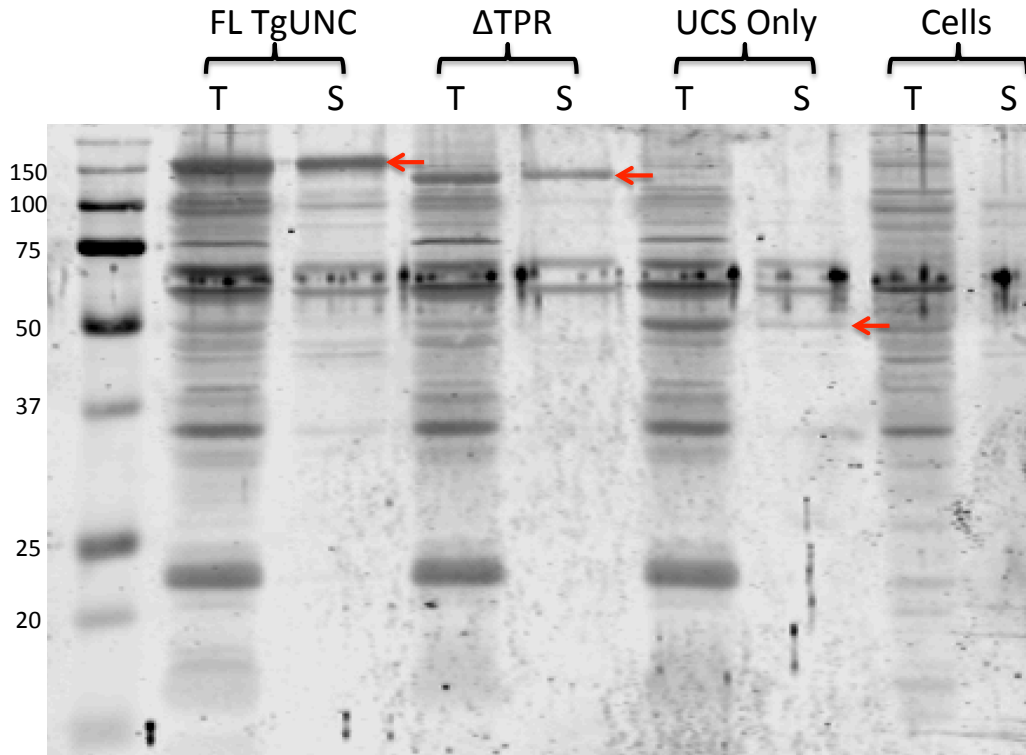
Appendix E – Figure 5: Western blot against *T. gondii* lysates using UVT149 and UVT150

RH $\Delta hxgprt\Delta ku80$, 3x-MYC-, and FLAG-tagged TgUNC parasite lines were probed with UVT149 and UVT150 bleeds at 1:500 (6 boosts, 070114) followed by goat anti-rabbit antibody (1:20000). UVT149 does not show reactivity with antibody, while UVT150 shows specificity in all three parasite lines (white box).



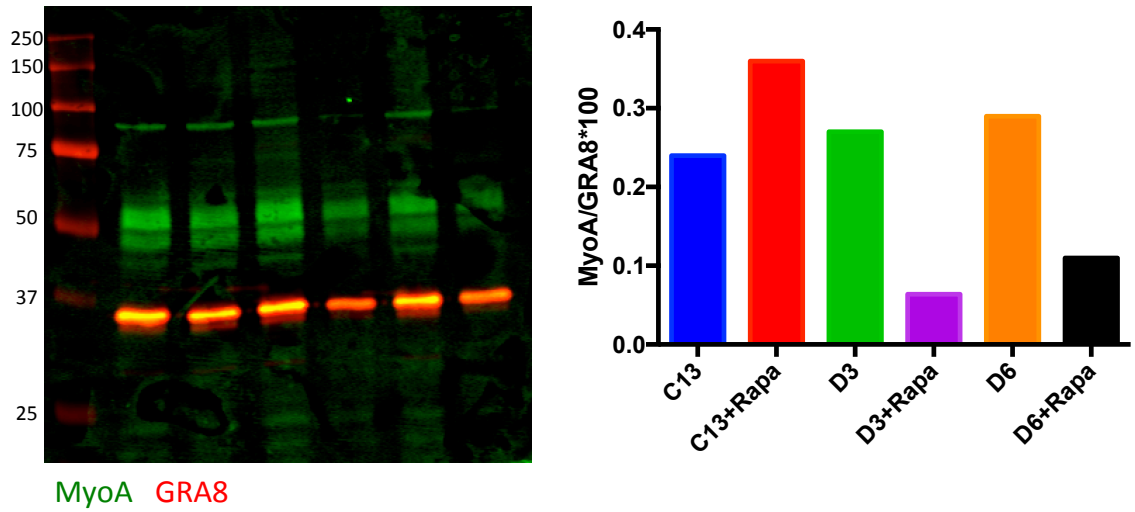
Appendix E – Figure 6: Immunofluorescence of UCS3xMYCIn1 parasites using UVT149 and UVT150

3x-MYC-tagged parasites were stained with UVT149 and UVT150 bleeds at 1:500 (terminal bleed, 102014) followed by goat anti-rabbit antibody (1:500). UVT149 (top, green) staining co-localizes with anti-MYC staining (red), while UVT150 appears non-specific (bottom, green).



Appendix E – Figure 7: Western blot against recombinantly expressed TgUNC (full-length and truncations) using UVT150

Baculovirus/Sf9 recombinantly expressed full-length TgUNC (FL TgUNC), TgUNC lacking the TRP domain (Δ TPR), and the UCS-domain (UCS only) of TgUNC probed with UVT150 terminal bleed. All recombinantly expressed forms of TgUNC are detected by UVT150, with little cross-reactivity in the cells only control.



Appendix E – Figure 8: Inducible knock-out of TgUNC results in loss of TgMyoA

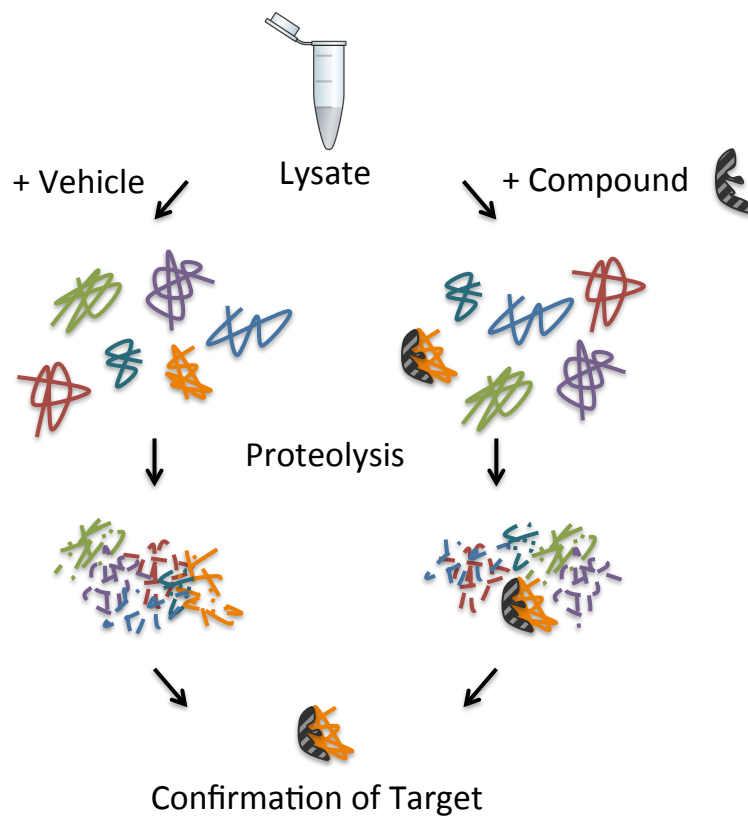
Quantified western blot of non-*loxP* flanked 3xMYC-tagged TgUNC (C13) versus *loxP* flanked 3xMYC-tagged TgUNC expressing parasites with and without rapamycin (TgMyoA=100 kDa, TgGRA8=38 kDa, n=1).

APPENDIX F: DRUG AFFINITY RESPONSIVE TARGET STABILITY AS AN APPROACH TO TARGET IDENTIFICATION

[N.B. Baculovirus expressing recombinant TgMLC1 was generated by Jacqueline Leung (University of Vermont).]

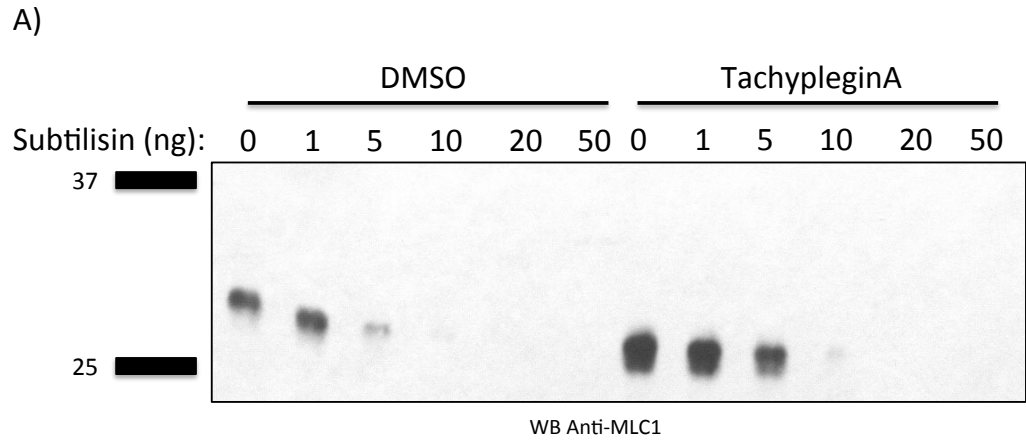
Drug affinity responsive target stability (DARTS) is a genomics-based approach to target identification. The approach is based on the assumption that the binding of a small molecule/drug of interest to a target protein may stabilize that protein's structure in such a way as to make it less susceptible to proteolysis (Lomenick et al. 2009, Lomenick et al. 2011, Pai et al. 2015). DARTS was chosen because it allows one to analyze lower affinity reactions that are typically lost using other techniques, it requires no chemical modification or derivatization of the target protein or small molecules, and can be used with any cell or tissue type. TachypleginA binds covalently to TgMLC1 and upon binding results in an electrophoretic mobility shift associated with the formation of a 225.118 Da adduct on the protein (Heaslip et al. 2010, Leung et al. 2014). This pair presented a unique way to visually troubleshoot DARTS, as unbound, unmodified TgMLC1 should be degraded while the bound form should remain intact (Appendix F – Figure 2B). The assay was performed using Sf9 cell extracts made using PBS supplemented with small amounts of CaCl₂ and a concentration of subtilisin between 5-10 ng per 10 μL of extract. It was found that the addition of TachypleginA to recombinant TgMLC1 did not protect the protein from proteolysis (Appendix F – Figure

2A). This is demonstrated by the disappearance of both the upper and lower bands in each TachypleginA treated sample. The same results were obtained using an alternate protease (pronase). This technique has been unsuccessful thus far in our hands and needs further optimization.



Appendix F – Figure 1: Schematic of DARTS mechanism

Lysate or extract is prepared and incubated with the small molecule/drug of interest (or vehicle control). The protease of choice is then added to each sample and incubated for a pre-optimized amount of time. Samples are prepared for running on SDS-PAGE gel followed by western blot or staining to visualize proteolysis.



Appendix F – Figure 2: DARTS using TgMLC1 and TachypleginA

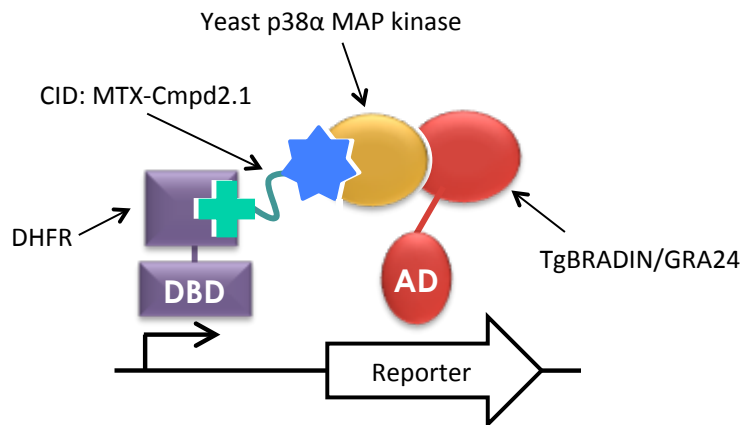
A) DARTS using whole cell lysate. Sf9 cells expressing recombinant Myosin Light Chain-1 were harvested and treated with 40mM TachypleginA or equivalent volume of DMSO. Samples were subjected to subtilisin digestion, run on an SDS-PAGE gel, and analyzed via western blot with an anti-MLC1 antibody. B) Predicted DARTS outcome for recombinant TgMLC1 protected by TachypleginA.

APPENDIX G: DETERMING IF TgBRADIN CAN INTERACT WITH p38 α MAP KINASE

[N.B. Appendix G – Figure 1 was generated by Gary Ward (University of Vermont).]

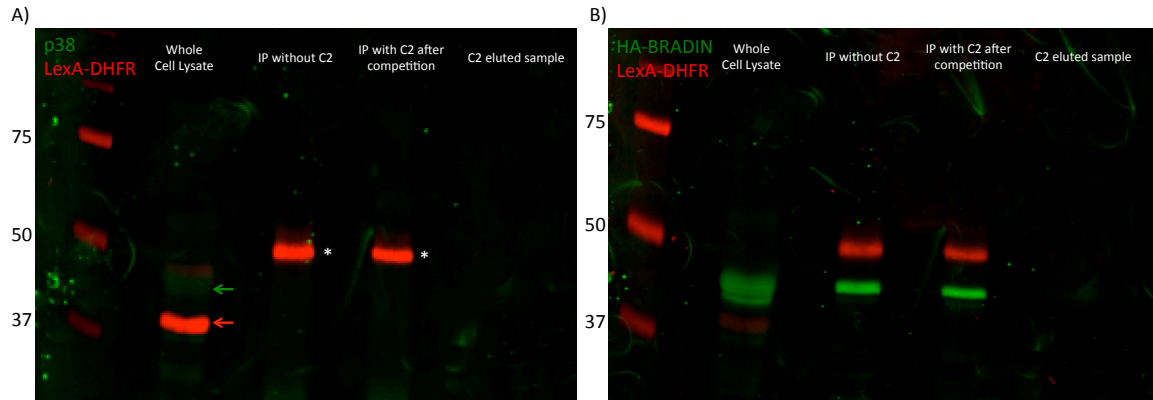
While our paper discussing TgBRADIN as a target of Compound 2 was under revision, another group published an analysis of TgBRADIN (which they named GRA24) (Braun et al. 2013, Odell et al. 2015). TgBRADIN/GRA24 was shown to be secreted by the parasite into the host cell cytosol where it associates with p38 α MAP kinase (p38 α MAPK). This presented us with the hypothesis that TgBRADIN/GRA24 interacts indirectly with Compound 2 through p38 α MAPK. To directly test this an immunoprecipitation of the entire yeast three-hybrid complex (Appendix G – Figure 1) was attempted, where protein G beads and an anti-HA antibody were used to pull-down the HA-tagged c-terminal portion of TgBRADIN (Screen 3 Hit#4). If an interaction is occurring one would be able to detect TgBRADIN, p38 α MAPK, and LexA in the presence of Mtx-Cmpd2.1. Additionally, immunoprecipitation with free Compound 2 (C2) should result in the disappearance of TgBRADIN. Standard western blots were performed and it was determined that both p38 and LexA were detectable in whole cell lysates, but only LexA was found in immunoprecipitations with (bound) or without Compound 2 competition. Both p38 and LexA were absent from the eluate collected after Compound 2 competition (Appendix G – Figure 2A). Upon stripping and re-probing the blot, it was determined that TgBRADIN was found in all samples except the eluate

(Appendix G – Figure 2B). Taken together, these data suggest that TgBRADIN is not interacting with Compound 2 through p38 α MAPK.



Appendix G – Figure 1: Hypothesized role of p38 α MAPK in yeast three-hybrid complex

Yeast three-hybrid schematic where p38 α MAPK (yellow) acts as a bridging protein between compound 2 (blue) containing CID (MTX-Cmpd2.1) and TgBRADIN (red). The methotrexate moiety of MTX-Cmpd2.1 (green) interacts with the DNA-binding domain (DBD, purple). The activation of reporter genes occurs upon interaction of the quaternary complex.



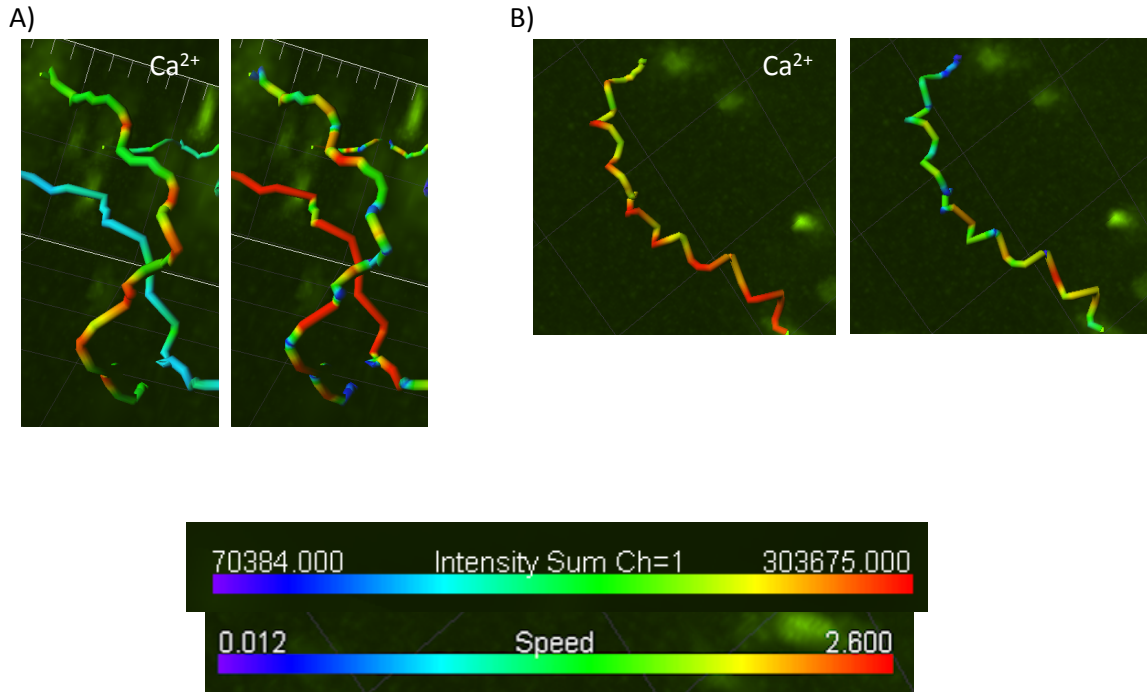
Appendix G – Figure 2: p38 α MAPK is not present in yeast three-hybrid complex

Yeast containing the functional TgBRADIN yeast three-hybrid complex were grown to log phase in the presence of CID. HA-tagged TgBRADIN was immunoprecipitated (IP) using protein G beads and an anti-HA antibody. The resulting IP was run on an SDS-PAGE gel including whole cell lysate, IP with and without compound 2 competition, and the eluate isolated from the compound 2 competition. The gel was prepared for western blot and probed for A) p38 α MAPK (green) and LexA-DHFR (red) and B) HA-TgBRADIN (green) and LexA-DHFR (red). * Indicates cross reactivity with heavy chain.

APPENDIX H: USING 3-DIMENSIONAL MOTILITY ASSAYS TO EXAMINE THE ROLE OF CALCIUM IN *T. GONDII* MOVEMENT

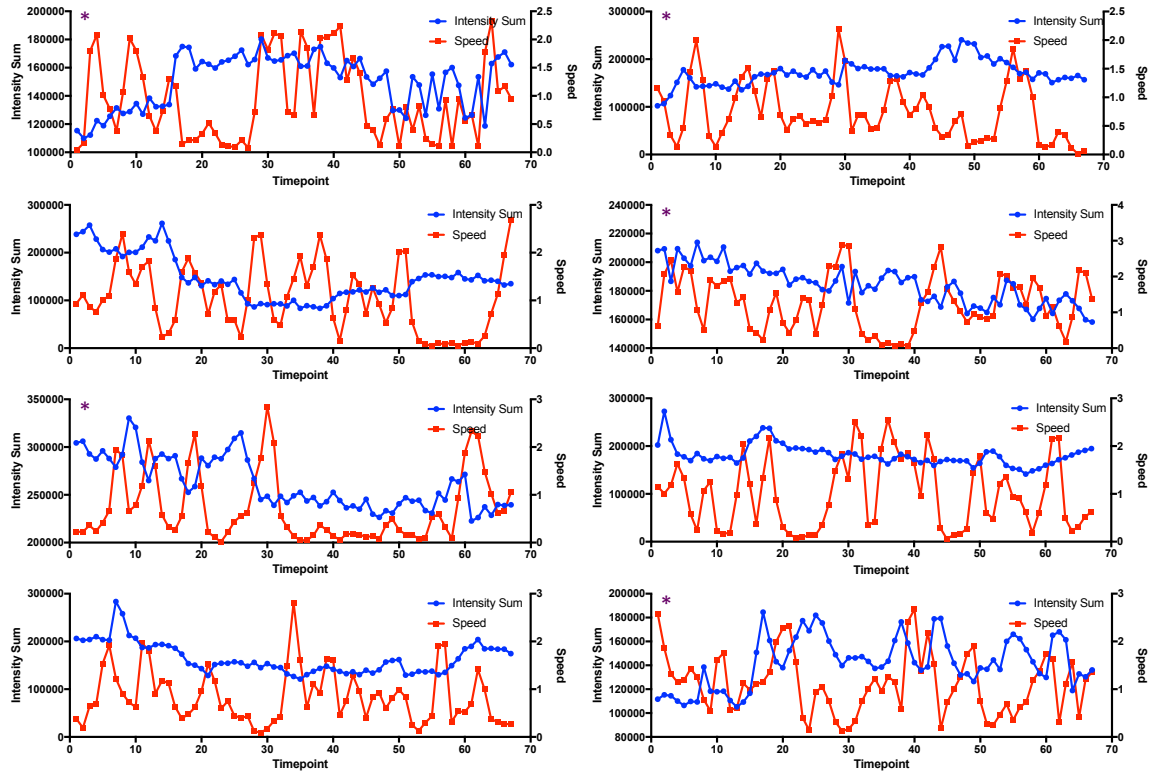
It has been shown that calcium is involved in parasite motility, conoid extension, microneme secretion, invasion, and egress (Carruthers et al. 1999, Carruthers and Sibley 1999, Lovett and Sibley 2003, Wetzel et al. 2004, Del Carmen et al. 2009, Borges-Pereira et al. 2015). However, the spatial and temporal dynamics of calcium fluctuations are unclear. For these experiments, we used a microscopic assay, first developed in our laboratory, which tracks parasites as they move in a three-dimensional matrix (Leung et al. 2014). We expanded on this powerful assay by using *T. gondii* parasites transfected with genetically encoded calcium indicators (i.e., GCaMPs) (Borges-Pereira et al. 2015) to track changes in calcium concentration as parasites move (Appendix H – Figure 1). This allows us to measure changes in intracellular calcium concurrently with velocity (Appendix H – Figure 2), displacement, twist, acceleration, and curvature with the objective of determining if there is a correlation between calcium fluctuation and any of these parameters. We have optimized the assay with respect to matrigel concentrations/batches, intensity of light, imaging time, heating conditions, and image interpretation methods. Using this optimized system, we have generated preliminary data suggesting that there is an increase in parasite calcium levels prior to increases in parasite speed (Appendix H – Figure 1 and Figure 2 *). Using the results of the aforementioned experiments, we have performed experiments using small molecules known to alter calcium oscillations in the parasites. We used caffeine, which has been shown to lengthen

calcium oscillations, calmidazolium, which shortens the oscillations (Wetzel et al. 2004), and thapsigargin, which can cause shallow rapid or long slow oscillations (Nagamune et al. 2007). These experiments have been completed in triplicate and have been run through the existing analysis software (designed to analyze velocity, curvature, torsion, and acceleration) generated with the help of Mark Rould, but no notable phenotypes were seen with respect to log KS values (Leung et al. 2014). Log KS values represent the statistical Kolmogorov–Smirnov test. This test is used to show variation both within (same treatment and parasite line) and between (different treatments and/or parasite lines) data sets. In these experiments, we noted a lot of variability within datasets, meaning that DMSO-treated samples of the same parasite line did not behave in the same manner across biological replicates. As such we cannot conclude that large variation in the data are due to compound treatment and not just day-to-day variation. Work is currently underway to modify the existing software such that it is capable of developing a spatially and temporally resolved model of calcium levels in moving parasites.



Appendix H – Figure 1: Increases in calcium precede increases in velocity along parasite trajectories

Visualization of calcium levels (intensity sum, left) and velocities (right) along two parasite trajectories (A and B).



Appendix H – Figure 2: Oscillations in intracellular parasite calcium levels during motility

Graphical representation of simultaneous measurements of intracellular calcium level (blue) and speed (red) of GCaMP6-expressing parasites as they move through Matrigel. * Indicates a pane where a spike in calcium can be seen before an increase in speed across the majority of the graph.